

THE COMBUSTION OF DUST SUSPENSIONS.

by

W. E. MASON.

A thesis submitted

for the

Degree of Doctor of Philosophy
in the Faculty of Engineering,
University of London.

Dept. of Chemical Engineering

and Chemical Technology,

Imperial College of Science and Technology,

LONDON.

July 1965.

Abstract.

The development of an apparatus for the stabilisation of laminar flames of dust-in-air suspensions is described. This apparatus makes use of batch fluidisation, and operates with relatively small quantities of powder - about 15 to 20g. It was used to study flames of lycopodium powder stabilised on a 10.9 mm. diameter burner without support from a furnace or gas pilot flame. Special attention was given to concentration differences arising in the suspension flow as a result of relative motion between the dust particles and the air; these have been neglected by most of the previous workers studying dust flames. Some of the flames were analysed in detail by the use of particle track photography; the results gave information on the relationship of flame shape to suspension flow pattern, and on the variation of the local burning velocity over the flamefront. It is shown that the mechanism of stabilisation of these flames is quite different from that usually operative in pre-mixed gas flames. It was also found that the burning velocity is constant over a smaller fraction of the flamefront area than for a comparable pre-mixed gas flame. This is attributed partly to the greater depth to which quenching effects penetrate in lycopodium flames, and partly to variation in the effective lycopodium concentration across the flame.

Acknowledgements.

The author wishes to express his thanks to the Department of Scientific and Industrial Research for the award of a Research Studentship, and to the Institute of Fuel for the award of the R.H. Gummer Exhibition. The helpful and stimulating supervision of Dr. M.J.G. Wilson is acknowledged with gratitude. The author also wishes to thank Dr. V.D. Long for many helpful discussions, Dr. P. Eisenklam, Dr. N. Dombrowski and Mr. David Smith for help with photographic work, Mr. E.S. Brett and the workshop staff for assistance in constructing apparatus, and finally his parents and his wife for their help in typing and duplicating the manuscript.

Contents.

	Page
Chapter 1. Introduction and survey of previous research	10
Chapter 2. Development of the apparatus	33
Chapter 3. The flow of the suspension in the burner tube	81
Chapter 4. Flame studies	97
Chapter 5. Results and calculations	109
Chapter 6. Discussion and conclusions	135
Appendix A	191
Appendix B	194
Appendix C	195
List of References	199

LIST OF FIGURES.

	Page.
1. Fluidised bed.	35
2. Measurement of elutriation rate.	38
3a,b. Variation of elutriation rate with time.	41
4a,b,c,d,e. Burners.	43, 44
5. Flames stabilised on Gooch crucible	46
6a Dispersion Apparatus.	50
6b Air Flow System.	51
7a Sampling System.	52
7b Millipore Filter Holder.	52
8. Flow pattern inside cone (zero sampling flow)	55
9. Variation of Concentration with time, relative humidity 40%.	57
10. Variation of Concentration with time, relative humidity 68%.	57
11. Dimensions of Tinplate Cone.	60
12. Variation of \bar{C}_k with time, run No. 29.	62
13. Variation of \bar{C}_k with height of sampling position.	62
14. Variation of W with q.	64
15. Variation of \bar{C}_k with q.	64
16a. Ultra-microscope system.	67
16b. Flow pattern in tube.	67
17. Position of sampling platform.	69
18a. Scheme of Combustion Apparatus.	69
18b. Details of Combustion Apparatus.	72

List of Figures (continued)	Page.
18c. Exhaust flow system.	74
18d. Filter Nozzle.	74
18e. Filter Nozzle in sampling position.	74
19. Manostat.	77
20. Modified Air flow System.	78
21. Flow pattern in burner tube.	78
22. Attachment of fine wire gauze.	84
23. Apparatus for Experiments on Particle-free Space.	87
24a. Flow pattern at tube entry, showing particle-free regions; total flow 2 litres/min.	90
24b. Effect of Flowrate on Boundary of particle-free region.	90
24c. Flow pattern at entry to bell-mouthed tube.	92
25. Combustion apparatus, showing position of flame trap.	93
26. Tube for measurement of Settling Velocity.	95
27a. Plan of Particle Track Photography Lay-out.	100
27b. Details of Illumination System.	100
28. Lycopodium flames - plates P36 and P43.	111
29. Lycopodium flames - plates P27 and P50.	112
30a,b,c. Particle Track Measurements.	115
31a. Velocity profile - plate P27 (with flame).	118
31b. Velocity profile - plate P50 (with flame)	118
32a. Velocity profile - plate P59 (no flame).	119

List of Figures (continued)	Page.
32b. Velocity profile - plate P41 (with flame)	119
33. Position of Stream-tubes on Photographs.	120
34. Definition of S_u .	120
35. Areas of flame-front cut off by Stream-tubes.	123
36. Variation of S_u over flamefronts (i)	124
Variation of S_u over flamefronts (ii)	125
Variation of S_u over flamefronts (iii)	126
37. Variation of S_{max} with \bar{C}_k .	129
38. Measurement of refraction at tube wall.	134
39. Flow of suspension from the burner tube, plates P4 and P59.	1424
40. Flow pattern at entry to plain tube.	147
41. Position of displaced outlet tube.	147
42. Flow pattern at entry to bell-mouthed tube.	149
43. Flow pattern at entry to burner tube.	149
44. Flow entering tube.	159
45. Comparison of measured and calculated velocity profiles for plate P.59, (i).	166
46. Comparison of measured and calculated velocity profiles for plate P.59 (ii)	168
47. Comparison of two theoretical profiles.	170
48. Variation of S_{max} with C_k^i	174
A1 Suspension flow in tube.	196

CHAPTER I.Introduction and Survey Of Previous Research.Introduction.

The practical significance of dust flames lies in their occurrence in dust explosions, and their application to the combustion of pulverised fuel. In both these cases the flame has a highly complex structure, since it propagates through the dust-air mixture under highly turbulent conditions, and particles of a wide range of sizes take part in the combustion. The published literature on dust flames shows that workers in this field have encountered severe practical and theoretical difficulties, so it is desirable to make the system chosen for investigation as simple as possible. In small-scale laboratory work the simplest system is a laminar flame burning in a suspension as nearly mono-disperse as practicable. Some workers have employed systems in which it is necessary to stabilise the flames by a gas pilot flame or by radiation from a furnace; this adds to the experimental complications, and makes interpretation of the results more difficult. Laminar flames may be studied in two situations: i) when stabilised on a burner, or ii) when propagating along a duct containing the suspension. In the second case, the expansion on combustion may set in motion the unburnt

11

suspension ahead of the flame, with the result that conditions at the flame-front are not accurately known, so the first condition seems preferable for detailed investigation of flame structure.

One of the chief difficulties in the experimental study of dust flames is that of producing a uniform suspension of dust in air at a controllable, steady rate; in the case of pre-mixed gas flames, it is a simple matter to ensure that the inflammable mixture is homogeneous, but for dust flames the preparation and control of the suspension is a major part of the problem. Suspensions of dusts in air are inherently unstable, since particles are continually being lost from the system by sedimentation, aggregation, and adhesion to the walls of tubes and containers. As a result of the large density differences between the particles and the air, whenever a suspension flows round bends or past obstacles the particle trajectories deviate from the air streamlines, and local concentration variations result. It is impossible to avoid dust deposition on the surfaces of equipment, or local concentration variations at points where the flow lines are curved, but these effects may be reduced by suitable precautions in the design of the apparatus. Many types of apparatus for the production of dust suspensions have been described in the literature, but some of these are mechanically complex, and none has been widely adopted.

Some workers have given details of the practical difficulties involved. The first object of the present work, therefore, was to develop a simple flexible method for the laboratory-scale production of dust suspensions in the inflammable range of concentration. The second object of the work was to use this method to investigate the structure of laminar dust flames.

Previous Research.

Published work relevant to the present research may be conveniently reviewed under three headings, viz:-

- (1) Properties of dust suspensions.
 - (2) Production of dust suspensions.
 - (3) Studies of dust flames.
- (1) Properties of dust suspensions.

In almost all dust suspensions of combustion interest, the particles are too large to show Brownian motion, and this review will therefore exclude suspensions in which Brownian motion is significant, such as smokes. Experimental work on dust-in-air suspensions has largely been concerned with sampling techniques, but much of the work on solid-in-liquid suspensions is also relevant to dust-in-air systems. The fluid dynamics of the interactions between particles in suspension is still obscure, but a number of workers have attempted to treat theoretically the behaviour of idealised systems.

A very comprehensive survey of the fluid dynamics of gas-solid systems has been made by TOROBIN and GAUVIN.¹

HAWKSLEY² gives a detailed review of relative motion between fluids and particles in sedimenting systems. Shorter surveys by Hawksley³ and Davies⁴ discuss various points of interest concerning fluid-particle systems.

BANISTER⁵ discusses the nature of the difficulties facing attempts to produce theoretical models of the flow of dust clouds and suggests possible ways of overcoming them. A number of workers have discussed theoretically special cases of particle motion in fluids; e.g. KYNCH⁶, following an early treatment by SMOLUCHOWSKI⁷, has discussed the interaction of several small particles settling in a fluid, and extends some of his conclusions to the settling of clouds of particles. BURGERS⁸, adopting a broadly similar approach, has treated the sedimentation of clouds of particles. One result he obtains is that such a cloud may fall as a unit through a large volume of fluid, the fluid within the cloud moving at the same velocity as the particles. In this case, the velocity of the cloud may considerably exceed the velocity of a single isolated particle falling through the volume of fluid. Kynch⁹ has also discussed the behaviour of suspensions from the point of view of viscosity.

Both Burgers and Kynch conclude that the settling velocity of a cloud of particles is a function of the arrangement of particles within it. Hawksley¹⁰ applies this conclusion to suspensions of volumetric concentration greater than about 10%, and argues that since particles of
/different

diameters settle at the same rate in such a suspension ('hindered settling') they must reach an equilibrium configuration, with approximately uniform spacing in any horizontal layer; Kynch⁶, however, suggests that disturbances produced at the cloud boundaries will spread inwards and destroy any long-range ordering of the particles. In deriving theoretically an expression for the sedimentation velocity in the hindered settling regime which gives good agreement with experimental results, MAUDE and WHITMORE¹¹ assumed random ordering of the particles. It appears, therefore, that at present no definite conclusion can be reached as to the existence of ordered particle arrangements in concentrated suspensions.

ROWE and HENWOOD¹² have measured the mutual repulsion between two spheres side-by-side at various distances apart in a water flow. Although their spheres were of $\frac{1}{2}$ in. diameter, the conditions were dynamically similar to those of dust particles in air. Such repulsive forces between particles would tend to produce a uniform particle spacing in any horizontal layer of a suspension if the particles were of fairly uniform size.

In general, an increase in the concentration of a suspension settling in a confined space leads to a reduction of the falling velocity of the particles¹¹. Several workers have suggested, however, that particle interaction at low concentrations may increase particle falling velocities above the free-fall values^{*} and recently KAYE and BOARDMAN¹³ have

* i.e. the value for an isolated particle in an infinite fluid.

produced clear experimental evidence of this. They observed that in the region of volumetric concentration from 0.1% to 3% the falling velocities of individual particles exceed the free-fall value, and they attribute this result to the formation of inter-acting doublets or clusters of particles, which fall faster than isolated individuals. It is not clear why previous investigators working on the sedimentation of suspensions (e.g. HAPPEL,¹⁴ McNOON and LIN,¹⁵) have not observed corresponding increases in sedimentation rates. In the case of inflammable dust suspensions, the concentrations of interest are mostly in the range 50 to 500 mg/litre, which represents a range of volumetric concentrations from 0.005% to 0.05% for particles of unit specific gravity. Kaye and Boardman's results for this range indicate that the settling velocity of the particles is practically equal to their free-fall velocity.

It is observed that dust clouds in air have a tendency to fall bodily at speeds much greater than the free-fall velocity of the particles¹⁶, and it seems likely that in such cases the air within the cloud is moving with the particles, as suggested by Burger's theoretical analysis. If a dust cloud is in a confined space, different parts of the cloud may settle at different velocities. This relative motion between different regions of the cloud probably arises from local variations in concentration, which cause bulk flow of the suspension in a manner similar to convection currents in a liquid.

PALMER¹⁷ has noted that in the case of dust falling through

air in a 17" diameter tube, circulating currents are set up which cause the dust to flow upwards at some points of the tube cross-section.

KHUDYAKOV¹⁸ has pointed out that in most flowing dust suspensions, the dust particles are rotating, and this may affect the relative velocity between the particles and the suspending air. This rotation may arise from irregularities in particle shape, velocity gradients in the flow¹⁸, or from the manner in which the particles are introduced into the air stream.

WALTON¹⁹ has given a very helpful qualitative discussion of the effects of the relative motion between dust particles and air in various situations. He suggests two useful theorems which are applicable to systems in which particle inertia may be neglected. These are:--

- (1) A change in air movement (due for example, to the introduction of a sampling flow) within a cloud of sedimenting, inertia-less particles whose concentration is initially uniform will not give rise to a change in particle concentration at any point within the cloud.
- (2) The number of particles passing per unit time through any given area within a cloud of sedimenting, inertia-less particles is equal to the number that would fall through if the air were stationary plus the product of the particle concentration and the flux of air through the area.

The behaviour of suspensions flowing through tubes is important in cases where dust flames are stabilised on

burner tubes. There is some evidence to show that particles undergo radial migration in suspensions flowing through tubes, leading to variations in concentration over the cross-section of the flow. TOLLERT²⁰ studied the fall of steel and glass spheres and sand through air and liquids in a tube, and observed the deposition of the solid material at the base of the tube. He found that in most cases the deposition per unit area of the base in the axial region of the tube was considerable higher than the mean value over the whole cross-section; e.g. for steel spheres falling through glycerine in a tube of 3.74 cm diameter, the deposition per unit area in the axial region was 25% greater than the mean value, and for sand in water the corresponding value was about 8%. Tollert considers that velocity gradients in the upward flow of displaced fluid caused rotation of the particles, and that this rotation in conjunction with the relative motion of the fluid and particles gave rise to a Magnus force impelling the particles towards the axis. However, interpretation of his results is^s complicated by the unsteady-state conditions obtaining during the sedimentation, and he did not ensure that the particles were uniformly distributed at the start of their fall.

STARKEY²¹ observed the behaviour of colloidal particles of dye injected into laminar flows of liquid in a tube. He found that the particles migrated towards the axis as they travelled along the tube, and that the rate of migration was a function of particle size.

SEGRE and SILBERBERG²² studied a suspension of perspex spheres, about 1 mm. in diameter, in laminar flow through a tube. The spheres were suspended in a liquid of the same density, and were found to concentrate in an annular region, which had a diameter of about half the tube diameter. OLIVER²³ carried out further experiments on the same system, and showed that the spheres rotated. If prevented from rotating by a slight imbalance, the final position of the spheres was somewhat nearer the tube axis.

The interpretation of these results remains obscure, and much more experimental work is necessary before a clear picture of the behaviour of suspensions in tube flow can be obtained. In particular, further information is required on the effects of particle size, concentration, fluid viscosity, and relative velocity between particles and fluids. The following two points are also important:-

(1) When there is relative motion between particles and fluid in a suspension, two definitions of concentration are possible - termed the 'static' and 'kinetic' concentrations by TAYLOR²⁴. The static concentration, C_s , is defined as the mass of particles in a given volume of the suspension at any instant, and the kinetic concentration C_k is defined as the mass flow-rate of particles through a given area divided by the flowrate of fluid through the same area. For upward flow of the fluid in a vertical tube, if u is the local fluid velocity, and v the relative velocity between the particles,

and the fluid, then

$$C_k = C_s \cdot \left(\frac{u-v}{u} \right)$$

Since the value of u varies over the tube cross-section, the shape of the concentration profile depends on whether the static or kinetic value is chosen. For stationary dust flames, stabilised on tubes, the kinetic value appears to be the more suitable, since it is the ratio of the rates at which dust and air approach the flame front.

(2) In studying the radial migration of particles occurring in tube flow, it is important that entry effects should be clearly distinguished from those effects occurring in fully developed laminar flow. Considering the steady laminar flow of a Newtonian fluid in the entry length of a tube²⁵, as the fluid moves downstream from the entrance the parabolic velocity profile develops, the fluid in the axial region accelerates, and the fluid streamlines converge towards the axis until the flow is fully developed. If particles are present in suspension, the pattern is still similar, and the particles may be expected to converge towards the axis in the entry length, as they follow the fluid streamlines, quite apart from any considerations of the Magnus effect. It is possible that Starkey's results were influenced by such entry effects, as his dye streams were injected only a short distance downstream of the tube entry.

The structure of a dust flame stabilised on a tube is in

part determined by the velocity profile of the suspension flowing in the tube. Velocity profiles in suspensions have been considered theoretically by HAPPEL and BRENNER²⁶. However, their treatment assumes that there is no radial motion of the particles in flow through a tube, and in view of the above discussion, this assumption seems questionable.

(2) Production of Dust Suspensions.

The choice of a method for producing dust suspensions in combustion work depends to some extent on the nature of the combustion to be studied. A review covering most of the techniques which have been used has been made by BROWN AND JAMES²⁷. Since it had been decided to study stationary flames on a burner in the present work, the methods reviewed below are those suitable for continuous production of dust suspensions.

One method used by a number of workers is based on the controlled feeding of dust into a metered air stream; this has been adopted by KAESCHE-KRISCHER and ZEHR²⁸, RAY, BASU and GHOSH²⁹, HATTORI³⁰, and LONG³¹. One difficulty is that of ensuring adequate dispersion of the dust; to overcome this, HATTORI used a cyclone mixer following his screw feed, Ray, Basu and Ghosh mixed their dust and air in a centrifugal blower, and Long fed his dust by a screw feed into the throat of a Venturi through which the air passed.

CASSEL, DAS GUPTA and GURUSWAMY³² prepared dust suspensions by directing air jets on to a layer of dust mounted on a vibrating plate.

Elutriation from a fluidised bed has been used to prepare

dust suspensions for combustion studies by SAKAE, YAGI and DAIZO KUNII³³, and LINE, CLARK and RAHMAN³⁴. The former used a screw feed of coal dust to a fluidised bed, with additional fluidised beds and a cyclone in series to act as stabilisers. Line, Clark and Rahman describe two designs of fluidised bed, both of which were operated on a batch system; i.e. the powder removed from the bed in the suspension was not replaced during operation. KANE, WRIGHT AND SHALE³⁵, in a study of the filtration of dust-laden gases, used a fluidised bed to prepare suspensions. They found that the incorporation of an agitator rotating at 800 to 2000 r.p.m to stir the bed decreased the number of aggregates in the dust suspensions produced.

A comprehensive investigation of elutriation from beds fluidised by air and gases was carried out by HYMAN³⁶, LANG³⁷, and RICHARDS³⁸ in conjunction with one another. They examined the effect on elutriation rates of a number of variables, including gas velocity and density, bed diameter and depth, and outage (i.e. the height of the top of the column above the bed surface). Several materials were used, including glass beads and various catalysts in granular form. The most important results may be summarised as:-

- (i) Elutriation rates decreased exponentially with increase of outage.
- (ii) Elutriation rates increased as a high power of the gas velocity.
- (iii) Elutriation rates decreased with increase of particle size.

- (iv) Elutriation rates were independent of bed depth if this was greater than 4 in. They decreased with reduction of the bed depth below 4 ins.
- (v) The effect of column diameter on elutriation rate varied with the solid material used, but Lang, who used bed diameters from $\frac{3}{4}$ in. to $5\frac{1}{4}$ ins. found the highest rates with the $\frac{3}{4}$ in. bed for his materials.
- (vi) For a fixed outage, the kinetic concentration of the suspension decreased with increase of height above the bed surface.

It was found that the effects of the different variables were not independent of one another, but that the effect of one depended on the values of the others. Lang reported elutriation rates up to 0.84 lbs per ft³ of air; this represents a kinetic concentration of the suspension at the top of the column of approximately 13 g./litre. These high concentrations were obtained at very high air flow rates, with turbulent flow conditions in the column. He mentions that the reproducibility of the measurements was poor, and that elutriation rates for runs carried out under the same conditions could differ by more than 50%.

Although Lang presents correlations expressing elutriation rates in terms of the linear dimensions of the system, the particle size and density, and the gas velocity, these correlations contain constants peculiar to the various materials he used, and therefore cannot be employed to predict elutriation rates from beds of other materials.

THOMAS, GREY & WATKINS³⁹ made a study of the effect of the distribution of particle sizes in fluidised beds. They found that in beds containing particles of two different size ranges, classification took place during fluidisation, resulting in a non-uniform distribution of the different sizes throughout the bed. The fine particles concentrated near the upper surface of the bed, and there was also a variation in fines concentration across the bed; e.g. in one case, at the bottom of the bed, a sample taken from the centre contained 42% of material less than 150 mesh B.S. whilst a sample from the bed wall contained only 16% less than 150 mesh. It seems probable that this variation in size distribution across the bed will lead to similar variations in the suspension above the bed.

(3) Combustion of Dust Suspensions.

²⁷
BROWN & JAMES have given a comprehensive review of the literature on flame propagation in dust suspensions. Work directly relevant to the present study will now be reviewed.

Many experimental coal-dust explosions have been carried out in special galleries or mines in the course of research into mining hazards, notably in France, U.K., U.S.A., and Poland. Owing to the difficulties of securing uniform dust dispersion and making detailed observation of conditions in the highly turbulent flames produced, these explosions have given no information about the flame structure in dust suspensions.

Small-scale work on pulverised fuel firing, e.g. that of ORNING⁴¹, and AUDIBERT⁴², has been carried out to obtain information for the design of industrial furnaces, but this also has given little insight into the mechanism of flame stabilisation and propagation.

Before going on to laboratory studies, the early work of TAFFANEL and DURR⁴³ on flame speed in coal dust suspensions may be mentioned. This is of interest as the only reported case of coal dust/air flames being stabilised without the support of a pilot gas flame or a surrounding furnace. These flames were stabilised in a conical burner lined with refractory; the dust suspension was injected at the narrow end of the cone, 25 cm. in diameter, and the large end open to the atmosphere was 75 cm. in diameter. The suspension was ignited at the open end, and the resulting flames moved slowly towards the narrow end as they heated the burner walls, until they reached positions of equilibrium. The flames were not very steady, and only rough values of flame speeds could be obtained; these lay in the range of 7 to 16 m/sec. DE GREY⁴⁴ later published further values said to be obtained in this investigation, but there is some doubt about the source of these results, as they cannot be traced in the records of Taffanel and Durr's work.

Laboratory studies of the combustion of dust suspensions may be divided into three groups, according to the systems used:-

- (a) Combustion in closed vessels or bombs.
- (b) Flames propagating along tubes or ducts open to the atmosphere.
- (c) Flames stabilised on burners.

(a) Combustion in closed vessels has been extensively used to give indications of the explosion hazards associated with inflammable dusts; the Hartmann⁴⁰ apparatus developed by the U.S. Bureau of Mines is an example of this type. The condition of the dust suspension during the combustion is very complex owing to the non-steady state conditions of heat and mass transfer, and the turbulence produced within the bomb, hence it is difficult to obtain information on flame structure from the results of experiments in such systems.

(b) Many investigators have worked with systems in which flames propagate through dust suspensions contained in tubes since the method was first described in 1875. Most of these workers were interested in measuring limits of inflammability of suspensions, and made no attempt to study flame propagation itself.

CASSEL, DAS GUPTA & GURUSWAMY³² measured flame speeds in suspensions of fine aluminium dust contained in a 1 in. diameter vertical tube, 4 feet in length. The suspensions were ignited at the open top end of the tube, and the flames propagated down towards the closed bottom end. The flame speed was uniform only for the first 20 ins. or so of flame

travel in most cases; beyond this point the flame tended to oscillate. The uniform flame speeds were up to 1 m./sec. When ignition was carried out at the closed end of the tube the flame accelerated up to very high speeds, approaching 300m./sec in some cases. These high velocities were attributed to turbulence arising from bulk flow of the suspension as a result of the release of products of combustion into the confined space between the flame and the closed end of the tube. The use of a 2 in. diameter tube resulted in lower flame speeds, and it was found that the flame speed also varied with the strength of the source of ignition.

KISLIG⁴⁵ also studied flame speeds in suspensions in vertical tubes. He used a tube into which the suspension was fed at the closed lower end, and the top end of the tube was partially obstructed by a filter. Flame speeds up to 16 m./sec. were obtained with suspensions of aluminium flake, but the speeds of the flames fluctuated as they travelled along the tube, and it seems probable that the results were affected by bulk movement of the suspension arising from expansion of the products of combustion into a confined space.

ESSENHIGH & WOODHEAD⁴⁶ measured flame speeds in cork dust clouds, using an apparatus which was designed to minimise the possibility of bulk movement of the suspension. The cork dust fell through a vertical tube 17 feet in length, open at the bottom end. When the suspensions were ignited at the bottom end of the tube, practically uniform flame speeds

were obtained over most of the tube length. Tubes of 2 in. and 3 in. diameter were used, and flame speeds were between 40 cm/sec and 100 cm/sec.

LINE, CLARK & RAHMAN³⁴ have described apparatus for the study of the combustion of dust suspensions in which the suspension can be produced either in a 'wall-confined' or 'wall-free' condition. In the 'wall-confined' condition the suspension flowed down a vertical tube, and in the 'wall-free' state the column of suspension was surrounded by an annular stream of oxidiser gas. LINE, RHODES & GILMER⁴⁷ report details of a study of the spark ignition of lycopodium dust clouds in this apparatus. They found that the minimum spark energy required to produce ignition was strongly dependent on the electrical characteristics of the sparking circuit, and obtained some evidence to show that this resulted from disturbances in the dust cloud produced by the spark.

(c) Several workers have studied dust flames stabilised on small burners with diameters ranging from a few mm. to several cm. The most important points may be summarised as follows.

FUHRMANN & KOTTGEN⁴⁸ stabilised coal dust flames by means of a gas pilot flame, and studied the influence of particle size on the temperature distribution in the flame. They also measured burning times of individual particles in the flame, but LONG³¹ points out that these values are in error, since the expansion of the gases on combustion was neglected in their calculations. KISLIG⁴⁵ extended this work to flames of lignin dust. He reported that flames were not

sufficiently steady to carry out burning velocity measurements.

WOLFHARD & PARKER⁴⁹ and CUEILLERON & SCARTAZZINI⁵⁰ measured the flame temperatures of aluminium and magnesium dust flames by various methods. Scartazzini⁵¹ also carried out similar work with coal dust flames. DE SALINS⁵² studied aluminium dust flames by spectrography.

STUBBS⁵³ stabilised flames in aluminium/air and magnesium/air suspensions, and found that within a range of concentrations the flames were stable without support from a gas pilot. He reported that the flames showed no well-defined inner cone, and hence no burning velocity measurements were made.

Cassel, Das Gupta & Guruswamy³², in addition to their work on flame propagation in tubes, mentioned under (b) above, also measured burning velocities of stationary flames of aluminium and dextrin dusts in air, burning on a 1 in. diameter tube. These flames were similar in appearance to pre-mixed bunsen flames, with a well-defined inner cone. They also exhibited flash-back and blow-off. Burning velocities for a flame of aluminium dust, with particle sizes between 3 and 40 microns, increased from 19.2 cm/sec at a concentration of 120 mg./litre to 23.8 cm/sec at 190 mg./litre. Later work by CASSEL, LIEBMAN & MOCK⁵⁴ on bunsen-type flames of aluminium dust over a wider range of concentrations showed that a reduction in the diameter of the burner tube led to higher burning velocities; a 1.4 cm.

diameter tube gave burning velocities up to 23% higher than the values obtained at the same concentrations on a 1.9 cm. diameter tube. Burning velocities were higher for the finer fractions of the dust. Subsequently flat flames burning on Mache-Hebra nozzles were used, and burning velocity measurements by particle-track photography showed that for flat flames an increase in the flame area resulted in an increase in burning velocity. Using a theoretical analysis of heat flow in the flame, the authors calculated from their experimental data on the relationship of flame area and burning velocity that the ratio of radiation heat transfer to total heat flux was about 0.3 for aluminium/air flames. The corresponding value for graphite flames was 0.6. ORNING⁵⁵ criticised their theoretical analysis on the grounds that the inhomogeneous nature of dust flames was ignored.

⁵⁶
GHOSH, BASU & RAY, using coal-dust suspended in oxygen-enriched air containing 60% oxygen, were able to stabilise flames on burner tubes in the open air without a pilot gas flame. The minimum diameter of burner tube on which a flame could be maintained under these conditions was 1.1 cm. These flames exhibited flash-back and blow-off, but no well-defined inner cone was present, and in some cases the flame-front was flat. The mean velocity of the suspension at the burner mouth was mostly in the range 25 cm/sec. to 45 cm/sec. for stable flames. ORNING⁵⁷ suggested that the flat flame-front observed was due to an increase in the burning velocity at the centre of the flame caused by radiant heat transfer.

LONG³¹ stabilised laminar coal dust flames on a $\frac{5}{8}$ in. diameter burner by using a gas pilot flame, or supporting radiation from a surrounding furnace. Some flames were also stabilised on a downward-pointing Mache-Hebra nozzle. These flames all had well-defined inner cones, although in preliminary experiments flat flame-fronts had been obtained in one or two cases. Burning velocities were measured at dust concentrations from 80 mg./litre to 300 mg./litre for three different fractions of dust, having mass mean sizes of 11μ , 33μ , and 45μ . All three fractions showed an increase of burning velocity with concentration up to concentrations of about 220 mg./litre. For concentrations between 220 mg./litre and 300 mg./litre, burning velocities remained practically constant. The 11μ dust gave the highest burning velocity, which was 18 cm/sec. for flames on an upward pointing burner tube, and 8.5 cm/sec. for flames on a downward-pointing nozzle.

Burning velocity measurements for lycopodium dust flames in the concentration region 180 mg./litre to 500 mg./litre were reported by KAESCHE-KRISCHER & ZEHR²⁸. These flames were stabilised on a 2 cm. diameter tube. They showed a well-marked blue inner cone, and were described by the authors as being very similar to rich hydrocarbon flames. No measurements were made on flames at concentrations below 180 mg./litre as these were found to be very unsteady, and did not show a coherent flame-front. The suspension was produced simply by a screw feeding the lycopodium into the bottom of the long

²⁸ The symbol μ is used for microns. $1\mu = 10^{-6}$ m.

burner tube, so poor uniformity of the suspension might have been responsible for the unsteadiness. The burning velocity was found to be approximately constant at 25 cm/sec. from 180 mg./litre to 400 mg./litre, and then dropped to a value of 16 cm/sec at 500 mg./litre, the highest concentration at which measurements were made.

One interesting point emerging from this review of the literature on laminar dust flames is the variation in the shape of the flame. Whereas Long's coal-dust flames had a conical flame-front, including those stabilised on a nozzle, most of the flames observed by Ghosh, Basu & Ray had flat flame-fronts, or showed no well-defined cone. Stubbs reported aluminium and magnesium dust flames as having no well-defined inner cone, but the aluminium dust flames stabilised by Cassel, das ^G Gupta and Guruswamy, and Cassel Liebman and Mock had clearly defined inner cones.

The stability of flames on burners depends to a considerable extent on the flow conditions at the burner mouth, and it is possible that concentration variations arise in the suspensions as a result of flow through burner tubes or nozzles. Of the investigators mentioned above, only Cassel, Liebman and Mock attempted to study the flow conditions of the suspension approaching a flame-front.

From the work of Cassel, Liebman and Mock, it appears that radiant heat transfer is important in some dust flames. In the conditions prevailing in dust flames, radiation transfer is effective over much longer distances than

convection, and hence the quenching effect of tube walls is likely to be important over longer distances than in gas flames. This may be the reason why it has been found impossible to stabilise unsupported dust flames on tubes smaller than about 1 cm. diameter.

It has frequently been accepted that the burning time of particles in dust flames is controlled by oxygen diffusion, but BEER & ESSENHIGH⁵⁸ have suggested that under the conditions prevailing in coal dust flames, the rate of reaction of the coal particles is also important.

CHAPTER 2.

Development of the Apparatus.

From the study of the literature on the preparation of dust suspensions mentioned in Chapter 1, it appeared that elutriation from a fluidised bed was a promising method of preparation. In comparison with the other methods mentioned elutriation has the following advantages:-

1. The apparatus is simple and compact.
2. It can be used for a wide variety of dusts, including some which are otherwise difficult to handle, e.g. KANE, WRIGHT AND SHALE³⁵ using this method readily produced suspensions from an air-cleaner test dust specially chosen for its difficult handling properties.
3. It is capable of producing suspensions over a wide range of concentrations, from very low values up to 13 g/litre as shown by Lang's work. (page 22.)
4. Its use avoids the difficulties caused by dust sticking in hoppers which occur with some other dispersion systems, e.g. that described by Long.

In a batch-fluidised bed, the rate of elutriation drops as material is removed from the bed, but it was considered that by the use of relatively deep beds the rate of decrease could be made quite small. Experiments were carried out to develop a suitable fluidised bed apparatus for producing dust suspensions and burning them.

Experimental work on elutriation.

If a fluidised bed contains a range of particle sizes,

the finer material is preferentially elutriated, and the particle size distribution in the bed changes continuously during fluidisation. In these circumstances it is necessary to carry out particle size analyses, and in order to avoid these, lycopodium powder was used for the initial experiments. Lycopodium powder has a practically uniform particle size of about 30 microns.

Lycopodium was fluidised with air in the apparatus shown in fig. 1. This consisted of a Gooch crucible diameter 4 cm. with a fritted glass filter of porosity No.2., extended by means of a glass tube of the same internal diameter. The depth of the bed of lycopodium before fluidising was roughly equal to its diameter. As the air flow rate was gradually increased from zero by opening valve C, the bed expanded, and began to fluidise. When the mean air velocity through the bed reached about 1 cm/sec., a few particles could be seen passing out of the top of the tube at A. As the velocity was further increased, fluidisation became more vigorous, and greater numbers of particles were carried out of the bed, until the tube was filled with a column of dense suspension which slowly 'poured' over its rim, and fell through the surrounding air. With mean air velocities above about 2 cm/sec., three regions could be distinguished in the tube - the dense phase (i.e. the fluidised bed itself), the transition region, and the disperse phase (fig. 1.) The upper surface of the bed 'boiled' violently, and masses of powder were constantly being projected from

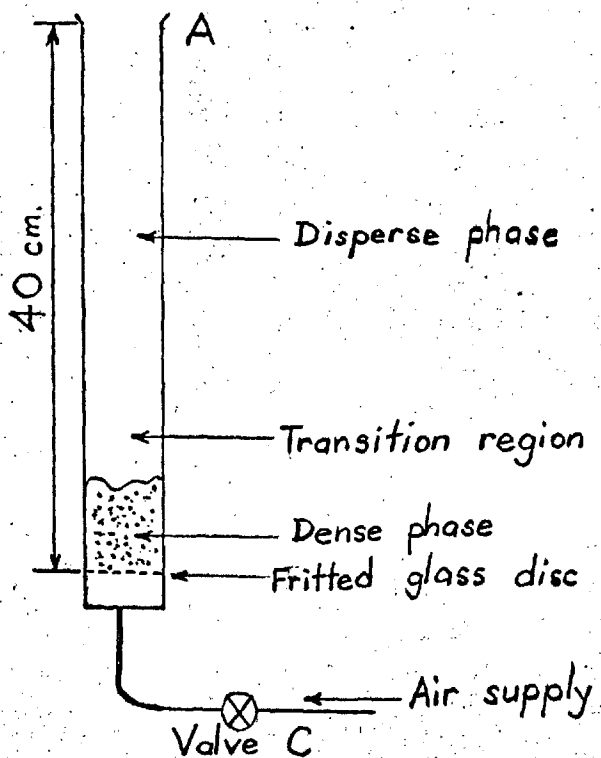


Fig. 1 Fluidised bed

different points on it into the transition region. Most of the lycopodium in these masses fell back immediately into the bed. In the transition region, therefore, the concentration of the suspension varied widely, the particles moved in an erratic manner, and large eddies could be seen. In the disperse phase region the eddies had died out, the concentration of the suspension appeared quite uniform to the eye, and the great majority of the particles moved steadily upwards along straight paths. However, some particles could be seen moving down the tube. When a small gas flame was applied to the top of the tube, the suspension ignited, and a flame propagated down the tube.

This simple experiment showed that suspensions in the inflammable range of concentration could be produced with air velocities sufficiently low for the flow to be well in the laminar regime. Under these conditions the transition zone, above which the suspension reached a steady concentration, was only a few centimetres in depth. Although the work on elutriation mentioned in the literature survey indicates broadly the effects of bed dimensions and fluidising flowrates on the elutriation rate, Lang emphasises that these effects are inter-related in a complex manner, the effect of one variable depending on the values of the others, so that experimental results cannot be reliably extrapolated. It was therefore necessary to make some measurements of elutriation rates from fluidised beds of lycopodium, and the apparatus shown in fig. 2 was

constructed for this purpose.

The fluidised bed rested on a fritted glass plate, porosity No. 1, (Gallenkamp), 65 mm. in diameter. The free-board above the bed (i.e. the distance between the top surface of the bed and the collecting funnel) could be varied by moving the funnel along the glass tube. A rubber washer sealed to the rim of the funnel with 'Bostick C' adhesive provided an air-tight seal between the funnel and the tube. The suspension produced passed through a $\frac{1}{4}$ inch rubber delivery tube fitted inside the brass tube supporting the funnel. The air velocity in the delivery tube was sufficiently high to prevent any accumulation of powder on its walls during operation of the bed. The upper end of the tube was connected to a glass cyclone, which collected the powder carried over. The overall length and weight of the collecting cyclone were limited by the necessity of weighing it on an analytical balance, so it was not possible to make it of the proportions recommended for the highest collection efficiency. However, it was found that in operation very few particles escaped into the outlet pipe, and these were retained by a plug of glass wool at the top of the latter. The compressed air supply to the bed was filtered through cotton wool to remove dust and oil, and the moisture content increased, if desired, by passing part of it through a wash-bottle. Alternatively, the moisture content could be reduced by passing part of the flow through a drying tower filled with anhydrous calcium chloride.

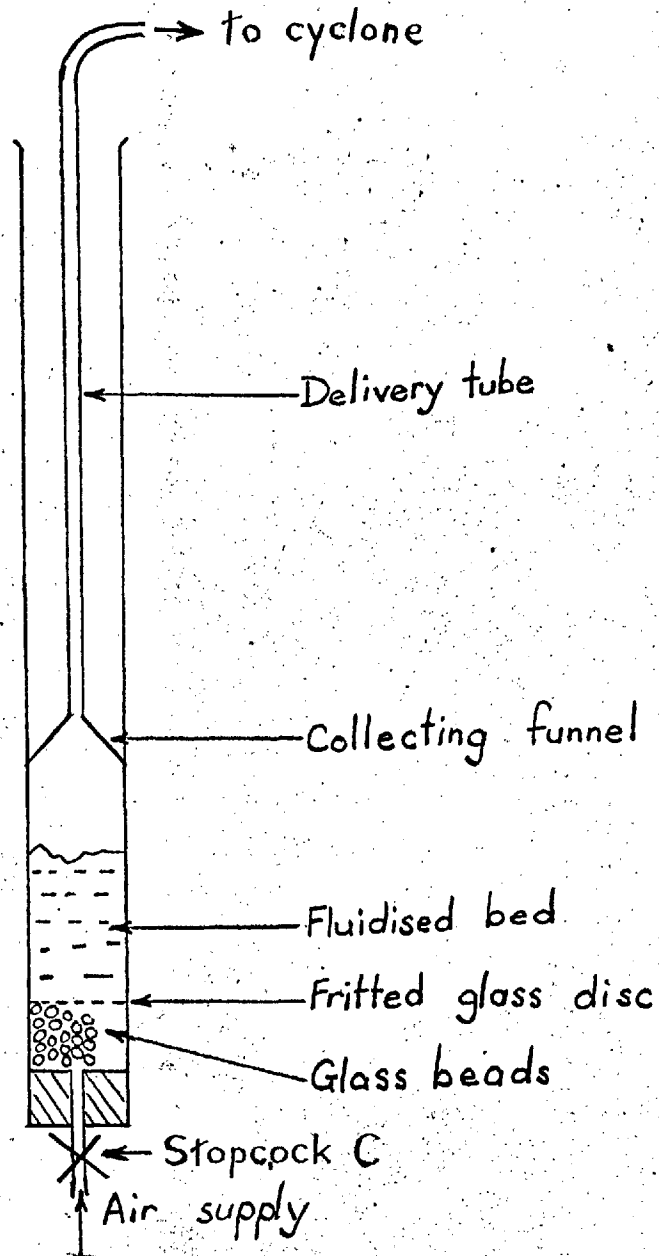


Fig. 2 Measurement of elutriation rate.

The humidity of the air supplied to the bed was measured before each run by passing it through a wet-and-dry bulb hygrometer.

The method of operation was as follows. The air flows were adjusted ~~by valves A and B (fig. 2)~~ to give the required relative humidity and fluidising flowrate, and then stop-cock C was closed, cutting off the air supply to the bed. The cyclone was emptied, weighed and replaced in the apparatus, then stop-cock C was opened, and fluidisation commenced. After a measured time interval, the stop-cock was closed again, and the cyclone was weighed to find the amount of lycopodium elutriated from the bed during the period of fluidisation. The fluidisation procedure was repeated several times at regular intervals under the same conditions, and for the same lengths of time. A typical run consisted of six one-minute periods of fluidisation at 5 minute intervals. Since the volume of the air in the tubing between the stop-cock and the bed was small, the flow rose quickly to the operating value when the cock was opened, and fell quickly to zero when it was closed. Runs were carried out with several different values of air flowrate and air humidity, and with the collecting funnel at different heights above the bed. The depth of the bed when fluidised varied from 5.5 in. to 7.2 in. The most important features of the results were as follows:-

1. Three levels of air relative humidity were used, 23%, 45% and 56%. In all the runs carried out using air

with relative humidities of 23% and 45% the elutriation rate decreased in a roughly exponential manner during the run, as shown in fig. 3a. In some of the runs at relative humidities of 56%, the elutriation rate remained roughly constant for some time, or increased slightly after the initial fall. (fig. 3b.)

2. Microscopic examination of lycopodium samples taken from the cyclone and from the bed after fluidisation showed no obvious difference in particle size between them. This eliminated the possibility that the elutriated material consisted of particles smaller than the mean size of the powder, or of fragments of broken spores.
3. Since the reproducibility between runs carried out under similar conditions was poor, and the amount of lycopodium in the bed could not be controlled accurately, no conclusion could be drawn about the effect of free-board above the bed on the elutriation rate. Lang, in his study of entrainment from fluidised beds, reports similar lack of reproducibility of elutriation rates. He found that elutriation rates from beds of glass beads and cracking catalyst fluidised under similar conditions could differ by 50% or more.

Stabilisation of flames.

Following the measurements of entrainment rates described above, the conditions required to stabilise dust flames were investigated. For this purpose, the collecting cyclone was removed, and various burners were attached to the

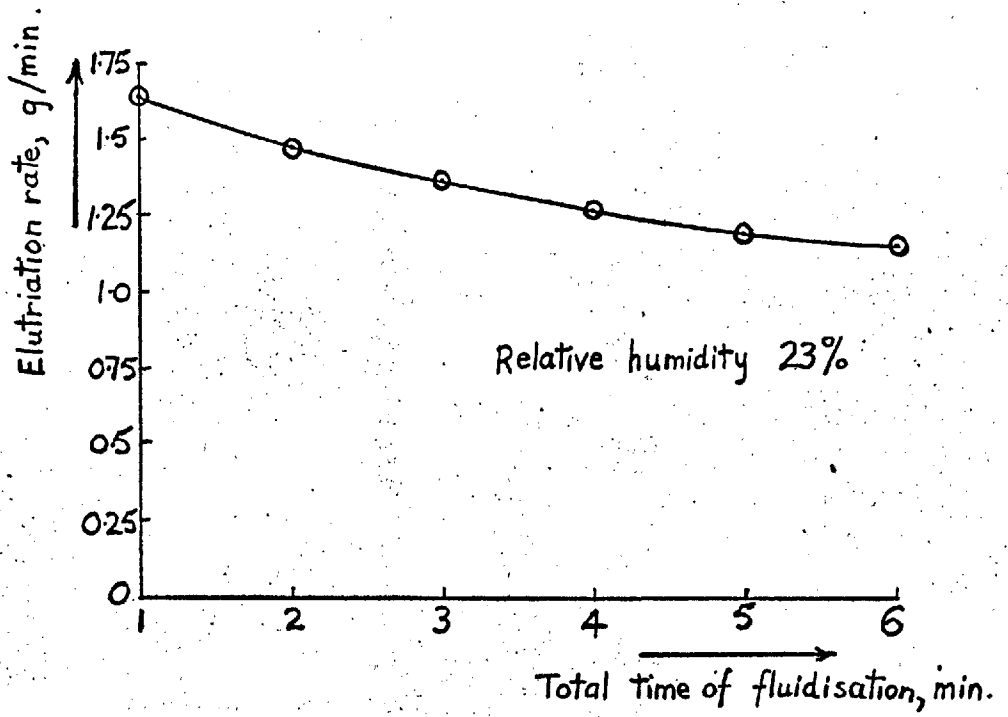


Fig. 3(a)

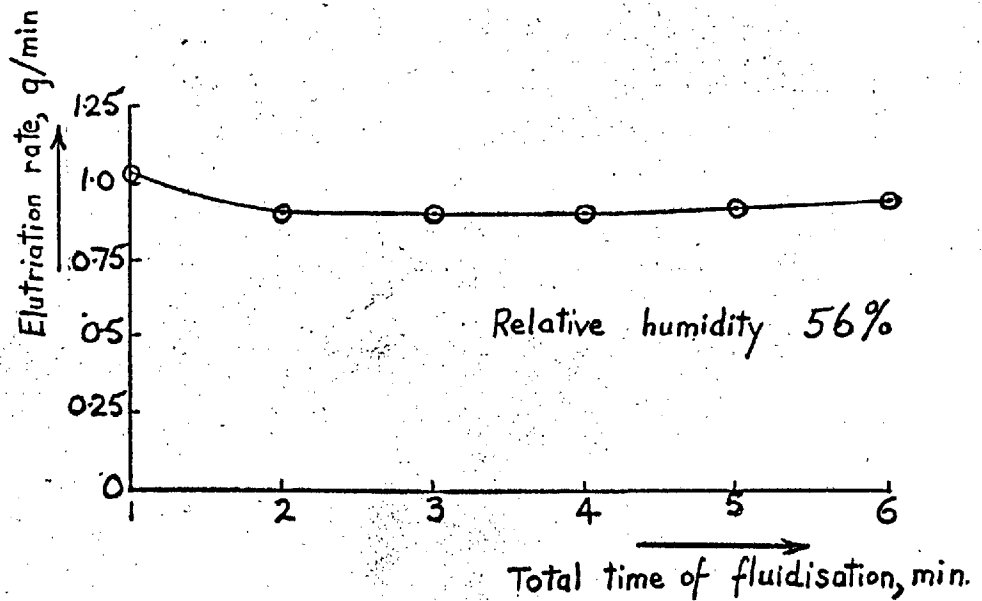


Fig. 3(b)

Fig. 3 Variation of elutriation rate with time.

delivery tube.

(i) The first arrangement used was based on a suggestion of Essenhigh, and is shown in fig. 4a. In principle it resembles the dispersion section of a Gonell elutriator. The cone was made of tin-plate, and its small end was closed by a rubber bung. The lycopodium suspension was fed into the burner along the axial tube A, which was attached to the delivery tube of the fluidised bed apparatus. Attempts were made to ignite the suspension in the cone with a bunsen flame, but no stable flame could be obtained with any of the flowrates and concentrations used. Large deposits of lycopodium accumulated on the walls of the cone at the narrow end.

(ii) The burner used in (i) was inverted, but it still failed to give any stable flame.

(iii) The tin cone used in (i) and (ii) was attached directly to the suspension delivery tube to act as a diffuser, and a gas pilot flame was fixed on its axis, as in fig. 4b. Stable flames were obtained at high flow rates and concentrations, but these were low down in the throat of the cone, and were turbulent in structure. They continued to burn after the pilot flame was turned off.

(iv) Attempts were made to stabilise flames on cylindrical burner tubes of various diameters between 1.5 cm. and 3 cm. These tubes were connected to the suspension delivery tube by conical diffusing sections made of stiff paper, and sealed with cellulose adhesive tape. (fig. 4c).

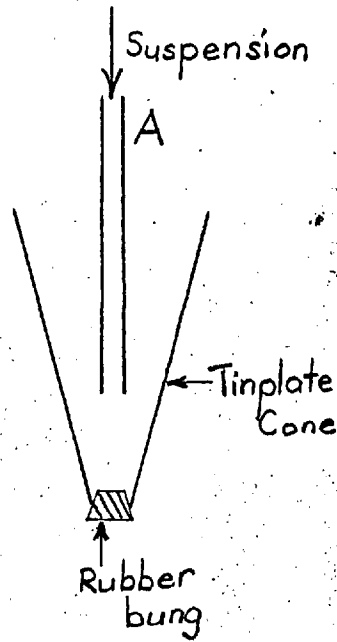


Fig. 4(a)

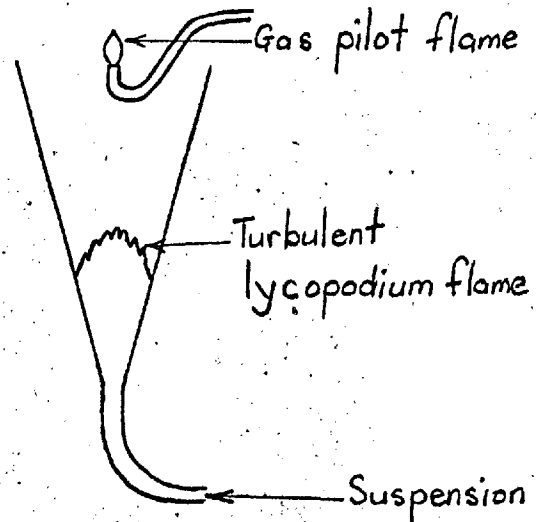


Fig 4 (b)

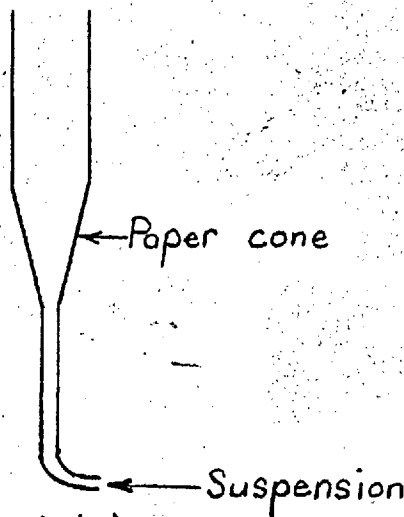


Fig. 4 (c)

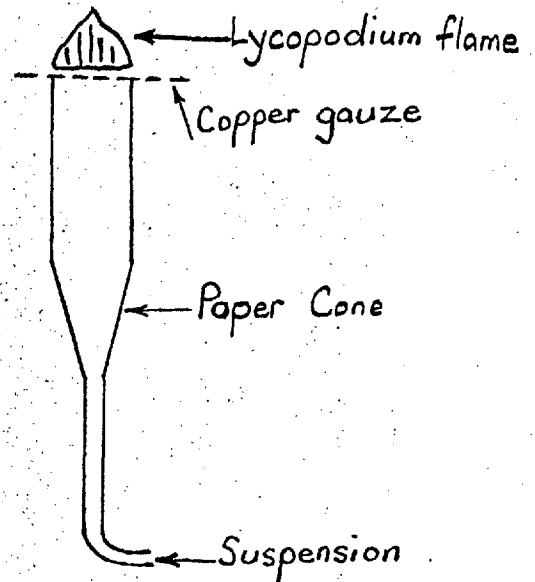


Fig. 4(d)

Fig. 4 Burners.

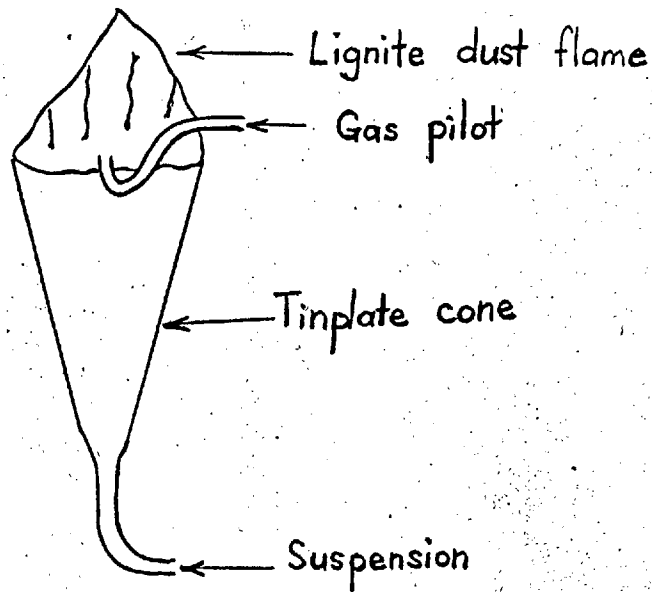
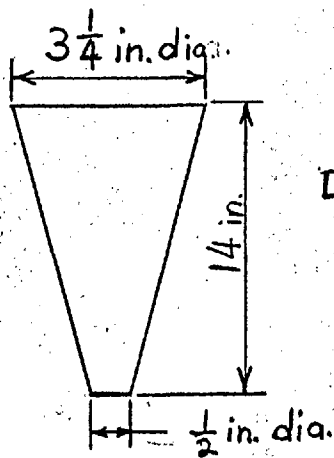


Fig. 4(e)



Dimensions of Tinplate cone
shown in Figs 4(a), 4(b), 4(e).

Fig. 4 (Continued)

Laminar flames could be stabilised with some difficulty on the smaller diameter tubes, but not on the larger ones. However, when pieces of copper gauze were placed over the tops of the tubes, stable flames were readily obtained in all cases. (fig 4d)

These experiments on flame stability were all repeated using a lignite dust in place of lycopodium. The behaviour of the lignite suspensions was similar to that of lycopodium except in the case of apparatus (iii). In this apparatus, stable laminar flames of lignite dust were obtained, burning near the top of the cone (fig.4e). These flames continued to burn when the pilot flame was turned off. They were of a dusky red colour, and the flame-front was practically flat. The tracks of individual burning particles were clearly visible within the flame envelope. The overall burning velocity of a typical flame was about 10 cm/sec.

Further experiments on the stabilisation of dust flames by gauzes were carried out using the apparatus shown in fig.5. Various dusts were fluidised in the Gooch crucible, the top of which was covered by a piece of 40-mesh copper gauze. When lycopodium was fluidised in this apparatus, a flame could readily be stabilised above the gauze as shown. At low velocities and concentrations the flame-front was about 1 mm. above the upper surface of the gauze, but as the fluidising velocity and concentration were increased, the flame-front moved further from the gauze. The 40-mesh

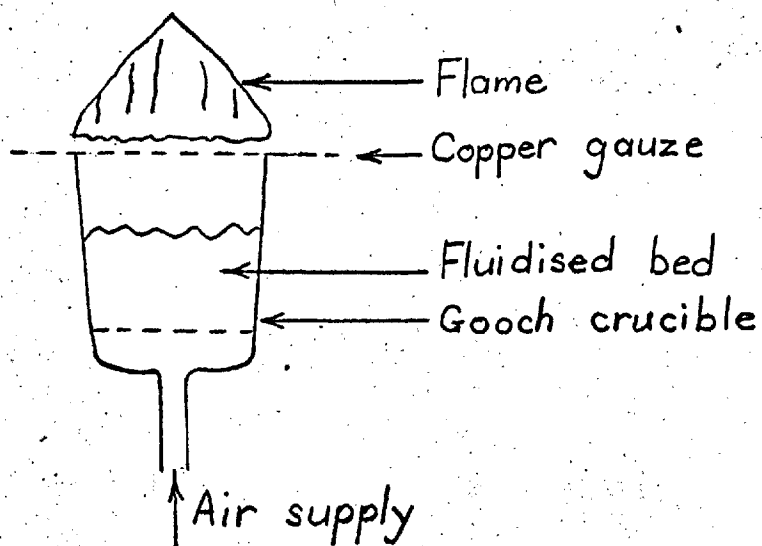


Fig. 5. Flames stabilised on Gooch crucible

gauze was replaced by a perforated zinc sheet, with perforations 2 mm. in diameter, which was also found to stabilise the flame. When a sample of South Devon lignite, supplied as large lumps, was ground in a hammer mill and then fluidised in this apparatus, no ignition could be obtained, but after the ground material had been allowed to dry under ambient conditions in the laboratory for a few days, ignition was readily obtained. The stable flame produced above the perforated zinc sheet was dark red in colour, and similar in shape to the lycopodium flames. A sample of a Chinese low-rank bituminous coal showed similar behaviour; whilst no ignition could be obtained with a freshly ground sample, after prolonged air-drying the coal gave a stable flame above the perforated zinc sheet. These experiments showed that under suitable conditions, flames of lignite dust and low rank coal dust in air can be stabilised without the use of a gas pilot flame or supporting radiation from a furnace. The only case reported in the literature of coal dust flames stabilised without the use of a pilot gas flame or supporting radiation is that given by Taffanel & Durr. (see p.24)

As a result of the experiments on flame stabilisation, it was decided that the large fluidised bed apparatus used for elutriation rate measurements was too inflexible and cumbersome for work with flames. With this apparatus, the concentration of the suspension produced could be varied by changing:- (a) the air flow rate, (b) the amount of powder

in the bed, or (c) the height of the collecting funnel above the bed. Of these, only alternative (a) offered a convenient means of control, since it was necessary to stop fluidisation before changing (b) or (c). Since the whole of the suspension produced in the bed passed to the burner, changing the concentration by alteration of the air flowrate involved a change in the velocity of the suspension at the burner, with the result that concentration and velocity could not be varied independently. It was also felt that the narrow-bore suspension delivery tube was an undesirable feature, since the highly turbulent flow within it might cause agglomeration of particles in the suspension, and also there was a tendency for particles to accumulate on the walls of the conical diffusing sections which were attached to the end of the delivery tube. A modified system for the production of the suspension was therefore investigated.

Modified Dispersion System.

The suspension was produced in a fluidised bed as before, but a diverging section was provided above the bed, in which the mean upward velocity of the suspension was reduced to a value below the settling speed of lycopodium particles. By this means the suspension was contained within the diverging section, which acted as a reservoir for the suspension. A new apparatus was constructed to investigate the behaviour of a

suspension in such a system.

The apparatus, shown in fig. 6a, consisted of a Gooch crucible, with a fritted glass filter of porosity No.3 (Callenkamp), extended by a short piece of glass tubing 4.6 cm. internal diameter, and a conical diverging section fitted to the top of the glass tube. The joints between the Gooch crucible, the glass tube and the diverging section were made airtight. The lycopodium was fluidised by air of controlled humidity, supplied by the flow system shown in fig 6b. The glass sampling tube, 1.02 cm. bore, was clamped vertically on the axis of the conical section. The sampling system is shown in fig.7. The flow of suspension induced by the 'Dymek' diaphragm pump passed through the Millipore filter unit, which collected the lycopodium particles. The Aerosol Assay type Millipore filter membrane was used, which has pores less than 1 micron in diameter. Since lycopodium particles are in the size range 30μ to 35μ effectively all the particles in suspension were collected by the filter. The sampling tube was connected to the filter unit by a short length of 1 mm. bore plastic tubing. Under all the sampling conditions used, the flow velocity through the plastic tubing was sufficiently high to prevent any deposition of particles inside it. The metal filter holder was of a type developed by the Chemical Defence Experimental Establishment, Porton. The arrangement of the filter holder and tubing is shown

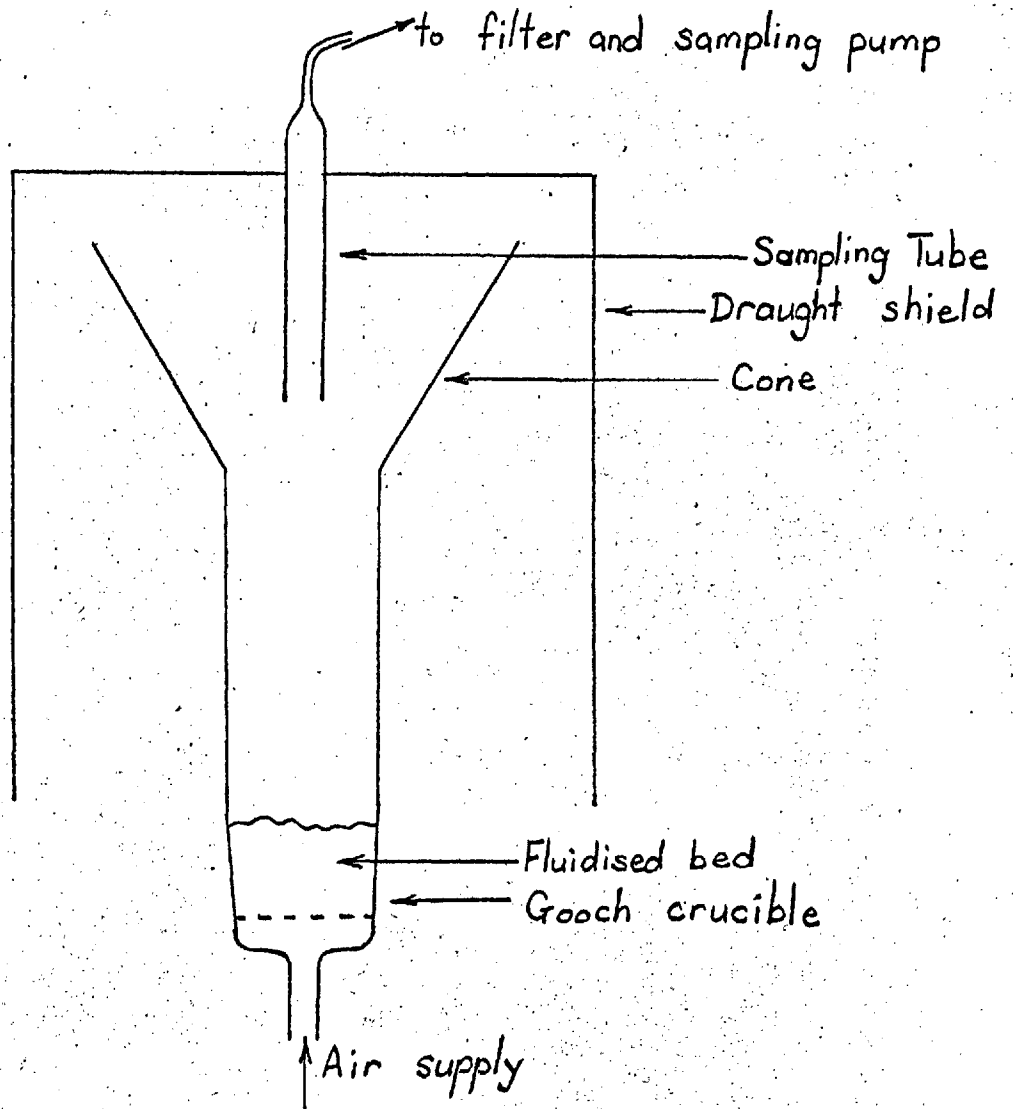


Fig. 6(a) Dispersion Apparatus

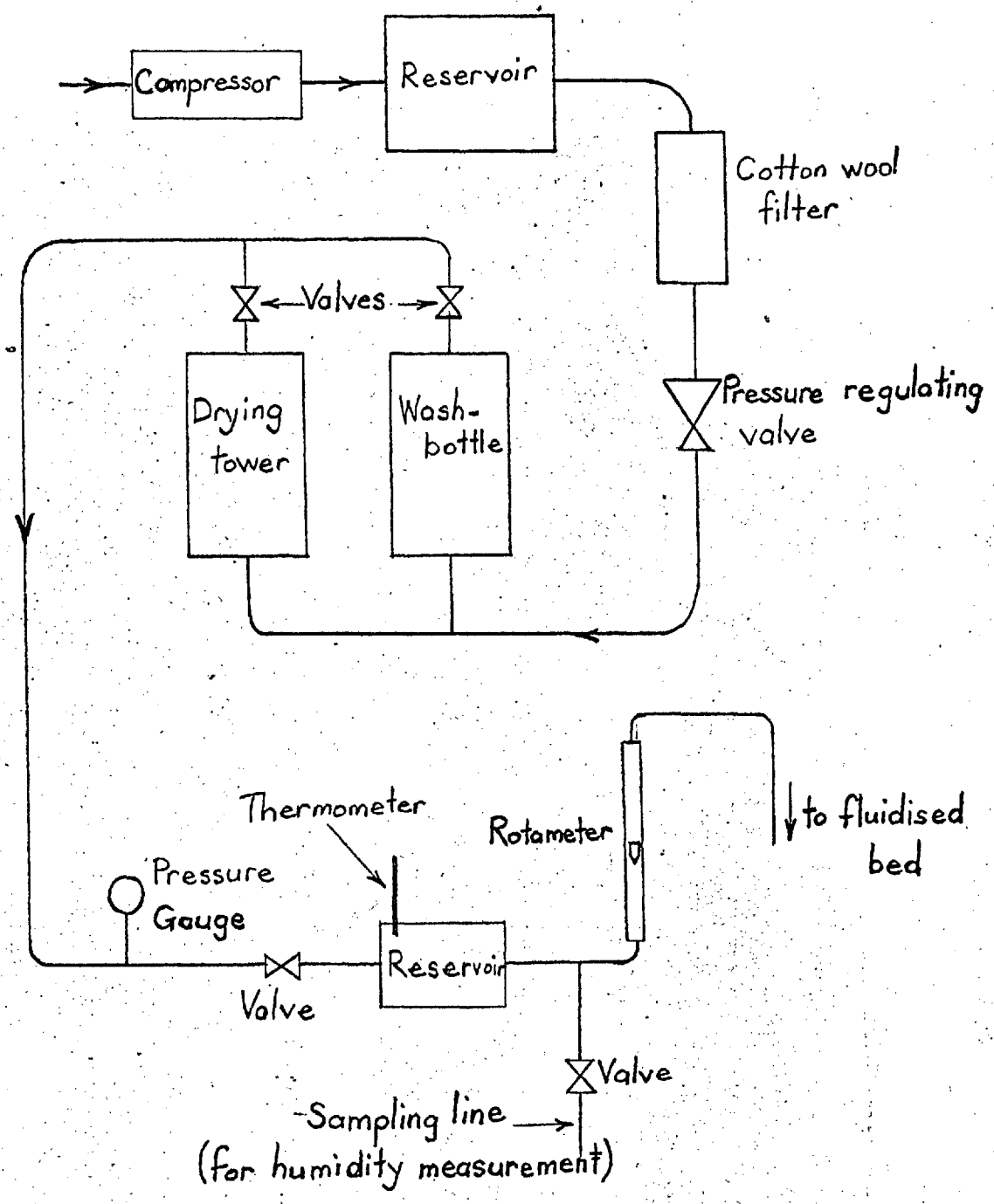


Fig. 6b Air Flow System

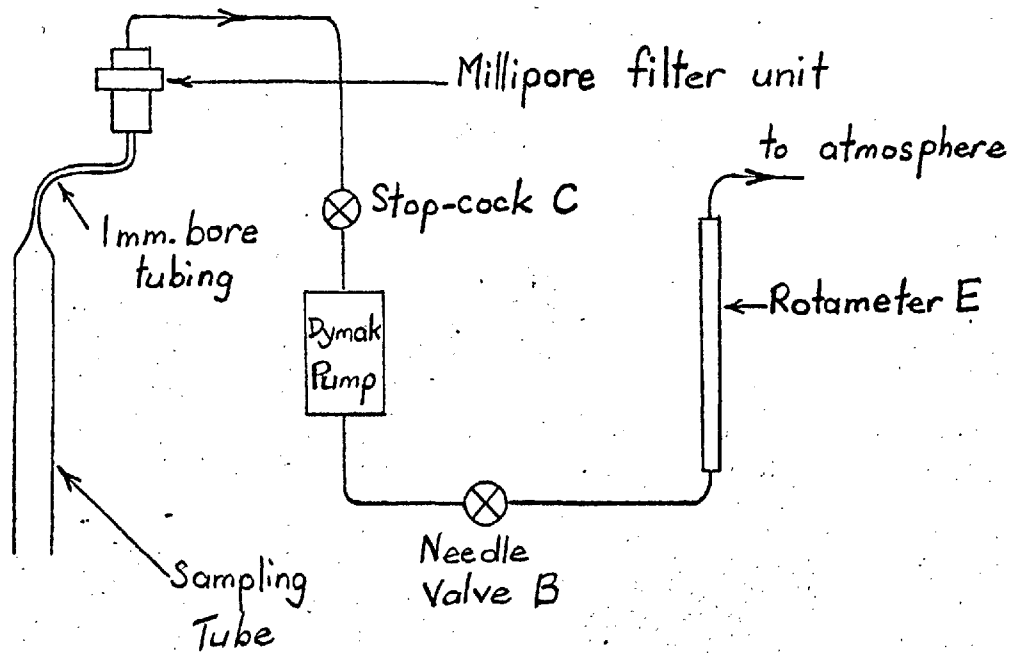


Fig. 7(a) Sampling System

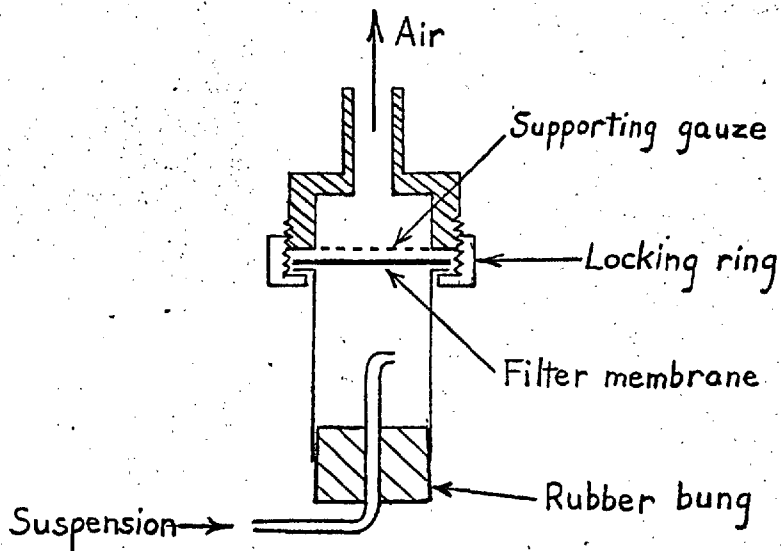


Fig. 7(b) Millipore Filter Holder

in fig. 7b. It was found that up to 1 g. of lycopodium could be collected in the filter unit without affecting the sampling flow through it. The sampling flowrate was controlled by needle valve B, and measured by either a rotameter or a soap-film meter at E. The quantity of lycopodium collected was found by detaching and weighing the filter holder. The draught shield was constructed of tin-plate, and provided with a Perspex top, which permitted observation of the flow pattern in the cone. The cone was at first made of stiff paper, so that its proportions could easily be changed, if necessary. Its greatest diameter was made large enough for the mean velocity of the air at this section to be well below the settling velocity of lycopodium particles, so that most of the particles elutriated from the bed did not pass out of the top of the cone. The radial velocity component of the air in the cone carried the particles outwards until they were deposited on the sides of the cone, where they accumulated and slid back into the bed. The air flowing out of the top of the cone was almost dust-free.

Under these conditions, the suspension contained within the cone was in a state of dynamic equilibrium; the powder removed from suspension by settling out on the walls of the cone was replaced by fresh material coming up from the bed. Since the material deposited on the walls eventually slid back into the bed, the rate of loss of powder from the system was very small, and the

conditions of fluidisation remained practically constant over a long period. The direction of particle flow in the cone could be observed through the Perspex top of the draught shield under a strong light. Fig. 8 indicates the basic flow pattern at zero sampling flow.

With about 10 g. of lycopodium in the bed, and fluidising velocities below 10 cm/sec., the transition region above the bed did not extend into the conical section, and the flow within the cone itself was steady with time. If the fluidisation velocity was increased above this value, eddies from the transition region penetrated into the cone.

The characteristics of this system were investigated by fluidising the bed continuously for periods up to 2 hours, and withdrawing samples of the suspension through the sampling tube at intervals. The fluidising velocities used were kept below 7 cm/sec., to ensure steady flow conditions at the entry to the sampling tube. The bed was charged with fresh lycopodium for each run.

First, a constant sampling flowrate was used. Before taking a sample, the filter holder was detached from the apparatus, emptied if necessary, and weighed on an analytical balance to the nearest 0.001 g. It was then replaced in the system, and the sampling pump was switched on, but stop-cock C was left in the closed position. After about one minute's delay, to allow the pump to reach its normal operating speed, the stop-cock

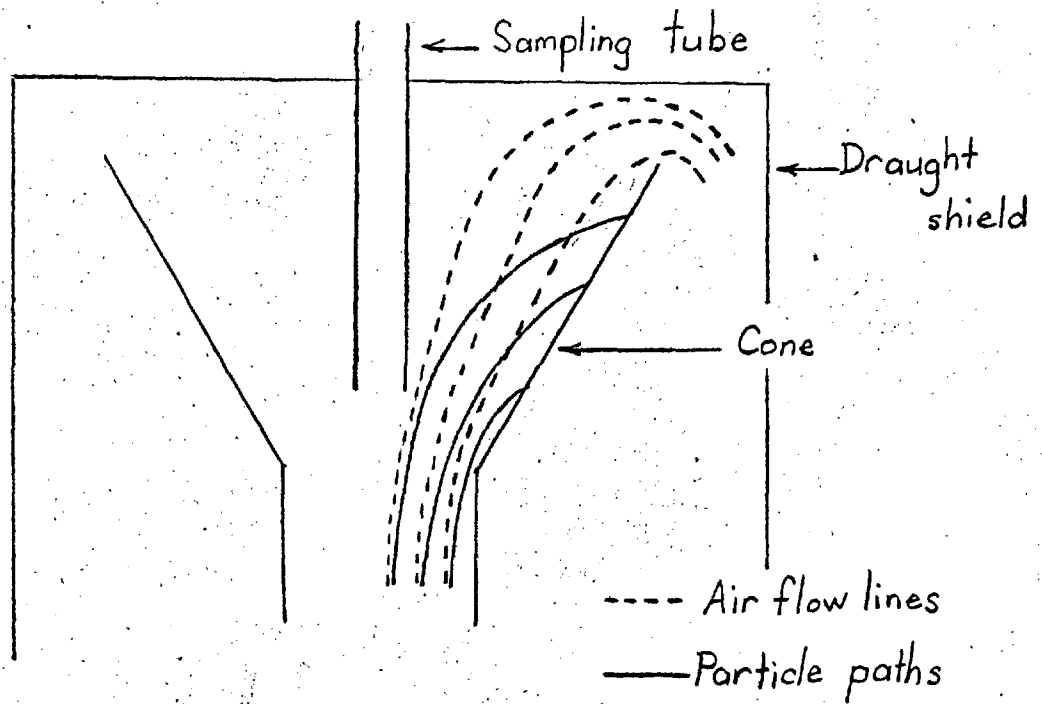


Fig. 8. Flow pattern inside cone (zero sampling flow)

was opened, allowing the pump to withdraw a sample at a steady rate indicated by the rotameter. After a measured time interval, the stop-cock was closed again, the pump switched off, and the filter holder detached and weighed. This sampling procedure was repeated at intervals of a few minutes whilst fluidisation continued.

By varying the sampling time in half-minute steps from $\frac{1}{2}$ min. to $2\frac{1}{2}$ min. at constant sampling flowrate, it was found that the weight of lycopodium collected per unit time was independent of the sampling time; this showed that end effects in sampling were negligible for times of $\frac{1}{2}$ min. or over. In all subsequent runs, sampling times were $\frac{1}{2}$ min. or longer.

Fig. 9 shows the results of two runs, Nos. 22 and 23, carried out under similar conditions. (Fluidising flow rotameter reading 4.5 litres/min., sampling flow-rate 0.63 litres/min.) In each case the bed was initially charged with 7.23 g. of lycopodium taken from the same supply bottle, and the relative humidity of the fluidising air was 40%. The graph shows the rate of collection of lycopodium in the sampling filter plotted against the time from the commencement of fluidisation. Fig. 10 shows the results for two runs carried out using the same fluidising and sampling flows as Nos. 22 and 23, but with air of 68% relative humidity. Since the sampling flow rate was constant throughout, the rate of collection of lycopodium in the filter was proportional

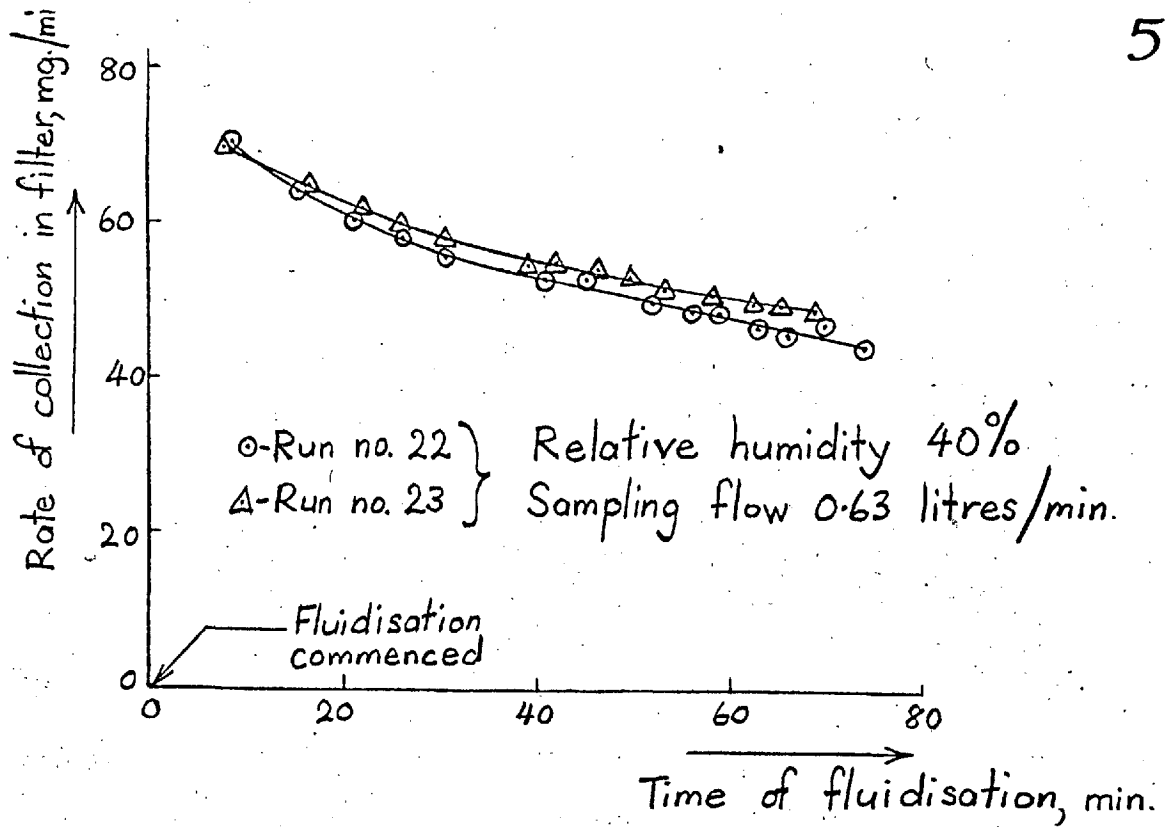


Fig. 9. Variation of Concentration with time, relative humidity 40%

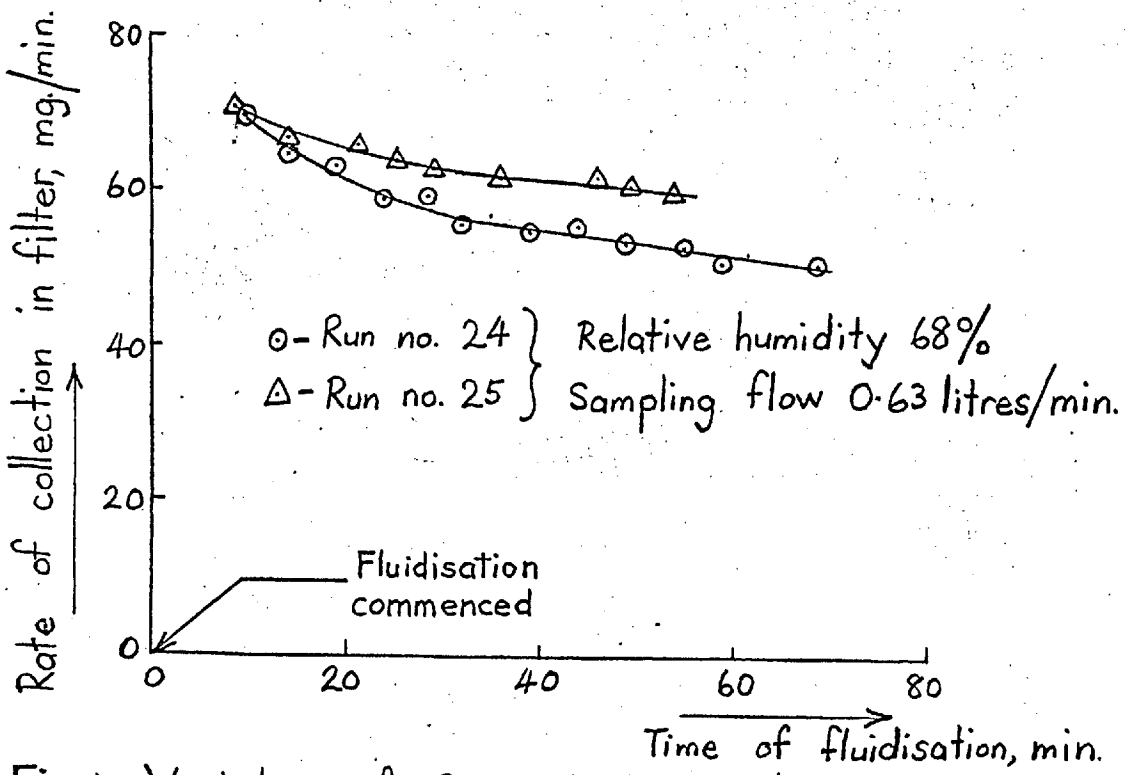


Fig. 10. Variation of Concentration with time, relative humidity 68%

to the kinetic concentration of the suspension flowing up the sampling tube. The local kinetic concentration, C_k , at any level in the tube will vary over the tube cross-section, since it is a function of the local air velocity, (see the definition of kinetic and static concentrations on p.19.) This point will be discussed further later on. If W is the rate of collection of lycopodium in the filter (in mg/min.) and the sampling flow rate is q (litres/min.) then $\frac{W}{q}$ (mg/litre) is the mean value of C_k taken over the whole tube cross-section. This mean value of C_k will be denoted by \bar{C}_k .

The four runs given in figs. 9 and 10 all indicated a rapid fall in \bar{C}_k at the beginning of the run, followed by a more gradual decrease. The curves were similar in form to those obtained with the previous fluidised bed apparatus, (fig. 3.)

It was suggested that this decrease in concentration of the suspension with time could be due to the accumulation of static charges on the particles during fluidisation, and that these charges might be reduced by earthing the bed. One run was therefore carried out with a loop of copper wire immersed in the bed, and during part of the run the loop was earthed. The earthing of the wire had no effect on the behaviour of the system.

Since the paper cone gave a stable region of suspension as originally intended, it was now replaced

by a tin-plate cone made to the same dimensions. The joint between the glass tube and the cone was made air-tight with sealing compound. A circle of 8-mesh copper gauze was placed horizontally in the cone, close to the lower end. (fig. 11.) This gauze was intended to damp out local fluctuations in the motion of the suspension caused by eddies originating in the transition zone above the bed. Observation of the particle motion in the cone confirmed that the gauze was very effective in improving the stability of the suspension, and that it largely suppressed the irregular eddies which otherwise penetrated into the cone at the higher fluidising velocities.

The highest values of \bar{C}_k so far obtained were of the order of 130 mg./litre, which corresponds approximately to the stoichiometric mixture for lycopodium/air flames. These concentrations were obtained in the initial stages of runs, and were only maintained for periods of a minute or so. In an attempt to produce higher concentrations, and to maintain them for longer periods, a series of runs was carried out using deeper beds, and relative humidities higher than most of those used previously. It was found that if the bed was initially charged with about 12g. of lycopodium, and fluidised with air of about 70% relative humidity, the concentration of the suspension increased with time at the beginning of a run, instead of decreasing as in the previous

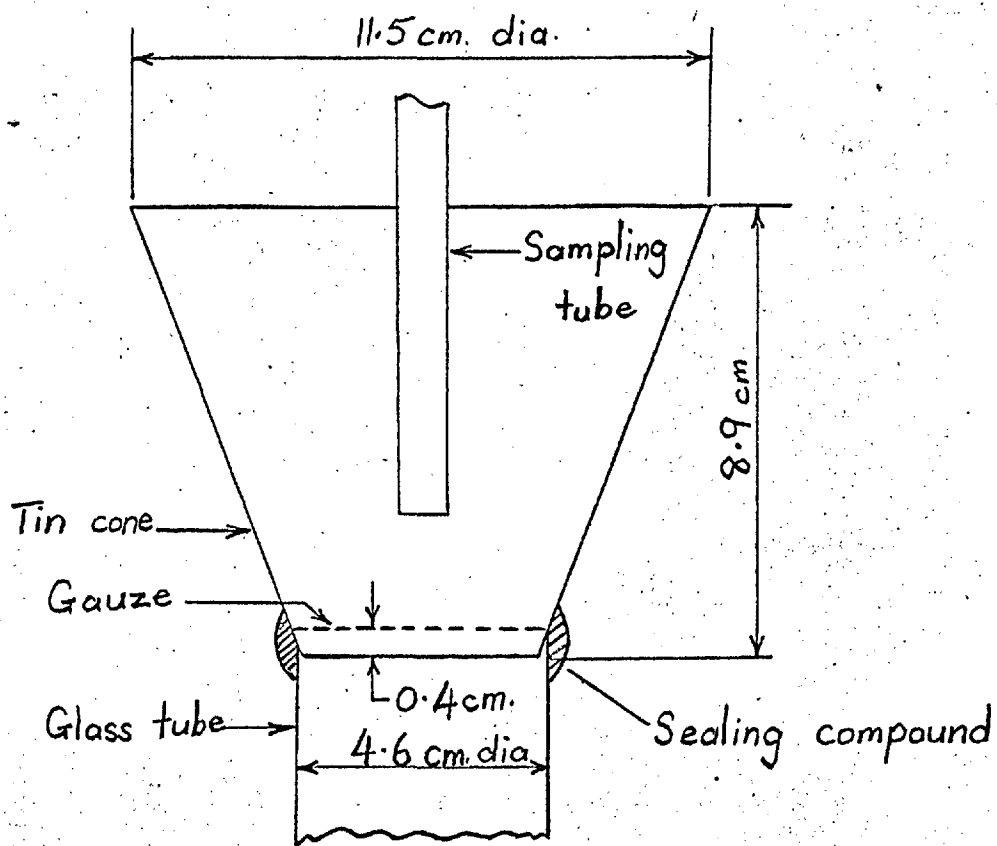


Fig. 11. Dimensions of Tinplate Cone

series of runs. A typical result for fluidisation under these conditions is shown in fig.12, which gives the variation of \bar{C}_k with time for run No. 29. (fluidising flow rotameter reading 4.5 litres/min, sampling flowrate $0.6\frac{4}{3}$ litres/min.) The bed depth was initially 11.53 g., and the fluidising air relative humidity was 70%. The curve for run No.29, after the initial rise, remained between 105 mg/litre and 110 mg./litre for a period of about one hour. The particle flow in the cone was steady under these conditions.

The type of behaviour shown by run No. 29 was much more promising than that exemplified by run No. 22, since in the former the concentration remained practically steady at the maximum value for a considerable period of time, long enough to give opportunity for a series of observations to be carried out at practically constant concentration. All subsequent experiments were therefore carried out with bed depths and relative humidities similar to that of run No. 29. It was found that under these conditions the moisture content of the lycopodium changed during fluidisation. Samples taken from the bed at the ends of runs and dried by prolonged exposure to silica gel in a desiccator showed a loss in weight of about 5%, compared with 3.5% for the lycopodium as supplied. Samples taken at the end of runs carried out under the conditions used previously (i.e. bed depths initially 7.23g., relative humidities 68% or less) showed no significant change in moisture content as a result of fluidisation.

The effect of variation in the height of the sampling

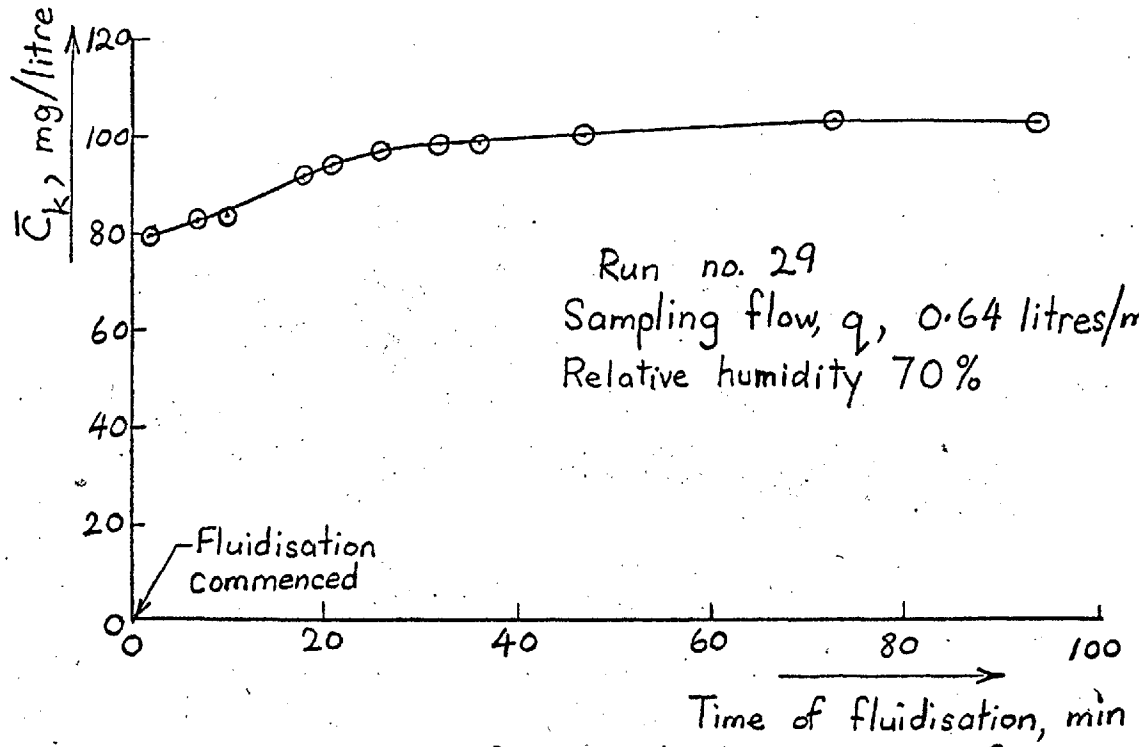


Fig. 12 Variation of \bar{C}_k with time, run no. 29

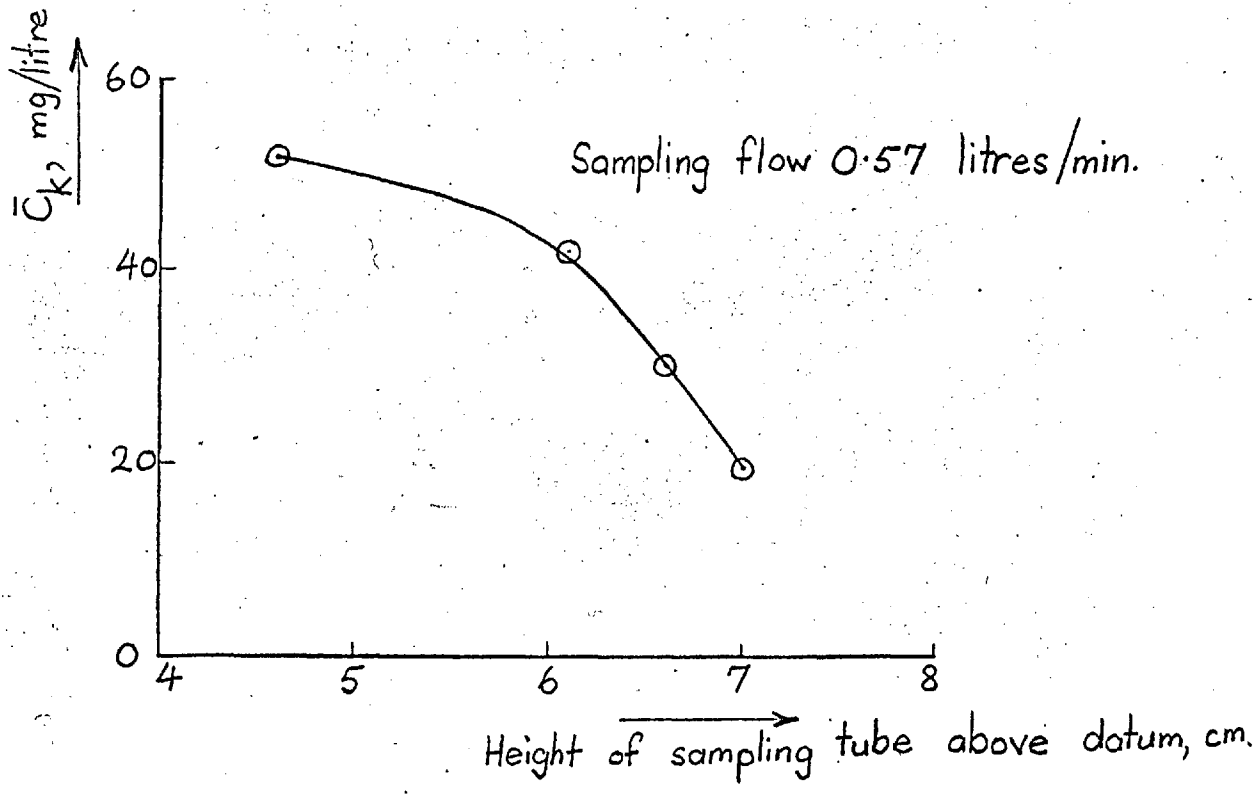


Fig. 13 Variation of \bar{C}_k with height of sampling position.

position on the sample concentration is shown in fig. 13. Samples were taken with the sampling tube mouth at different positions along the axis of the cone, using a constant sampling flowrate. The concentration of the suspension at a fixed level in the cone remained constant during these measurements.

The effect of sampling flowrate on the kinetic concentration of the samples was also investigated. The results are shown in fig. 14, where W , the weight in mg. of lycopodium collected per minute in the filter, is plotted against q , the sampling flow in litres/min. The internal diameter of the sampling tube was 1.02cm., although the entry was slightly smaller than this, as a result of flame-polishing. Fig. 15 shows values of \bar{C}_k (\bar{C}_k is given by W/q) plotted against q ; this graph indicates that the value of \bar{C}_k becomes practically independent of q as the latter approaches a value of 0.6 litres/min.

The flow pattern of the suspension in the upper part of the sampling tube was investigated by means of the ultra-microscope system shown in fig. 16a. The illumination was provided by a microscope lamp with a heat filter and two vertical slits, producing a parallel beam of light about 1 mm. thick. The beam was adjusted to shine along a diameter of the tube, thus illuminating any particles in a cross-section of the flow: this illuminated zone was about 1 cm high, and about 9 cm. above the bottom of the sampling tube. Screens were used to exclude extraneous light, and

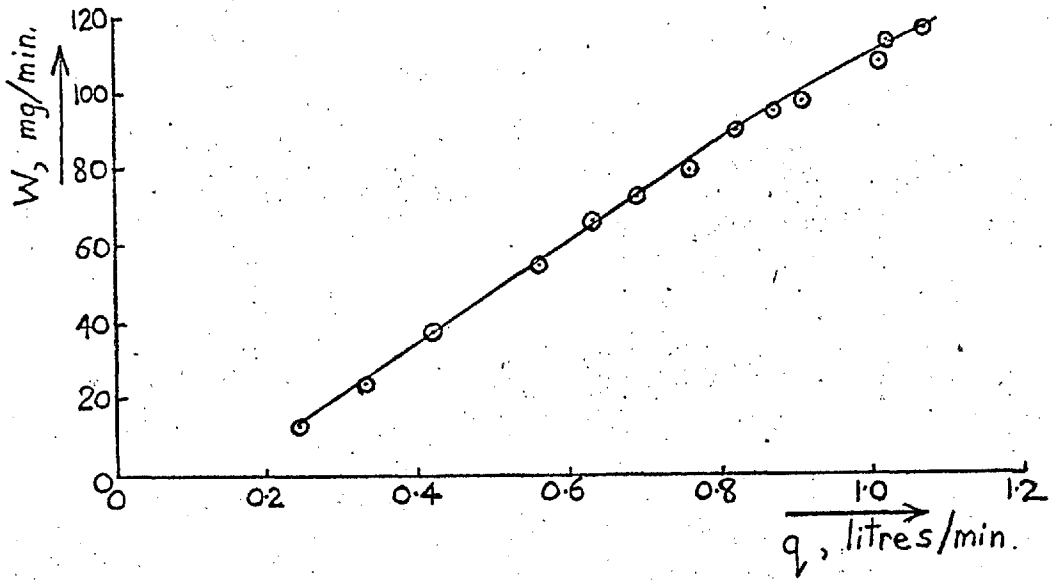


Fig. 14. Variation of W with q .

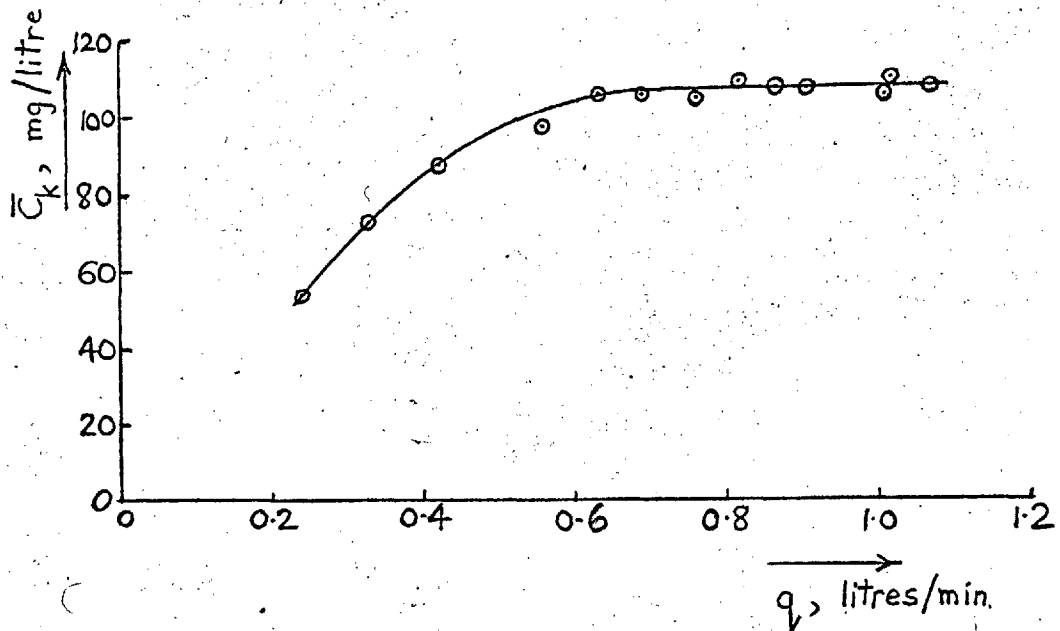


Fig. 15. Variation of \bar{C}_k with q .

the tube was thoroughly cleaned inside and outside with a proprietary window cleaning material. The observations were made as follows. The bed was fluidised, with the sampling pump switched off and the sampling needle valve B (fig.7a) closed. The pump was then switched on and the valve B opened slightly, whilst the illuminated portion of the tube was observed closely. At first no particles were visible, then as the valve was gradually opened further, particles could be seen rising slowly up the tube. They appeared to be practically uniformly distributed over the tube cross-section, and rose steadily along straight paths, except for a narrow region at the tube wall in which no particles appeared. Then as the flow was increased further, more particles became visible, and most of these moved at higher speeds; a few, however, could be seen moving downwards. At higher flows, these downward falling particles became concentrated on the tube axis; they appeared to be much larger than those flowing upwards. When the sampling flow was increased to 0.26 litres/min., the falling particles abruptly reversed their direction and moved upwards out of the illuminated region. With sampling flows higher than this value, no particles could be seen falling down the tube.

These observations of the particle flow were repeated using a larger diameter sampling tube of 1.5 cm bore, with its lower end in the same position as that of the 1.02 cm bore tube. The flow pattern observed in the larger bore was similar to that just described; the stream of particles moving slowly down the tube axis became very marked, and in

this condition the illuminated portion of the flow had the general appearance shown in fig.16b. The axial region was occupied by particles appearing much larger than the rest, which were stationary or drifted slowly downwards. Outside this axial region was a zone in which the particles followed a sinuous course, swaying from side to side as they moved up the tube. Outside this region the particles pursued a steady upward course, moving in straight lines. Immediately adjacent to the wall, a few particles could be seen drifting slowly downwards. The stream of downward-moving particles in the axial region abruptly disappeared when the sampling flow reached 1.06 litres/min., in a manner similar to that observed in the smaller bore tube. When the flow was reduced slightly below this value, the stream of falling particles was re-established. It was thought that this stream might consist of large agglomerates formed by collision of individual particles or smaller agglomerates in the portion of the tube above the illuminated zone, and in an attempt to test this idea, a small 'Perspex' platform, about 7 mm. across, was introduced into the tube to collect a sample of these particles for microscopic observation. This platform was held in the axial region of the tube on a long wire, as shown in fig. 17. The sampling flow was switched on, and adjusted to a value of 0.6 litres/min, when particles in the downward-moving stream were observed to fall on the platform. After some seconds, the fluidising flow to the bed was turned off, then when the particles ceased to rise up the sampling tube, the sampling

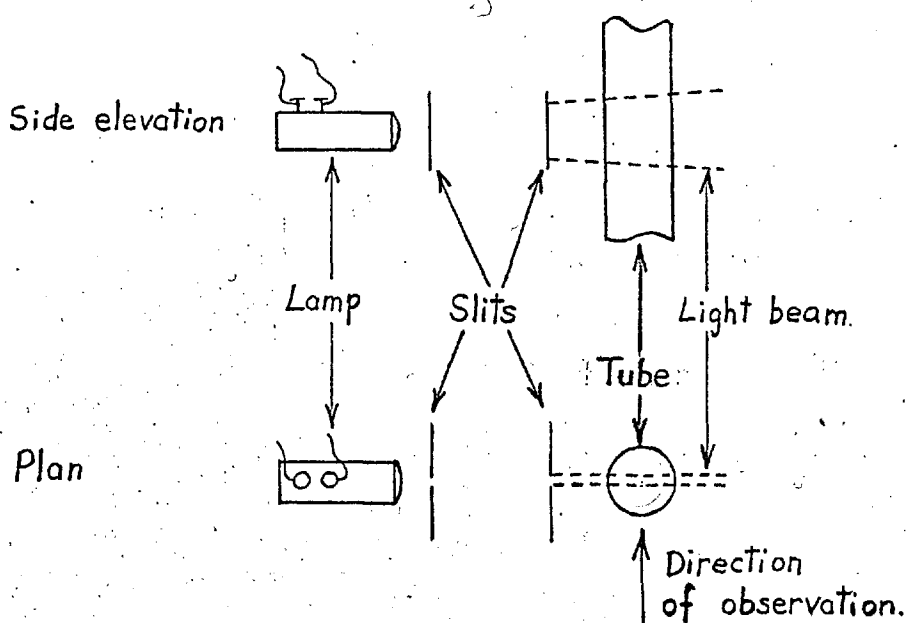


Fig. 16a. Ultra-microscope system.

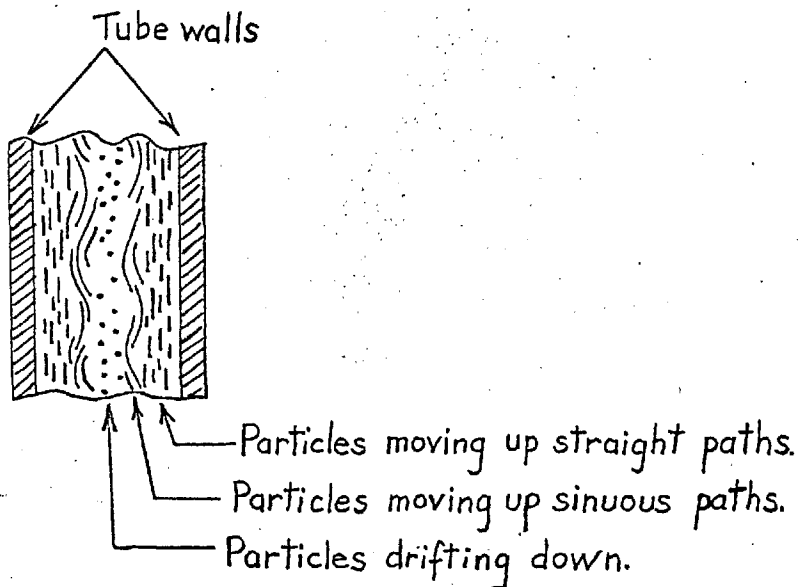


Fig 16b. Flow pattern in tube

pump was switched off, and the platform carefully removed for observation. The central portion of the platform was too densely covered with powder for any details to be distinguishable, but in the outer portions over 100 agglomerates, mostly containing between 4 and 20 particles could be distinguished. Hardly any single particles could be seen. Some of the agglomerates had long chain-like structures; others were more compact.

The presence of agglomerates in the suspension entering the sampling tube was investigated as follows. Whilst the bed was fluidised, a small glass slide was lowered slowly in a horizontal position into the suspension in the cone, until it was at the same level as the bottom of the sampling tube; the bed flow was then turned off, and the suspension allowed to settle. The slide was then removed and examined under the microscope, when it was seen that the deposited material contained many agglomerates as well as single particles. The largest agglomerates contained up to 10 or 11 particles.

These observations were not conclusive, but support the idea that the falling particles observed at the lower sampling velocities were agglomerates formed by collision in the upper part of the sampling tube. Further observations of suspension flow in tubes will be described in chapter 3.

Modification of the Apparatus for Flame Studies.

These investigations of the fluidisation system with a conical diverging section showed that the original idea of producing a reservoir of suspension with a steady

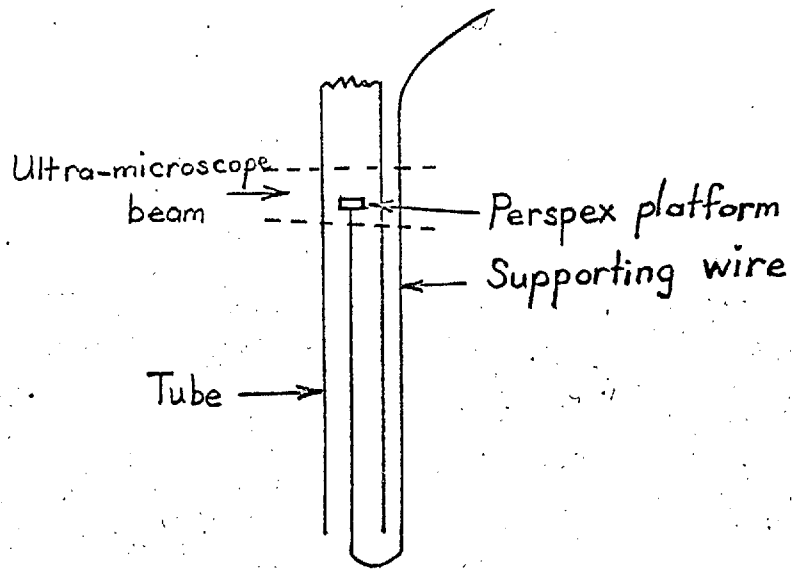


Fig.17. Position of sampling platform.

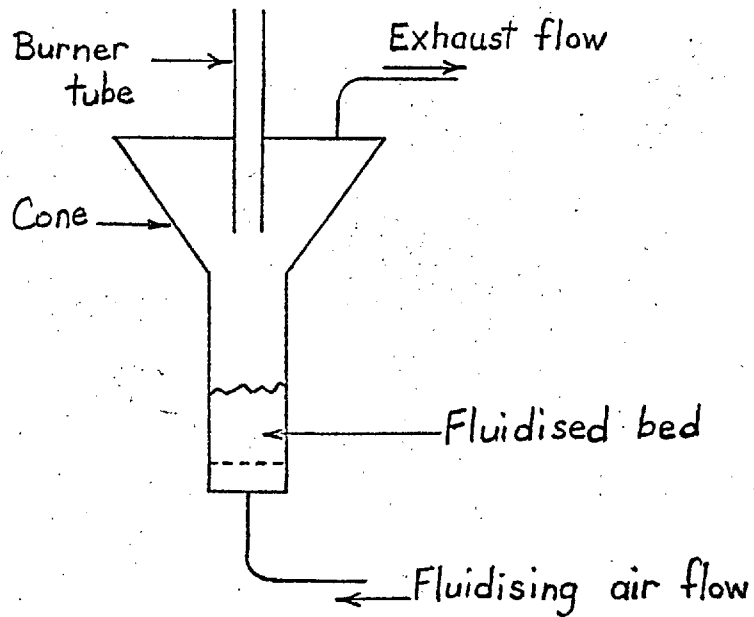


Fig.18a Scheme of Combustion Apparatus

concentration above a fluidised bed was practicable. The next step was to modify this system to permit stabilisation of flames on a burner supplied with suspension from the conical reservoir. The most direct way of doing this appeared to be to modify the sampling tube to permit its additional use as a burner. The top of the cone was enclosed, and the air which formerly passed out to atmosphere was exhausted at a controlled rate by a pump. The original sampling tube was replaced by a plain tube, which could be used either for sampling or as a burner tube. The provision for exhausting air at the top of the cone presented some difficulty, and a number of different arrangements were tried before a satisfactory one was found. Preliminary tests during the modifications showed that lycopodium flames could be stabilised on a burner tube of 10.9 mm. inside diameter, so this size of tube was used in the modified apparatus. The layout finally adopted is shown in principle in fig. 18a, and details are shown in fig. 18b. The concentration of suspension produced could be controlled by varying the fluidising air flow, and the flow velocity at the burner could then be adjusted to any required value by altering the exhaust flow from the top of the cone. In this manner it was possible to vary the concentration of the suspension independently of its velocity at the burner mouth, and so overcome one of the disadvantages of the earlier fluidised bed system. (p.48).

The top of the cone was closed in by a Perspex disc, which was bolted to brackets on the cone itself, and

sealed round the edges with Plasticine, so that it could easily be removed for cleaning purposes. The air was exhausted from the top of the cone through a short brass tube surrounding the burner tube. Washers made from rubber tubing sealed the ends of the brass exhaust tube, and located it on the burner tube. Air entered the bottom of the brass tube through circumferential slots, and left at the top through a side tube. The slots were covered by a cylinder of 40-mesh copper gauze; this was intended to provide a symmetrical resistance to flow, and so prevent any tendency for more air to be drawn through the slots on the side into which the side-tube opened. Since the air arriving at the top of the cone was not completely dust-free, the arrangement of baffles shown was adopted to remove most of the remaining dust from the air-stream. The ends of the burner tube were ground smooth and perpendicular to its axis, and it was clamped in a vertical position. The pressure within the cone was indicated by a water manometer.

The exhaust flow system is shown in fig. 18c. The air passed from the brass exhaust tube to a cyclone, followed by a millipore filter, in which the last traces of lycopodium were removed. From the filter, the air passed to a rotameter then to the needle valve A. This valve had a bypass, with needle valve B, and a stop-cock, by means of which the bypass could be quickly opened or shut. The reservoir, of about 1 litre capacity, was placed before the pump to smooth out small fluctuations in the flow.

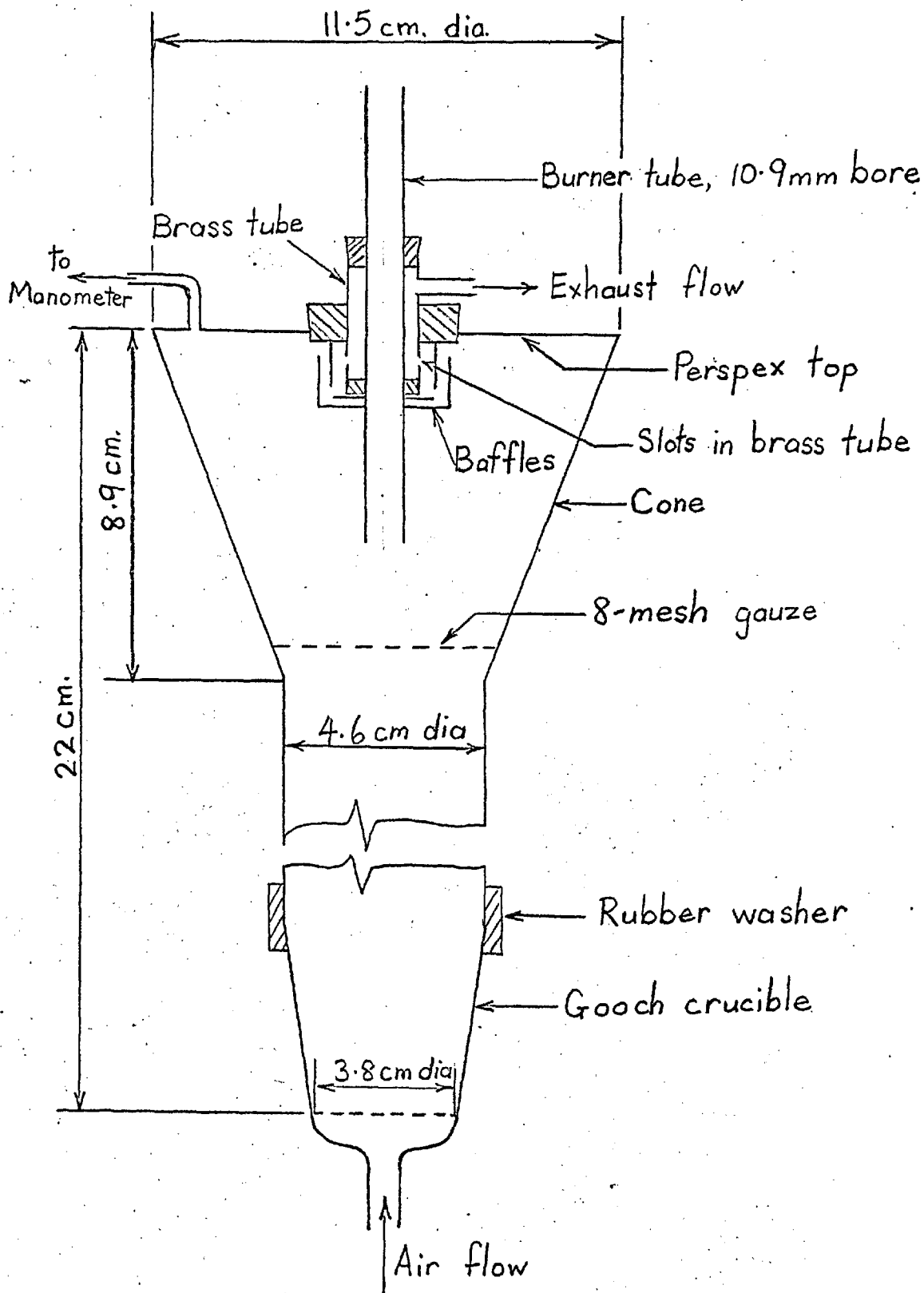


Fig. 18b. Details of combustion apparatus.

The modified apparatus was operated as follows: The fluidising flow was adjusted to give the required concentration, and the burner flow rate was then controlled by needle valve A in the exhaust flow line, with the bypass closed. When the burner flow was not required, it could be conveniently turned off by opening the bypass. Valve B was adjusted to give zero burner flow with the bypass open; under these conditions the exhaust flow was equal to the fluidising flow.

The concentration of the suspension flowing out of the burner tube was measured by the same sampling system as before. (fig. 7). The sampling flow was metered by a soap-film meter, in place of the rotameter used formerly. The burner tube was connected to the filter holder for sampling purposes by the filter nozzle shown in fig. 18d. The nozzle consisted of a short piece of glass tubing, having the same diameter as the burner tube at one end, and drawn out at the other end to take the short length of 1 mm bore plastic tubing which connected it to the filter holder. The wide end was fitted with a short piece of rubber tubing which could be slipped over the top of the burner tube when required. The bore of this rubber tube was widened at the lower end, so that as it was slipped over the burner tube the seal with the latter was made gradually; when the nozzle was pushed home onto the burner tube (fig. 18e) the joint between the two was airtight. Before a sample could be taken, the flows had to be balanced, so that the sampling flow through the filter was exactly equal to the difference between the fluidising and exhaust flows. If the flows

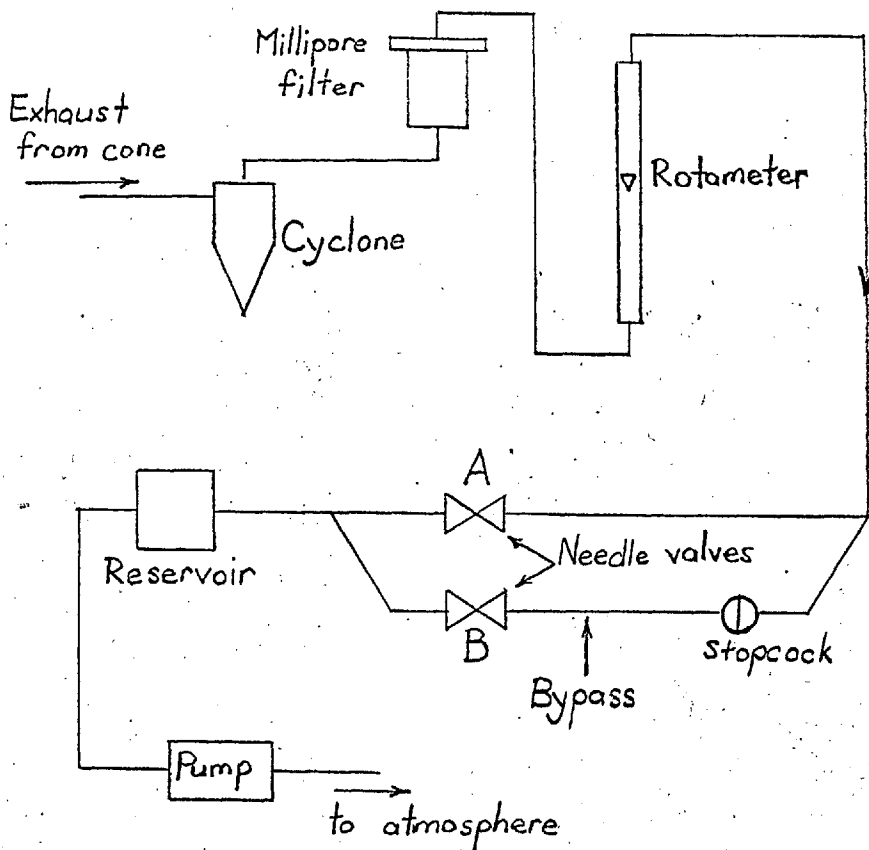


Fig. 18c Exhaust flow system

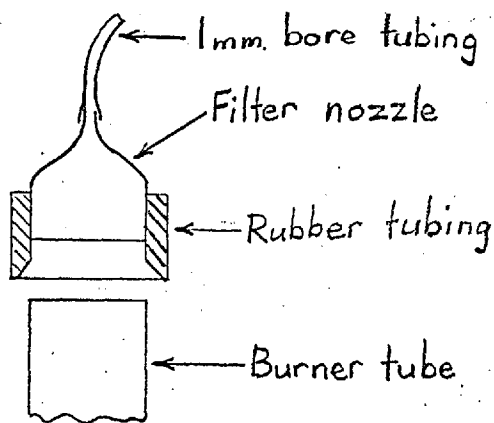


Fig. 18d. Filter Nozzle

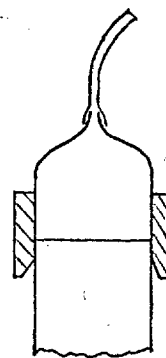


Fig. 18e. Filter nozzle in sampling position

were not balanced when the filter was connected to the burner tube, the pressure within the cone changed, causing changes in the flowrates themselves. Since the pressure drop along the burner tube was very small under all conditions of flow, the water manometer connected to the cone indicated zero whenever the burner tube was open to the atmosphere. When the burner tube was connected to the filter, any imbalance in the flows could readily be detected by departure of the manometer from a zero reading. The balancing procedure was carried out as follows: The sampling pump was switched on, and the filter nozzle was connected to the filter. The exhaust bypass was closed, causing the suspension to flow out of the burner tube, and the filter nozzle was slowly lowered on to the burner tube. The manometer was watched carefully, and the sampling flow was adjusted as necessary to maintain the zero reading. After the nozzle had been pushed home, sealing the joint with the burner tube, a final adjustment of the sampling flow was made. When the manometer reading remained steady at zero, the sampling flow was equal to the flow in the burner tube with the latter open to atmosphere. When the flows had been balanced, the sampling nozzle was disconnected, and the exhaust bypass opened to turn off the burner flow. The filter unit and sampling nozzle were weighed on an analytical balance, replaced in the system, then the suspension was sampled by closing the exhaust bypass, and immediately connecting the filter to the burner

tube for a measured time interval (usually 1 min.). The connection and disconnection of the sampling nozzle could be carried out in less than $\frac{1}{2}$ sec. Re-weighing of the filter unit and nozzle gave the weight of lycopodium collected. The sampling flowrate was measured during the sampling period by means of the soap-film meter in the sampling system. The water manometer was observed whilst sampling was in progress, to check that no significant change in cone pressure occurred. Dividing the rate of collection of lycopodium in the filter by the sampling flowrate gave \bar{C}_k as before.

It was found during the development of the modified apparatus that the fluidising and exhaust flows required to stabilise lycopodium flames on the burner were in the region of 5 litres/min. and $3\frac{1}{2}$ litres/min. respectively. Precise control of these flows was necessary to achieve a steady burner flow, and it was found that fluctuations in the fluidising flow could cause changes of up to 10% in the burner flow. In order to reduce these fluctuations, a manostat was incorporated in the fluidising air supply. This manostat (fig. 19) was a modification of a design described in the 4th edition of Findlay's 'Practical Physical Chemistry'. The air humidifying arrangements were modified, and air of approximately 70% relative humidity (at ambient pressure) was supplied by passing the whole of the air supply through the wash-bottle at a pressure of 6 psig. This produced air of constant relative humidity irrespective of the condition of the compressed air supply. The modified air supply system is shown in fig. 20.

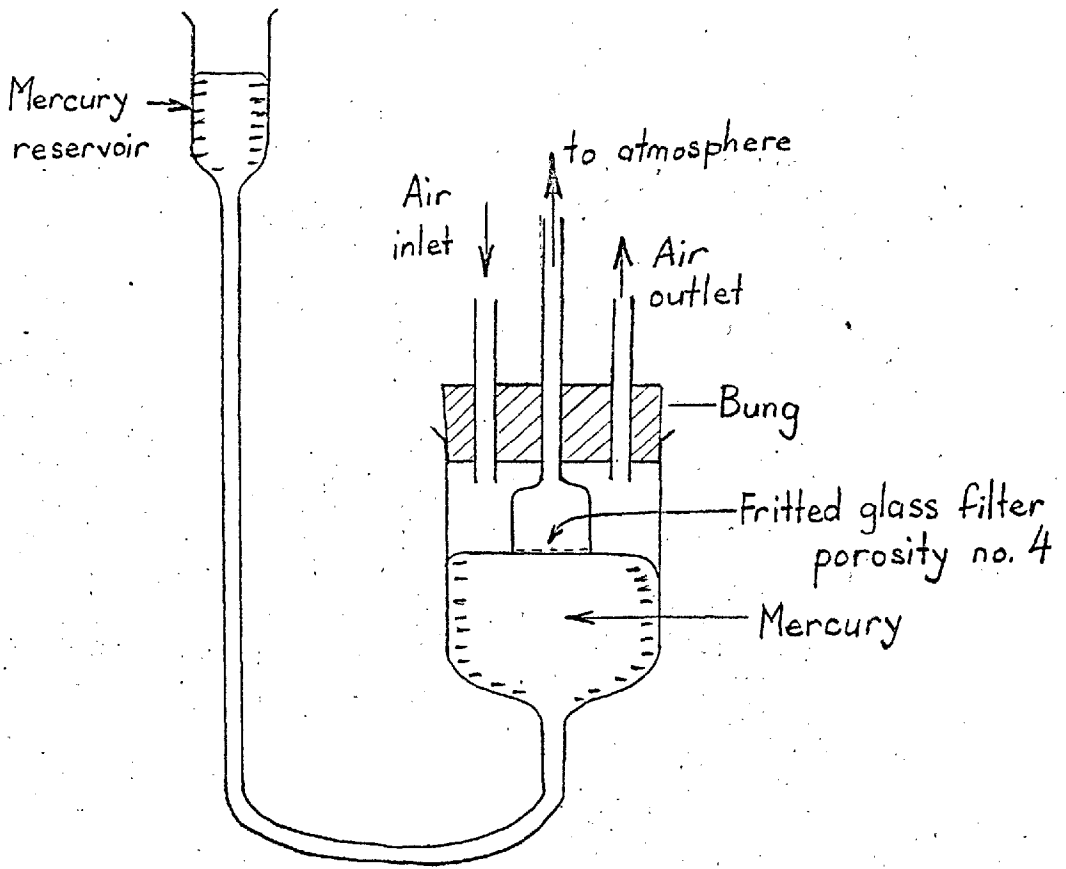


Fig. 19. Manostat.

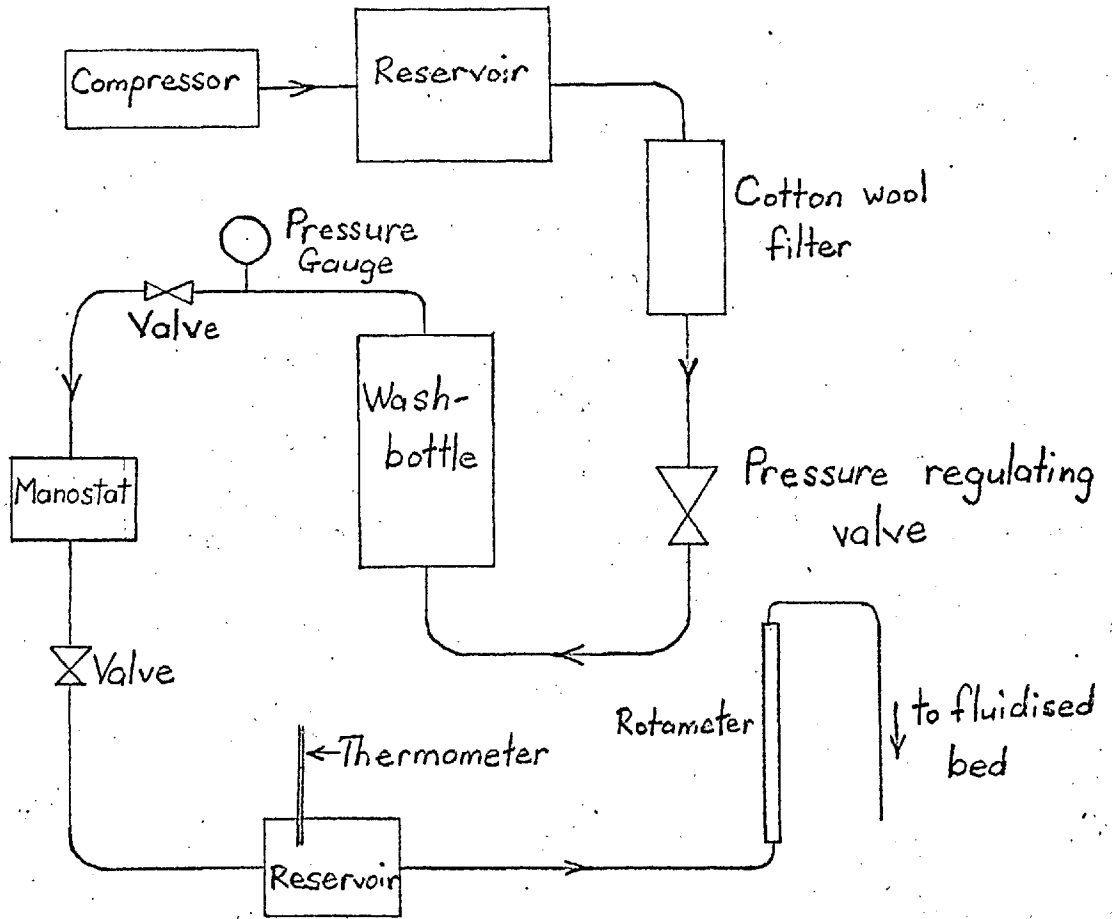


Fig. 20. Modified Air flow System

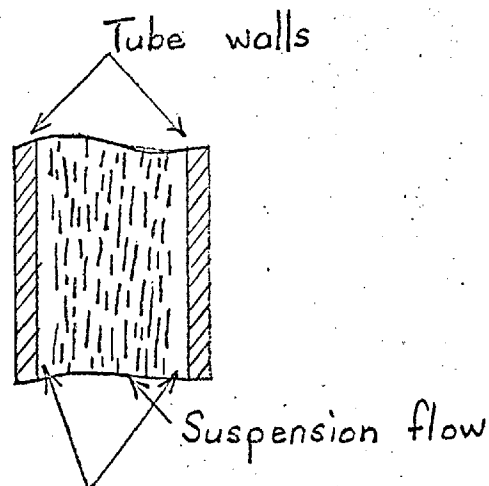


Fig. 21. Flow pattern in burner tube

Measurements were made to determine the changes in \bar{C}_k and burner flowrate caused by the slight fluctuations in pressure which still occurred after the incorporation of the manostat. The procedure was as follows. \bar{C}_k was measured, taking the mean of three successive measurements, and then a slight change was made in the sampling flowrate, resulting in a slight change of cone pressure. \bar{C}_k was then measured for the new conditions, again taking the mean of three values. The results in Table I show the changes in \bar{C}_k and burner flowrate associated with the changes in cone pressure.

Table I

Fluidising flow (litre/min)	Cone pressure (ins. water gauge)	Burner flow (litre/min)	\bar{C}_k (mg/litre)	% change in:-	
				Burner flow	\bar{C}_k
4.75	{ -0.1 +0.7 }	1.23 1.19	102 101 }	3	1
4.75	{ -0.2 +0.6 }	1.04 1.00	93 89 }	4	4
4.75	{ -0.1 +0.5 }	1.56 1.52	78 76 }	3	3
6.10	{ -0.1 +0.6 }	1.51 1.47	103 101 }	3	2

Since pressure fluctuations seldom caused changes in cone pressure exceeding 0.3 ins. water gauge it was considered that the errors involved in the sampling procedure were acceptable.

This completes the account of the development of the apparatus used for the combustion studies of lycopodium

dust flames. Before going on to the study of the flames stabilised with this apparatus, some experiments were carried out to observe the flow of dust suspensions in tubes. Details of these are given in the next chapter.

The Flow of the Suspension in the Burner Tube

As mentioned in chapter I, the structure of a flame stabilised on a tube burner depends on the nature of the flow in the tube itself. None of the workers who have studied dust flames burning on tubes have investigated the behaviour of dust suspensions in tube flow, and it was therefore thought desirable to make further observations of the flow of suspensions in the burner tube of the combustion apparatus, using the ultra-microscope system described on p. 63.

First, experiments were carried out to develop a flame trap for the burner tube; these will be described next. It was necessary to provide a flame trap in order to prevent a flashback in the burner tube igniting the suspension within the cone. The experiments with flames stabilised on gauzes, (p. 45) suggested that a piece of metal gauze across the bottom of the burner tube would provide an adequate flame trap. The effect of different gauzes on the suspension flow in the tube was studied as follows.

The flow was observed in a 1 cm. length of the burner tube about 2 cm. below the top, without a gauze across the tube. (The burner tube itself was 14 cm. long.) The light beam was adjusted to shine along a diameter of the tube, thus illuminating a cross-section of the flow in a vertical plane. The concentration and flowrate of the suspension were adjusted to values at which flames could be stabilised on the tube, but no flames were burnt whilst the flow was

under observation. The general appearance of the flow was as sketched in fig. 21. Well-defined regions adjacent to the tube walls contained no particles, whilst the stream of suspension appeared practically uniform, with sharp boundaries between it and the particle-free regions of the walls. The width of the particle-free regions fluctuated rapidly but was of the order of 1 mm. Flames stabilised on the burner under these conditions tended to be unsteady; the flame-fronts did not remain horizontal, but tilted from side to side. The flowrate in the burner tube was in excess of 1 litre/min, considerably higher than those used in the flow observations described in Chapter 2.

The observations of the flow in the burner tube were repeated with a piece of 16-mesh copper gauze made of 27 S.W.G. wire (0.0164 in. diameter) stretched across the bottom of the tube. The particle-free spaces at the walls were still present, but their width fluctuated much less than in the previous case, and the flow appeared much steadier. However, narrow particle-free zones could also be seen in the flow of suspension, standing out as dark streaks on the bright background of illuminated particles, and it was found by rotating the tube that these zones were above the wires of the gauze. This showed that the particle-free regions produced by the wires obstructing the flow extended downstream a distance of at least 14 cm., to the top of the burner tube. Flames burning on the tube were similar in appearance to those observed without a gauze in position

but burned much more steadily.

In an attempt to avoid the particle-free zones produced by the gauze of 27 S.W.G. wire, a gauze was made from much finer wire. The circle of 24-mesh gauze was made from 0.0045 in. diameter wire, stuck to a short piece of brass tubing with 'Araldite'. The brass tube was of slightly larger diameter than the burner tube, and was held in position at the bottom of the latter by a short length of rubber tubing. (fig. 22). This gauze of fine wire was found to improve the stability of the flow and steadiness of the flames burning on the tube in the same manner as the gauze of 27 S.W.G. wire used in the previous case. When the burner flow was first turned on, after placing the fine gauze in position, the illuminated stream of suspension was quite uniform in appearance, but after the suspension had been flowing for $\frac{1}{2}$ min. or so, dark streaks appeared in the stream, indicating regions of low particle concentration. These regions were found to be caused by deposits of lycopodium accumulating on the gauze wires; after gentle brushing of the gauze to dislodge the deposits, the stream of suspension became uniform in appearance once more. The particle-free regions at the tube walls were present as in the previous tests.

The effect of the gauzes in steadying the flow in the burner tube was probably due to their flow-resistance damping out small fluctuations in the flow entering the tube. The persistence of the particle-free regions above

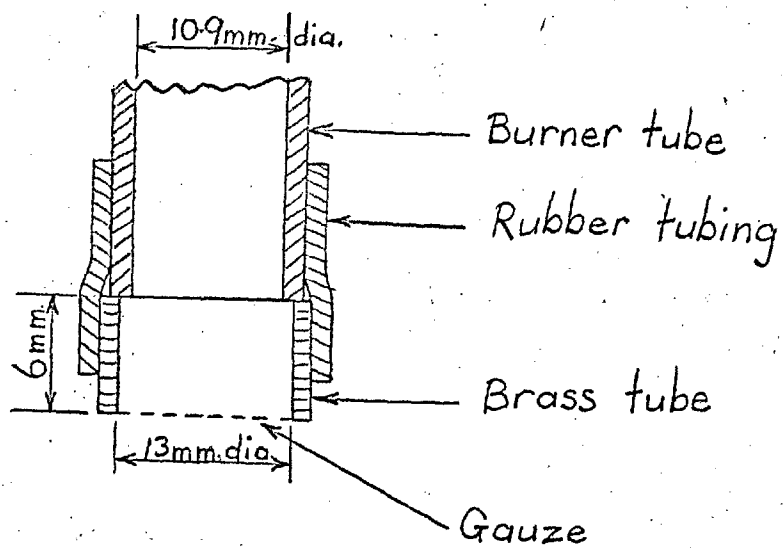


Fig. 22 Attachment of fine wire gauze

the wires of the coarse gauze to the top of the tube indicated that little radial movement of the particles took place as they moved up the tube. For a lycopodium suspension of 200 mg./litre concentration, the average interparticle distance is approximately 0.038 cm. (This is based on figures for the number of lycopodium particles per g. quoted by GREGORY)⁵⁹ In comparison, the diameters of the coarse and fine wires used in the gauzes were 0.0416 cm. and 0.011 cm. respectively. It would be expected, therefore, that the presence of the finer wires in the flow would not produce significant particle-free regions in the suspensions used in the present work.

Since the fine wire gauze improved the steadiness of the flames, it was used in all the subsequent experimental work. Its performance as a flame-trap was not tested at this stage, but later experiments on flame quenching, to be described in the next chapter, showed that it was an effective flame trap.

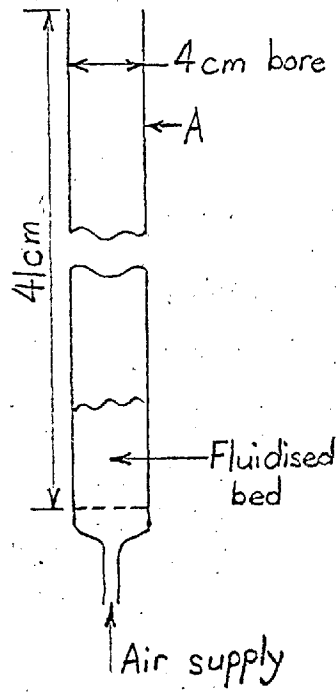
In order to reduce to a minimum disturbance to the flow caused by deposits of powder building up on the gauze wires, the gauze was brushed immediately before igniting flames, and observations on the flames were made within $\frac{1}{2}$ minute of igniting them.

Some experiments were carried out to discover if the particle-free region adjacent to the tube wall was influenced by the shape of the tube entry. The apparatus used is shown in fig. 23. and consisted of a fluidised bed for

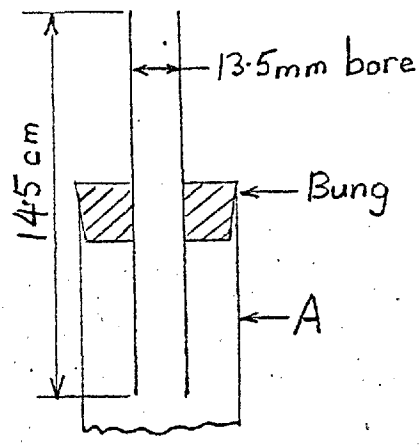
producing a lycopodium suspension surmounted by the vertical tube A, 4 cm. in diameter, up which the suspension flowed. The top of tube A could be closed by any one of the four pieces of apparatus shown in the figure, i.e.,

- i) A rubber bung carrying a plain tube, 13.5 mm. bore and 14.5 cm. long. The ends of the tube were ground flat and perpendicular to its axis. (fig. 23b)
- ii) The same bung and tube as in (i), but with a 24-mesh gauze made of 0.002 in. diameter aluminium wire fitted to the bottom of the tube. (fig. 23c)
- iii) A 13.5 mm. bore tube provided with a bell-mouthed entry 4 cm. in diameter at its widest part. The bell-mouth was sealed to the top of tube A with plasticine (fig. 23d)
- iv) A disc having a central orifice 13.5 mm. in diameter. The disc was sealed to the top of tube A with plasticine when in use (fig. 23e)

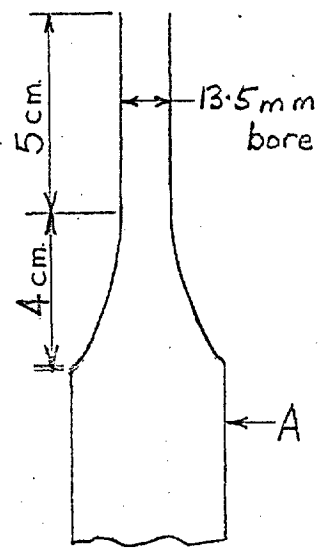
The flows through the tubes and the orifice were observed in turn, under similar conditions of flowrate and concentration, and in order to compare the widths of the particle-free regions in the four cases, the diameters of the columns of suspension emerging from the tubes or the orifice were measured. The measurement was made to the nearest millimetre with a ruler, the suspension being illuminated by a strong light from a direction perpendicular to the direction of observation. Owing to



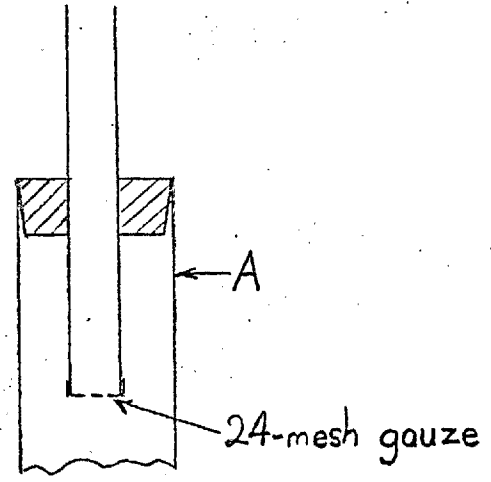
(a)



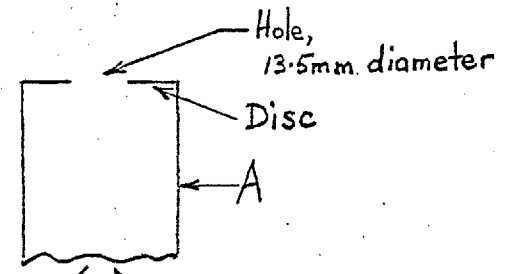
(b)



(d)



(c)



(e)

Fig. 23 Apparatus for Experiments on Particle-free Space

fluctuations in the widths of the streams of suspension, precise measurements were not possible.

The results of the measurements for two different values of suspension flowrate (2.0 litres/min. and 3.0 litres/min.) are shown in Table II. In the case of the tubes, the measurements were made at the tube outlets, but for the orifice the measurements were made at a point about 1 cm. above the disc, where the column of suspension was at its narrowest; this column contracted its diameter by about 1 or 2 mm. immediately above the orifice. Since the concentration of the suspension produced by the fluidised bed increased with increase of the air flow, the concentration of suspension flowing was higher for the higher flowrate; the measurements for the two different flowrates were therefore not directly comparable with each other.

TABLE II.

Suspension flowrate (litres/min.)	Diameter (mm.) of stream of suspension emerging from:-			
	Plain tube.	Plain tube with gauze.	Bell-mouthed tube.	Disc with orifice.
2.0	6	6	6	5
3.0	7-8	8	7	6-7

Internal diameter of tubes and orifice = 13.5 mm.

The values in the table indicated that within the range of flowrates covered it was not possible to eliminate the particle-free region at the burner tube walls by adopting a bell-mouthed tube entry. It was therefore decided on the

grounds of simplicity to use a plain burner tube fitted with a fine gauze at the bottom for the subsequent flame studies, to be described in Chapter 4. The results obtained for the orifice showed that a particle-free space was present at the edge of the flow in the plane of the orifice itself, which suggested that the particle-free spaces observed in tube flow originated at the tube entry. The flows in the tubes were therefore examined further, using the ultra-microscope system to illuminate a cross-section of the flow along a tube diameter as already described. The observations may be summarised as follows.

In the case of the plain tube without a gauze, the particle-free space increased slightly in width from the bottom of the tube up to a point about $\frac{1}{2}$ cm. above the bottom, after which it remained roughly constant in width up to the top of the tube. The flow pattern at the tube entry for a suspension flowrate of 2.0 litres/min. is sketched in fig. 24a. The lines a a in the figure represent the boundaries between the suspension flow and the particle-free regions. A particle-free space several mm. in width was observed immediately beneath the tube rim, and it was also noted that the column of suspension contracted slightly in diameter during the first $\frac{1}{2}$ cm. or so of its travel up the tube. The change observed in the boundaries of the suspension flow on increasing the flowrate of suspension from 2.0 litres/min. to 3.0 litres/min. is shown by the sketch in fig. 24b; the boundary between the suspension and the

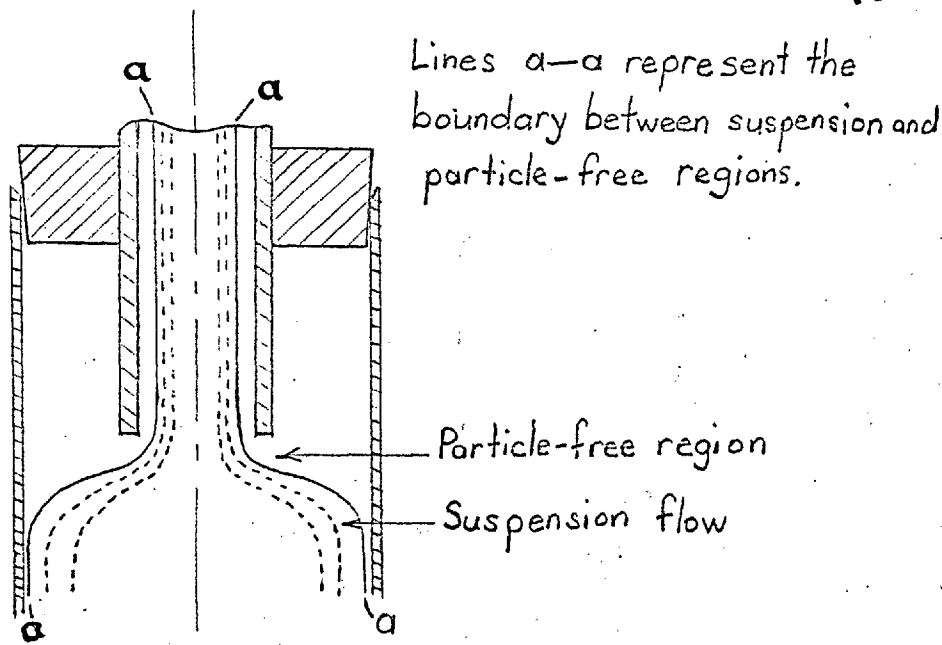


Fig. 24a. Flow pattern at tube entry, showing particle-free regions; total flow 2 litres/min

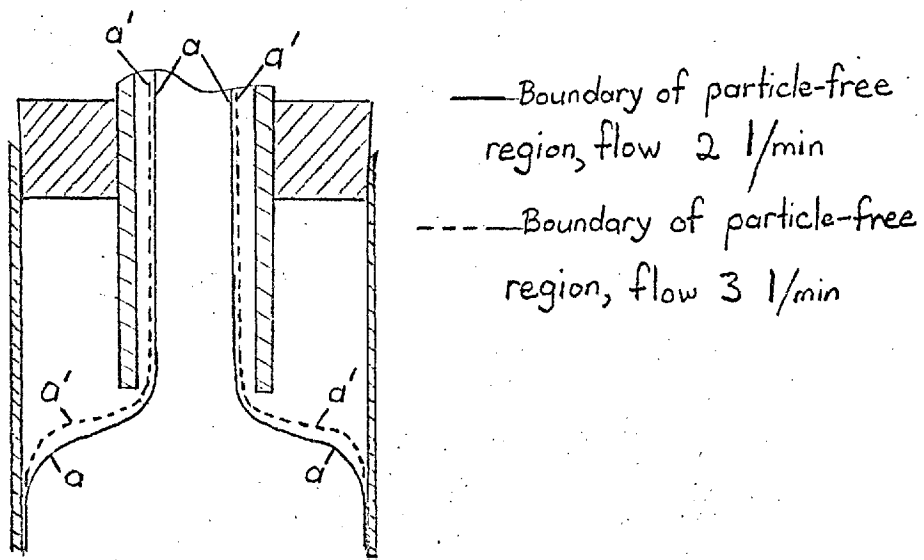


Fig. 24 b Effect of Flowrate on Boundary of particle-free region

particle-free region, a a, moved up to the position a' a' as the flow was increased, and the width of the particle-free space beneath the tube rim was reduced.

In the plain tube with the gauze fitted, the flow was obscured for the bottom $1\frac{1}{2}$ cm. of the tube by the fitting carrying the gauze, but above this point, the width of the particle-free space remained approximately constant up to the top of the tube. In the bell-mouthed tube, the particle-free space was seen to be present from the widest part of the bell onwards, as sketched in fig. 24c. In the parallel portion of this tube, the particle free space was of constant width.

These observations confirmed that the particle-free space arose adjacent to the tube entry, and showed that in the case of the plain, parallel-bore tubes the particle-free space was practically constant in width over most of the tube length. Their significance will be discussed in Chapter 6.

The apparatus developed as described in Chapter 2 was fitted with a 24 mesh gauze of 0.0045 in. diameter wire, made as previously described, at the bottom of the 10.9 mm. bore burner tube, to act as a flame trap. This completes the account of the development of the combustion apparatus, shown in its final form in fig. 25. This apparatus was considered to fulfil the first object of the present research, i.e. the development of a simple, flexible method for the laboratory-scale production of dust suspensions in the inflammable range of concentration. (p.12). The next chapter

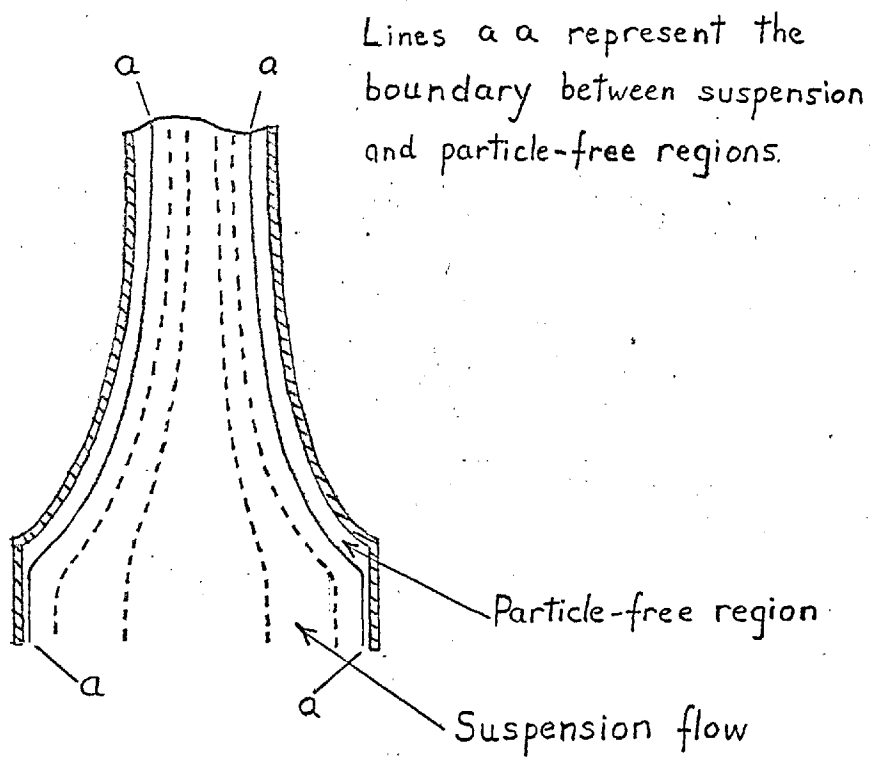


Fig 24c Flow pattern at entry to bell-mouthed tube.

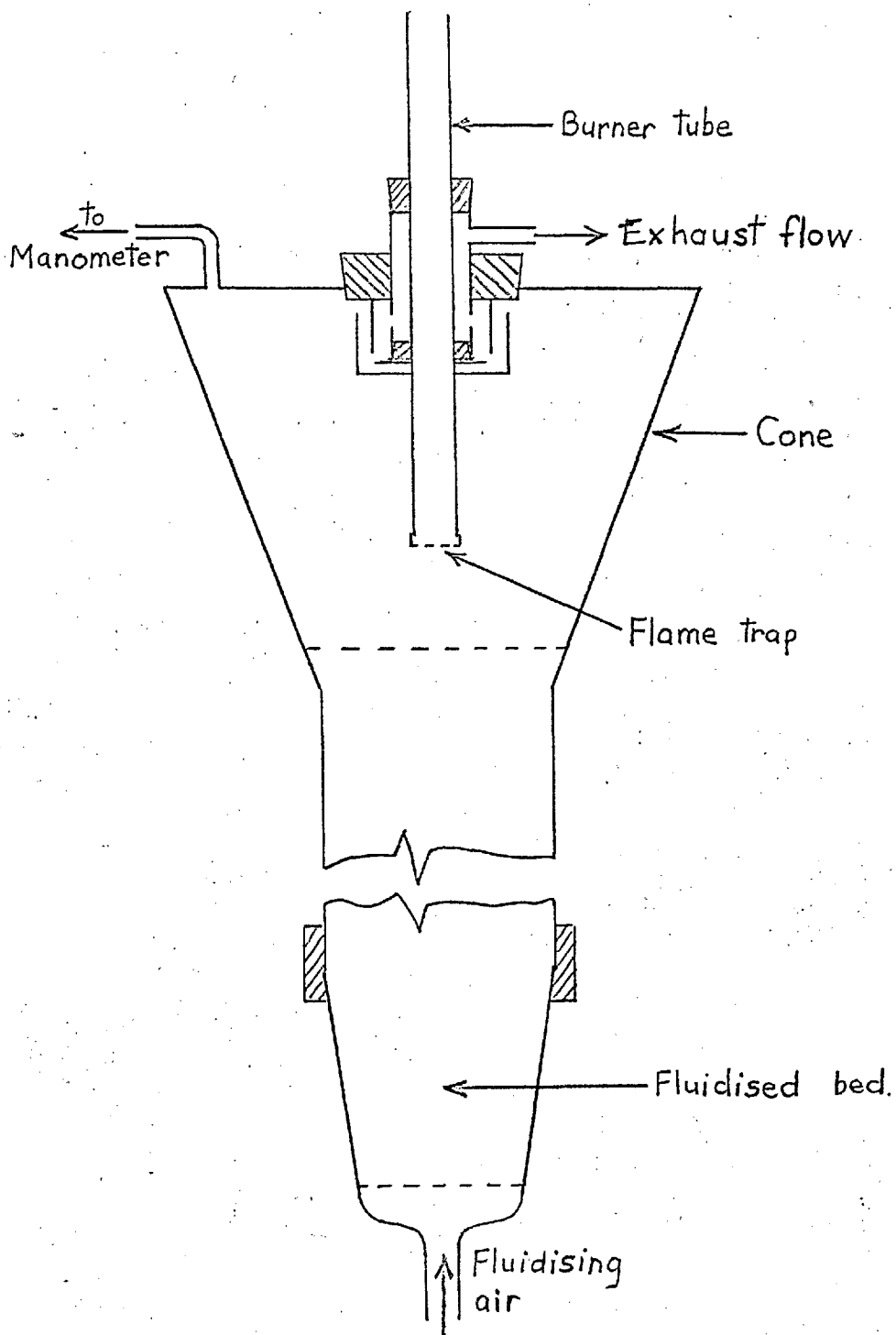


Fig 25. Combustion apparatus, showing position of flame trap. For dimensions, see fig 18b

describes the work carried out on the second object of the research, i.e. the investigation of the structure of dust flames. Before going on to the flame studies, however, it is convenient to describe at this point the measurement of the settling velocity of lycopodium particles.

It was proposed to study the structure of lycopodium flames by taking particle track photographs (see Chapter 4), and in order to interpret these photographs, a value for the settling velocity of lycopodium particles in air was required. The theoretical and experimental studies of sedimentation discussed in the literature review all indicate that at the concentrations used in the present work, the settling velocity of the particles relative to the air is not significantly different from the value for an isolated particle. Since it is simpler to observe the fall of individual particles than the sedimentation of suspensions, the settling velocity of single particles was measured in the apparatus shown in fig. 26. This consisted of a vertical glass tube, 46 cm. in length, closed at the bottom by a rubber bung. The tube diameter, 10.3 mm, was chosen to be similar to that of the burner tube. Two marks 10 cm. apart were made on the lower part of the tube, between which the settling particles could be timed. The lycopodium particles were introduced into the tube in the following manner; a small brush was dipped into the powder, then most of the powder was shaken off by tapping the brush several times. The brush was then stroked over the top of the tube, and this dislodged a few of the remaining particles from the brush. These particles

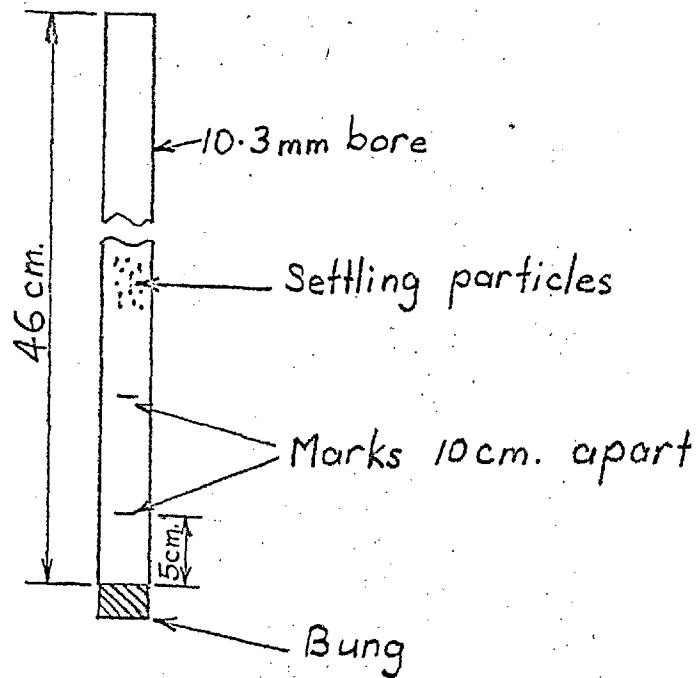


Fig. 26 Tube for measurement of
Settling Velocity.

settled through the stationary column of air in the tube. If the quantity of powder on the brush was too great, large aggregates fell into the tube, but under suitable conditions the number of particles introduced into the tube by this procedure was about 20 or 30. The tube was illuminated by a light beam, and individual particles could be distinguished by viewing the tube against a dark background from a direction perpendicular to the light beam. Individual particles or small groups of particles falling together could easily be timed between the two marks. There was considerable variation in settling velocities; values obtained from ten measurements varied from 1.4 cm/sec. to 2.7 cm/sec, with a mean value of 2.1 cm/sec. This variation was probably partly caused by slight differences in the size and shape of the particles, and possibly also by the presence of aggregates. P.H. GREGORY⁵⁹ quotes values of 1.76 cm/sec and 2.14 cm/sec. for the settling velocity of lycopodium particles in air. In view of the considerable variation between individual particles, a value of 2 cm/sec was taken as the approximate settling velocity, and this was used in the interpretation of the particle track photographs.

CHAPTER 4.Flame Studies.

The second object of the present work was the study of the structure of laminar dust flames burning in the combustion apparatus developed as described in the preceding two chapters. Details of the experimental work carried out to investigate the structure of these flames will now be given.

Preliminary experiments were carried out to find the range of conditions under which lycopodium flames could be stabilised on the 10.9/^{mm.} burner tube, and to observe the main characteristics of the flames.

It was found that, in general, burner flow rates above 1.1 litres/min. were required to stabilise flames, and that no flames could be stabilised at values of \bar{C}_k below 125 mg./litre. The highest value of \bar{C}_k that could usefully be produced at the burner was about 190 mg./litre. If attempts were made to increase this value by adding further material to the fluidised bed, or by increasing the fluidising flow-rate, the transition zone extended up into the cone, producing instability in the flow of suspension at the bottom of the burner tube.

A marked feature of the flames produced was the large dead space, in excess of 2 mm. in most cases, between the flame-front and the burner rim. Considerable quantities of suspension were seen to pass through this space, and by-pass the flame completely. A detailed description of the appearance and behaviour of these flames will be given in the results section (Chapter 5).

When the main characteristics of these flames had been established, consideration was given to the choice of a technique for investigating their structure. Most previous workers with laminar dust flames confined their attention to the measurement of overall burning velocities or flame speeds, e.g. Long, Kaesche-Krischer & Zehr, Cassel, Das Gupta & Guruswamy, and Ghosh, Basu & Ray. These obtained values of overall burning velocity by dividing the suspension flowrate at the burner by the total area of the flame-front. This method was not applicable in the present case, since some of the suspension by-passed the flame. In these circumstances, the flow of suspension into the flame-front could only be determined from a knowledge of the local suspension velocities approaching the flame-front. Particle track photography appeared to be the only method of obtaining this information. The use of particle track photography could also yield detailed information about the flow pattern of the suspension through the burner tube and into the flame, which has an important influence on flame shape and stability. Moreover, since this technique gives local velocities across the flame front, it would permit calculation of the variation of burning velocity across the flame.

Particle track photography was therefore used to study the flame structure. A few subsequent measurements were made on flame temperatures and flame quenching.

1. Particle Track Photography.

The layout of the apparatus for illuminating the particles and photographing the tracks is shown in plan

in fig. 27a. Fig. 27b shows the illumination system in detail.

The camera was of the quarter plate double-extension type, with an $f/4.5$ lens of 13.5 cm. focal length. It was used fully extended to give approximately 1:1 magnification. As a result of space limitation, it was impracticable to use an illumination system with a condenser and collimator, so a parallel light beam was produced by means of a flash-bulb and two slits. The chopper for interrupting the light beam was made of thin card, and was rotated at a speed of 2400 r.p.m. by a small induction motor. It was necessary to use a very narrow light beam to obtain a suitable number of illuminated particle tracks, as the particle concentrations in dust flames are many times greater than those used in particle track photography of gas flames. The slits were each formed by the edges of two razor blades spaced with strips of paper. Preliminary experiments showed that the slit width which gave the clearest photographs was 0.007 in. Further trials were necessary to synchronise the flash-bulbs with the camera shutter, as the latter was not provided with a synchronising device, and to find the most suitable bulbs. The lycopodium flames were very sensitive to air currents, and the mica draught shield shown in fig. 27b was used to reduce these to a minimum. Additional shielding, not shown in the figure, was necessary to prevent stray light from the flash-bulb or from external sources entering the

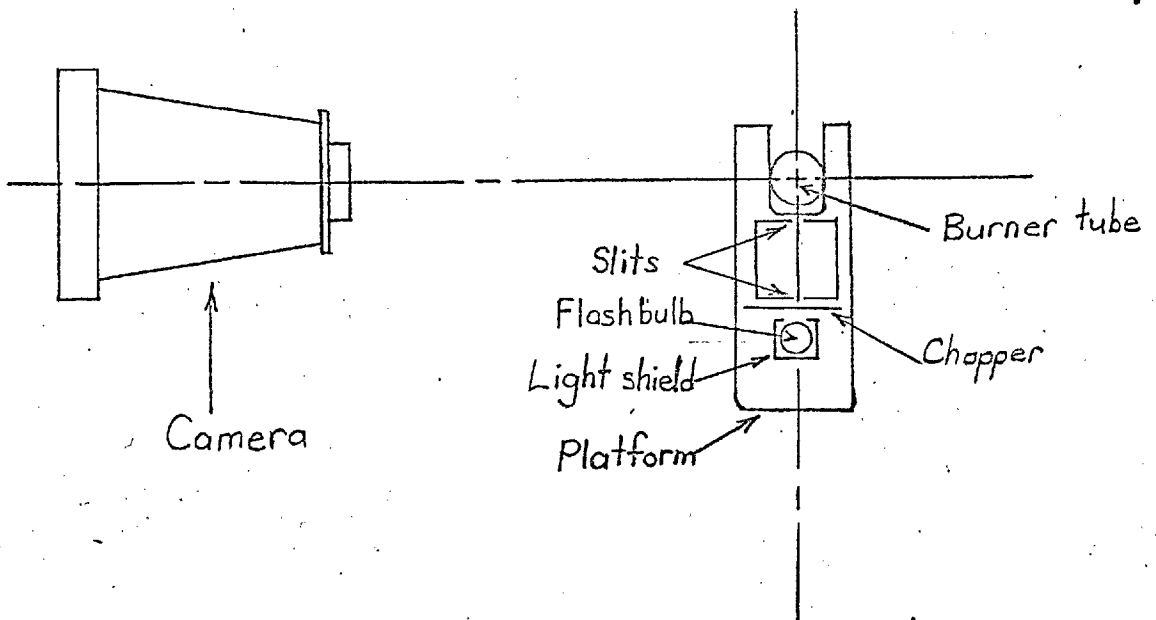


Fig. 27a Plan of Particle Track Photography Lay-out.

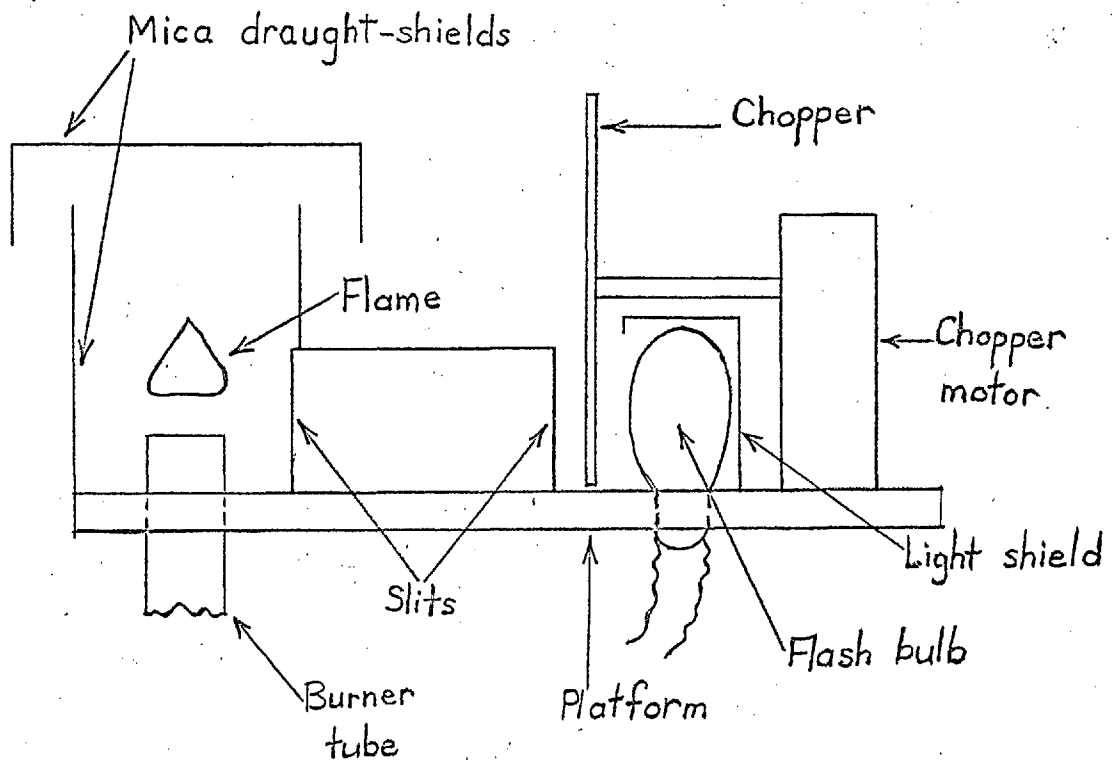


Fig. 27b. Details of Illumination System.

camera lens. Ilford HP3 plates were used, and these were developed in 'Promicrol' for 20 minutes at 60°F.

The only flames suitable for burning velocity measurements were those with flat or saucer-shaped flame-fronts, since in these the entire flame-front was visible. As will be described in more detail in the next chapter, in some lycopodium flames only a small portion of the flame-front was visible, in which case the flame area could not be determined.

Measurements on flames stabilised on the 10.9mm. diameter tube were restricted to values of \bar{C}_k in the region 125 mg/litre to 185 mg/litre. It was found to be impossible to stabilise flames at concentrations below the lower figure on this burner, and \bar{C}_k values higher than 190 mg/litre could not be produced satisfactorily in this apparatus for the reasons already mentioned. (p.97.)

Whilst the flames were burning, a sticky deposit consisting of charred or partly burned lycopodium particles gradually accumulated on the rim of the burner tube, and inside the top of it. These deposits affected the flow of the suspension, causing irregularities or asymmetry in the flame. Deposits of lycopodium also collected on the wires of the fine gauze at the bottom of the burner tube, with similar results. In order to eliminate these irregularities as far as possible, the burner tube and gauze were carefully cleaned before the burner flow was turned on and the flame ignited, and the photograph

was taken as soon as the flame appeared to be burning steadily, i.e. in most cases between 5 and 20 seconds after ignition.

The procedure for taking a particle track photograph was as follows. The bed was fluidised, and samples were taken at intervals until the concentration of the suspension produced reached an almost steady value; the fluidising flow was then adjusted until the concentration was in the region of the value desired. The exhaust flow was adjusted to give a burner flow in the region of 1.2 to 1.5 litres/min., and the burner tube was cleaned. This was done by gently brushing the gauze, the inside of the tube, and the tube rim with a fine squirrel-hair brush. The draught-shield was placed round the top of the burner tube, the exhaust by-pass was closed, and the suspension issuing from the burner tube was ignited by applying a small gas flame. The resulting flame was observed, and the burner flow was adjusted by means of the exhaust needle valve until the whole flame-front was clearly visible, and as nearly flat as possible. The flame was then blown out, and the exhaust by-pass opened. Any deposit on the burner tube rim was carefully removed with a knife, and the concentration was measured at the same burner flow as used for the flame, following the procedure already described. Next, the chopper motor, which took several minutes to reach its working speed, was switched on, the burner tube was cleaned with a brush as before,

and in addition any dust on the outside of the tube which would interfere with the observation of the particle tracks was brushed off. The draught shield for the flame was brushed clean and placed in position, and the light shields round the flash bulb were also positioned. The exhaust by-pass was closed, and the suspension ignited. The flame was observed for a few seconds, and if it appeared to be symmetrical, and was burning steadily, the camera shutter was operated. Immediately afterwards, the flame was blown out, the by-pass opened, and the deposit was scraped from the tube rim, then another concentration measurement was made. If the flame appeared to be asymmetrical, or did not burn steadily, no photograph was taken, but the flame was extinguished and the tube was cleaned again before re-igniting the flame.

The time interval between the concentration measurements made before and after taking each photograph was usually in the region of 10 minutes; the setting of the sampling flow needle valve remained constant for both of these measurements. During the measurements a careful watch was kept on the water manometer indicating the pressure within the cone; any slight fluctuation in the flowrate was reflected in a change in the manometer reading. If the mean pressure in the cone during either of the measurements deviated from

atmospheric by more than 0.4 in. water gauge, the results of the run were rejected. The error in the measurement of concentration and flowrate resulting from any such deviation was estimated from Table I (p.79), which refers to a range of flowrates similar to that used in the flame studies. The results there indicate that the maximum change in the values of concentration and flowrate caused by a change of 0.8 in. water gauge in the cone pressure was 4%. Since the change in cone pressure was small compared with the pressure drops over the fluidising flow and exhaust flow systems, the changes in concentration and flow may be taken as roughly proportional to the change in cone pressure. A fluctuation in cone pressure of 0.4 in. water gauge would therefore indicate an error of about 2% in the measured concentration and flowrate. Another source of error was the gradual change in concentration with time, occurring as material was lost from the fluidised bed; in most cases there was a small drop in concentration between the measurements made before and after taking the photograph. For the flames analysed in detail, this drop did not exceed 2% of the concentration, and the mean of the two values was taken as the concentration of suspension burning in the flames. The measurements of concentration and flowrate were therefore accurate to within 3 or 4%.

In order to study the flow of the suspension through the burner tube in the absence of flames, particle-track photographs were taken for several values of concentration and burner flowrate using the procedure just described, but omitting ignition of the flame.

2. Temperature Measurements.

A few measurements of flame temperatures were made using a platinum - 13% rhodium-platinum thermocouple. The thermocouple wires were 0.001 in. in diameter.

To measure flame temperatures, a flame was first stabilized, and the suspension concentration and flowrate were measured in the usual manner. The suspension was then re-ignited, and the thermocouple junction was moved into position in the flame, just above the flamefront. Whilst the thermocouple ^e.m.f. was read on a millivoltmeter, a photograph ^P_λ of the flame was taken to give the position of the thermocouple junction relative to the flamefront.

A temperature profile of the flow approaching the flamefront was obtained in the following manner. The thermocouple was mounted on a screw movement, so that it could be moved vertically along the axis of the burner tube.

A telescope fitted with an eyepiece graticule carrying a vertical scale was used to measure the heights of the thermocouple junction and the centre of the flamefront

above a fixed datum. When conditions of concentration and flowrate which gave a suitable flame had been established, the flame was extinguished, and the burner cleaned, then the thermocouple junction was positioned on the axis of the burner tube, just clear of the top of the tube. The suspension was ignited, and a millivoltmeter reading was taken simultaneously with a telescope reading of the thermocouple and flame-front positions. The thermocouple was then moved vertically through two turns of the screw movement, and the telescope and millivoltmeter readings were taken again. This procedure was repeated until the thermocouple was in the flame. The presence of the thermocouple caused some instability in the flame, which oscillated in a vertical direction, and on this account it was impossible to obtain precise readings of temperature or positions. When the thermocouple was moved up into the flame-front, the latter moved down about 2 mm., so that no temperature reading could be obtained immediately above the flame-front.

3. Flame Quenching Measurements.

Flame quenching in the 10.9 mm. diameter burner tube was investigated by the following procedure. The suspension concentration and flowrate were adjusted to permit a flame to be stabilised on the burner tube. The flame was blown

out, and the suspension flowrate was gradually reduced by slowly opening the exhaust flow needle valve. At intervals a 1 in. long gas pilot flame was passed slowly over the top of the burner tube, to see if the flame would flash back into the tube. When a flame flashed back for some distance along the burner tube, the suspension concentration and flowrate were measured, then the tube and gauze were cleaned, and a series of ten ignitions was carried out for these conditions. Each ignition was carried out as follows. The exhaust valve bypass was closed, and when a steady stream of suspension was issuing from the burner tube, the gas pilot flame was passed slowly over the mouth of the tube. The approximate distance for which the flame propagated down the tube was noted. The bypass was then opened. Intervals of at least ten seconds were allowed between ignitions, which was sufficient to prevent the tube becoming hot to the touch, and the tube was brushed clean at frequent intervals.

With the 10.9 mm. diameter burner tube, the flame did not flash back along the whole length of the tube under any of the conditions of concentration and flowrate obtainable, but was quenched after passing a few cm. down it. The apparatus was therefore modified slightly to allow a tube of larger diameter to be fitted, in an attempt to obtain flame propagation along the whole length of the tube (14.5 cm.) A flame trap gauze, 24-mesh and made of 0.002 in. diameter aluminium wire was fitted to this tube, in a similar manner to that used with the 10.9 mm. tube.

With the larger tube of 13.5 mm. internal diameter, it was possible to obtain flame propagation along the whole of its length; the flame flashed back as far as the gauze at the bottom of the tube, and then continued to burn steadily in the tube above the gauze.

CHAPTER 5.

Results and Calculations.

1. Lycopodium Flames Stabilised on the 10.9mm. Burner.

As already mentioned in Chapter 4, flames were stabilised on the 10.9mm. diameter burner tube in the range of \bar{C}_k values from 125 mg/litre to 185 mg/litre. (\bar{C}_k , the mean kinetic concentration, represents the mass flow of particles up the burner tube divided by the volumetric air flow up the tube; see p. 58). No flames could be stabilised at concentrations less than the lower figure, and the apparatus was unsuitable for the production of suspensions with \bar{C}_k values above about 190 mg/litre. The general characteristics of these flames were as follows.

At values of \bar{C}_k between 125 mg/litre and about 135 mg/litre, flames tended to be unstable, and frequently went out abruptly. They could not be stabilised close to the burner rim, but burned with the flame-front several millimetres above it, e.g. plate P36, fig. 28. The flame-fronts were blue in colour, and usually flat or saucer-shaped in profile. Above the flame-front, the tracks of individual burning particles could be distinguished within the flame envelope. If the flowrate of suspension was gradually increased, the flame would move further away from the burner until it became unstable and went out; in some cases flames were stabilised for brief periods with their fronts more than 1 cm above the burner rim. If the suspension flowrate was gradually reduced,

the flame moved down towards the burner, becoming smaller and going out when the front was of the order of 0.1 cm. above the burner rim.

Flames in the approximate range of \bar{C}_k from 135 mg/litre to 170 mg/litre burned more steadily than the leaner flames, were more luminous, and could be stabilised closer to the burner rim, with dead spaces between the flame-front and the rim of the order of 0.1 cm. By adjustment of the burner flow, the flame-front could be made practically flat, e.g. plate P27, fig. 29. If the burner flow was then increased, the central portion of the flame-front moved upwards, and the whole flame became much more luminous, resembling a gaseous diffusion flame. No inner cone of the Bunsen type could be observed through the luminous outer envelope, and only the periphery of the blue flame-front remained visible. These flames became very irregular in shape as the central portion of the flame-front lifted.

Flames for values of \bar{C}_k greater than about 170 mg/litre showed a type of behaviour not observed at lower concentrations; when first ignited they were similar in appearance to those in the intermediate range of concentration just described, but when the burner flow was adjusted to give a flat flame-front, after burning for $\frac{1}{2}$ min. or so, the periphery of the flame-front gradually moved down on to the burner rim, so that the flame-front itself took on the shape of a shallow cone, similar to a Bunsen cone of wide

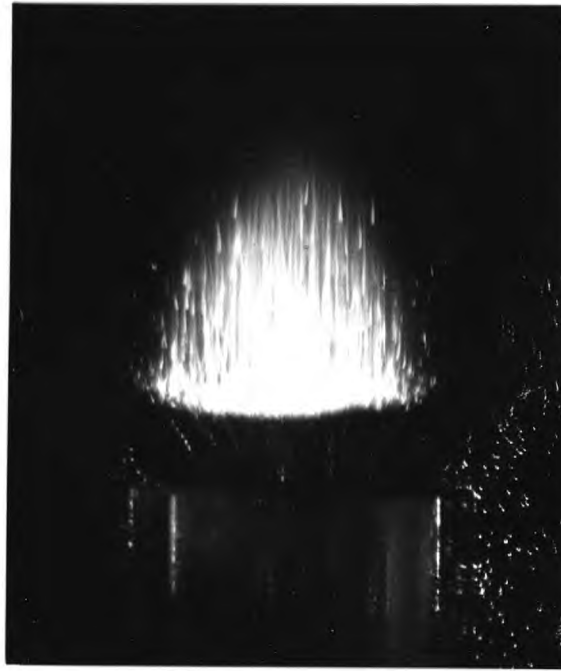


Plate P.36

$$\bar{c}_k = 133 \text{ mg/litre}$$

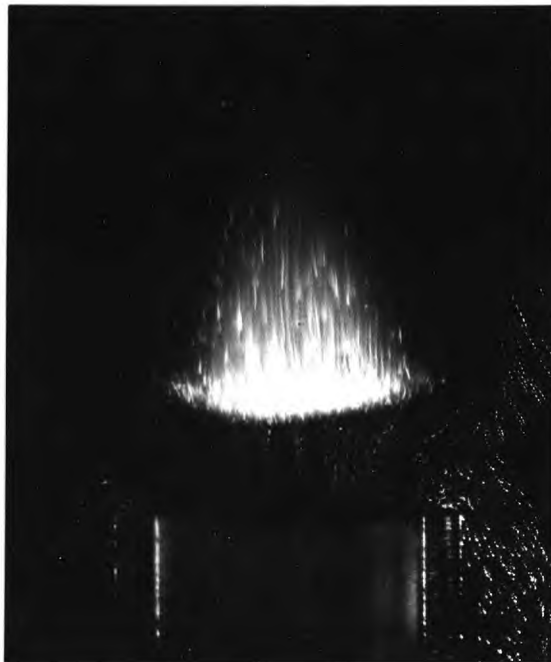


Plate P.43

$$\bar{c}_k = 149 \text{ mg/litre}$$

Fig.28. Examples of Lycopodium Flames.

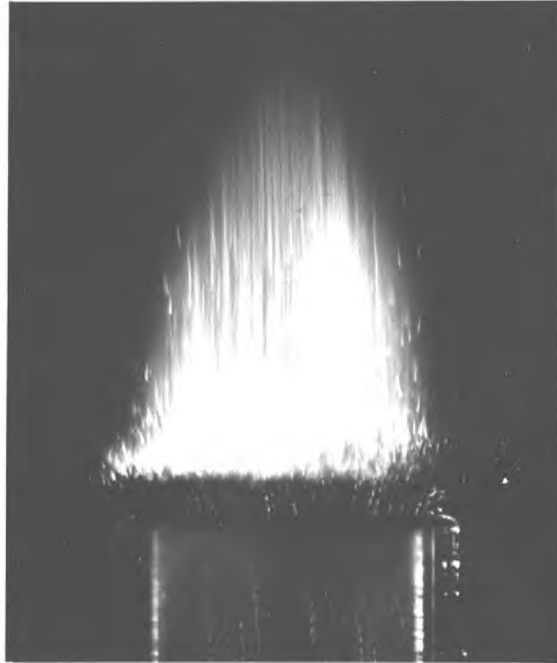


Plate P.27

$\bar{C}_k = 156 \text{ mg/litre}$

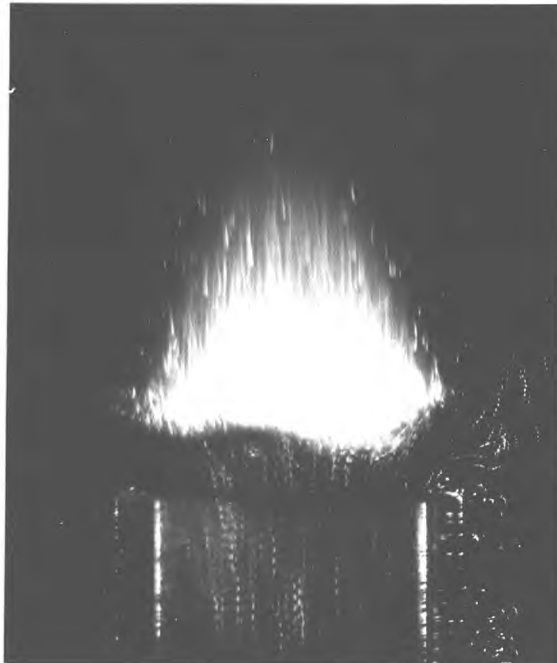


Plate P.50

$\bar{C}_k = 159 \text{ mg/litre}$

Fig. 29 Examples of Lycopodium Flames

angle. This cone was somewhat unsteady, and fluctuated in shape, so these flames were not suitable for the measurement of burning velocity. In this condition, the dead space at the burner rim appeared to be of the same order as for a gas flame. When the burner flowrate was gradually reduced, the flame moved slowly back into the burner tube, where it continued to burn with a smoky red flame.

2. Analysis of Particle Track Photographs.

In analysing particle track photographs of gas flames, it is assumed that the particles accurately follow the gas flow-lines. The particles used in such work are mostly of the order of 5μ in diameter, in which case this assumption does not involve serious error. In the present case, since the lycopodium particles are about 30μ in diameter, inertial effects are more important, and the particles would be expected to deviate from the air flow-lines where the latter are sharply curved. However, since the calculation of particle trajectories was quite impracticable, it was necessary to assume that the particle tracks followed air flow-lines for the purpose of analysis. Since in laminar dust flames there is usually an appreciable relative motion between the dust particles and the air, the burning velocity of the suspension may be defined using either the air velocity or the particle velocity. In the present case a burning velocity based on the air velocity was chosen, following Long.³¹

The analysis of the photographs was carried out as

follows. As the analysis assumes symmetry of the flame about the burner tube axis, all photographs showing markedly asymmetrical flames were rejected as unsuitable. The remaining photographs were enlarged to ten times actual size, and printed on extra hard bromide paper. Three prints, using different exposure times, were made from each plate, as it was found that comparison of several prints facilitated identification and measurement of the tracks. Co-ordinate axes were drawn on each print, as shown in fig. 30a, the y-axis was drawn along the tube axis, and the x-axis 1 in. below the top of the tube. Particle tracks were picked out and measured, using spring-bow dividers. In most cases the clearly defined portion of a track included at least two cycles, where a cycle is taken as the distance between the commencements or terminations of successive streaks. (fig. 30b). The information noted for each track consisted of the mean length of cycle for the track, the inclination of the track to the x-axis, and the co-ordinates of its commencement. Velocity profiles of the flow were then constructed from these measurements. In order to construct a profile, it was necessary that a sufficient number of tracks distributed over the cross-section of the flow should commence at similar values of y. The longest particle tracks on any of the photographs were just over 1 cm. in length on the print, and it was found by measuring the length of successive cycles in these tracks that no significant

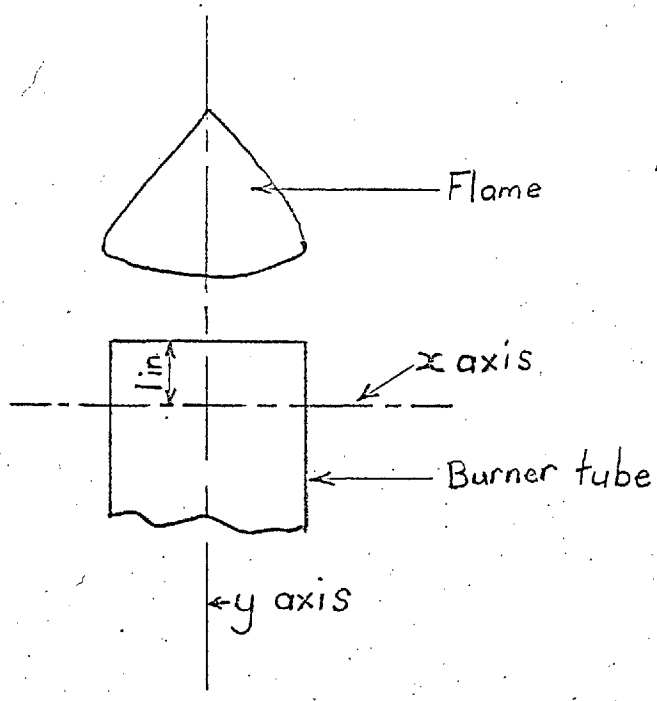


Fig. 30a Position of Axes on Flame Photographs

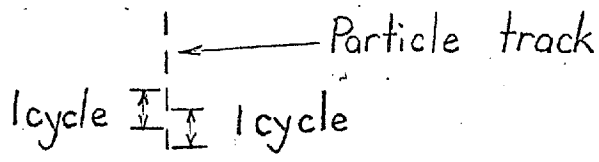


Fig. 30b Cycles in a Particle Track

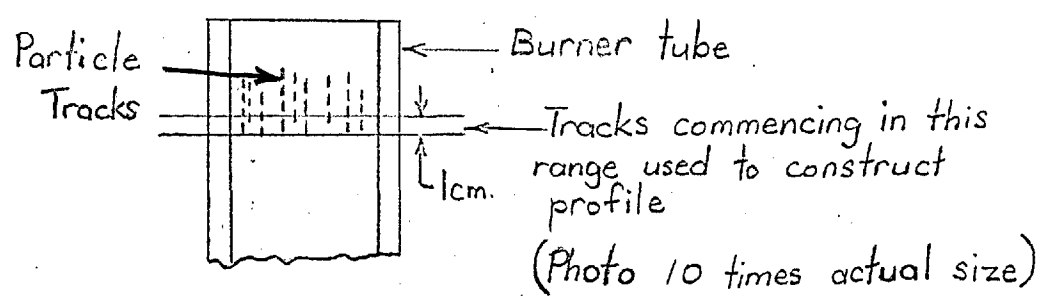


Fig. 30c

Fig. 30 Particle Track Measurements

change in velocity took place over the length of the track, except in^{the} case of some tracks actually entering the flame-front. It was therefore considered that a velocity profile could legitimately be constructed from tracks commencing in a 1 cm. range of values of y on the print (fig. 30c), provided that the profile was not too close to the flame-front. Values of y were chosen to utilise the maximum number of available tracks in each case. In constructing the profiles, the vertical components of the measured particle velocities were taken, and the settling velocity of lycopodium (taken as 2 cm/sec. - see chapter 3) was added, to give the vertical components of the air velocities. The resulting velocity profile of the air flow was taken to apply at a cross-section having a y -co-ordinate equal to the mean of the y values at the commencements of the tracks used in constructing the profile.

It was found that the majority of the flame photographs did not show a sufficient number of clearly defined tracks for any velocity profile to be obtained, and therefore could not be analysed. Of over 30 photographs taken, only eight proved suitable for detailed analysis. One photograph taken in the absence of a flame, P.59, was also analysed. The particle tracks were very poorly defined for suspensions with \bar{C}_k values greater than about 160 mg/litre, and as a result none of the flames burnt at concentrations higher than this could be analysed.

Figs. 31 and 32 show velocity profiles typical of those obtained. In some cases it was possible to obtain two or three profiles at different cross-sections of the same flow. When the profiles had been constructed, the procedure was as follows. In the case of the flow sketched in fig. 33, profiles were obtained for the sections y_1 and y_2 . Several stream-tubes of different diameters, co-axial with the burner tube, were marked on the print at section y_1 and these were extended from y_1 to y_2 and then on to the flame-front by sketching along the particle-tracks on the print. The outermost stream-tube was constructed so that it just embraced the whole flame-front; this was done by starting from the edges of the flame-front, and sketching back down the particle-tracks to sections y_2 and y_1 . Assuming that the particles follow the air flow-lines, the flow along each of these stream-tubes remains constant from section y_1 to the flame-front. The air flow through each of these stream-tubes was calculated at section y_1 by graphical integration of the velocity profile for this section over the appropriate diameters measured from the print, and the calculation was repeated for section y_2 . (The prints were ten times actual size). Comparison of the two values thus obtained for the flow through each stream-tube gave an indication of the accuracy of the method; some of the results for P.39 are set out in Table III as an example.

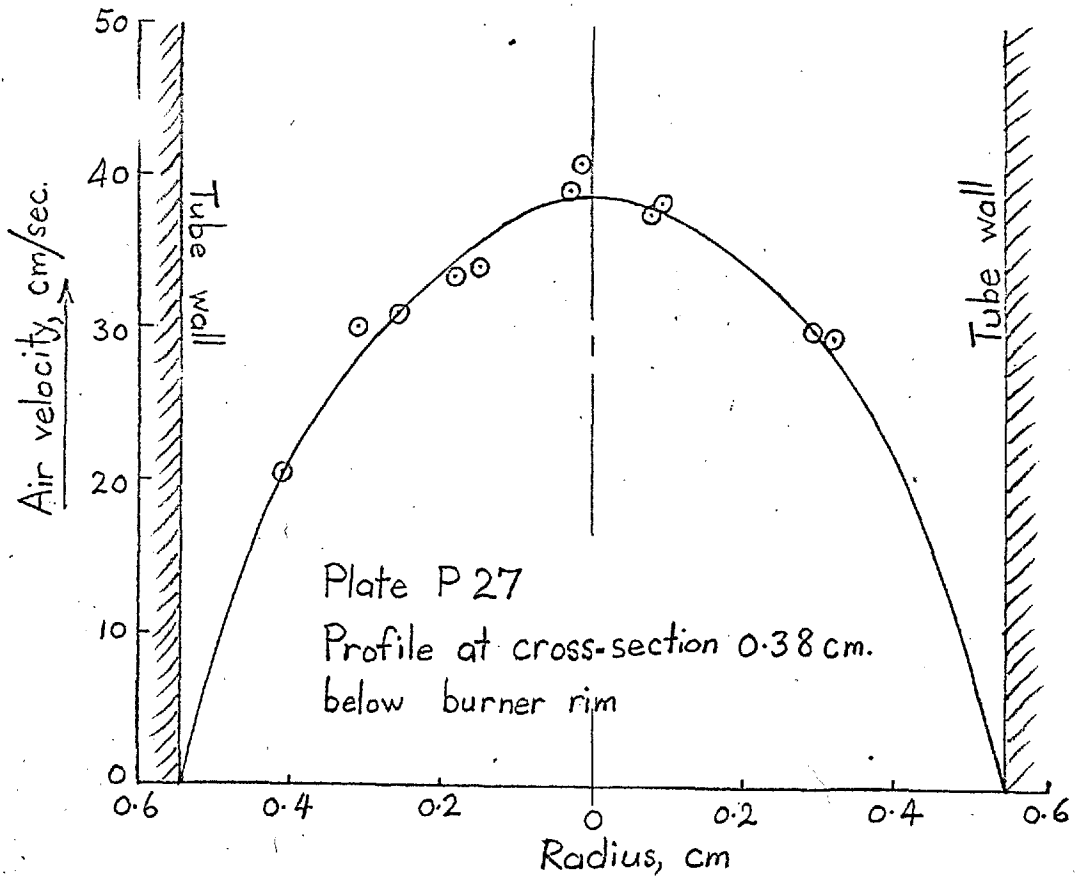


Fig. 31a. Velocity profile - Plate P27, (with flame)

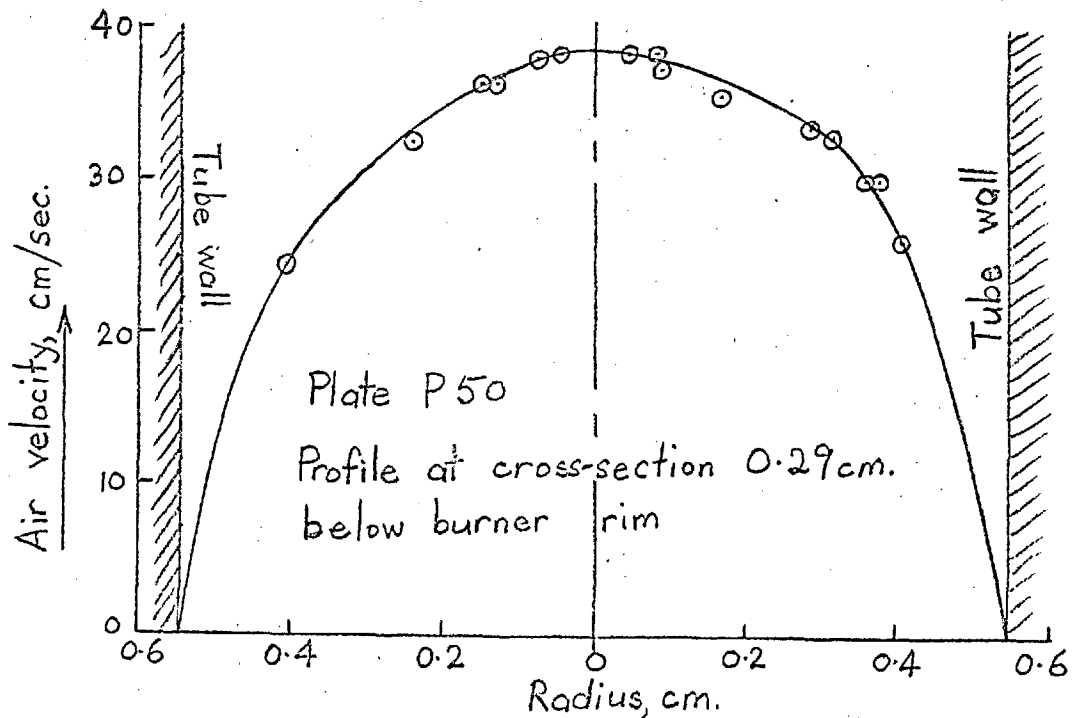


Fig. 31b. Velocity profile - Plate P50, (with flame)

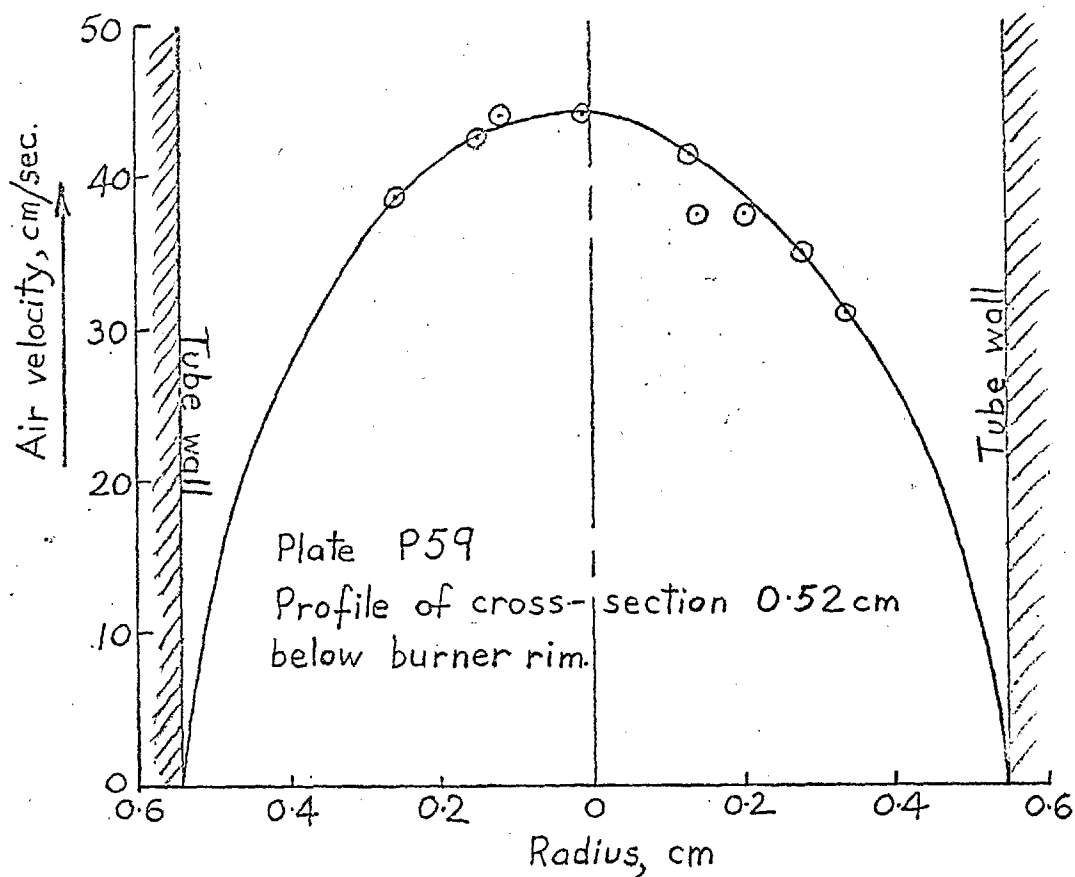


Fig 32a. Velocity profile, Plate P59 (no flame)

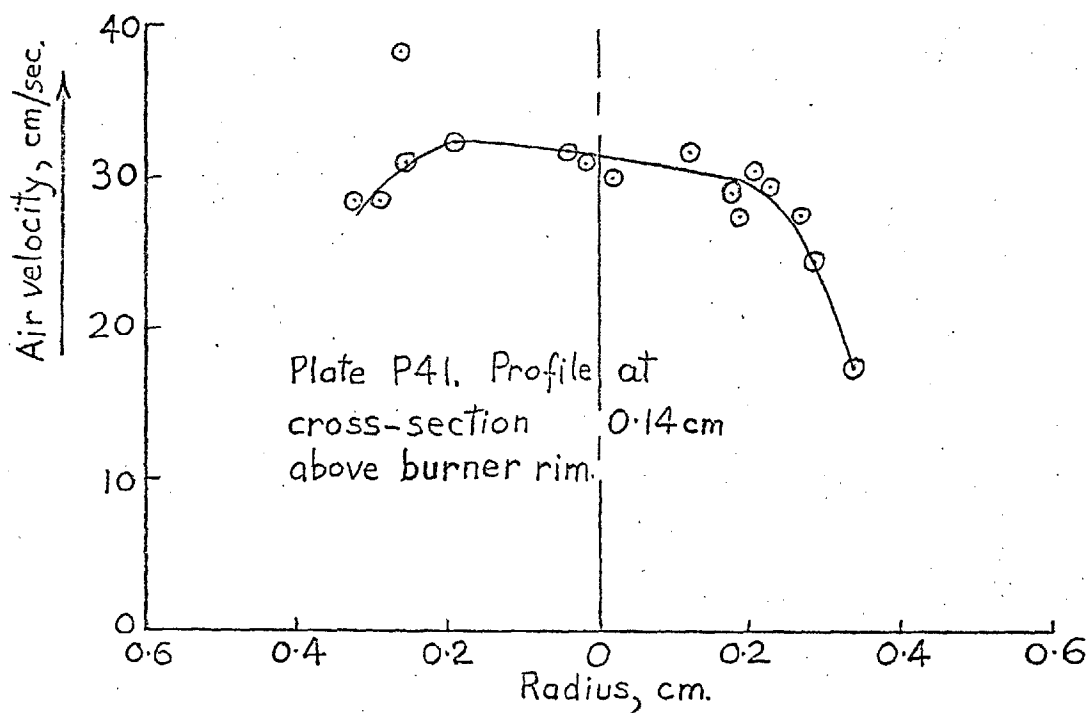


Fig 32b. Velocity profile, Plate P41, (with flame)

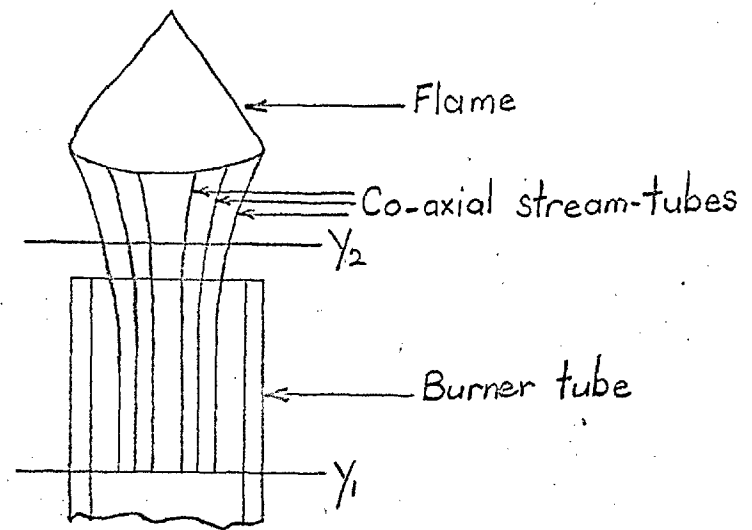


Fig. 33 Position of Stream-tubes on Photographs

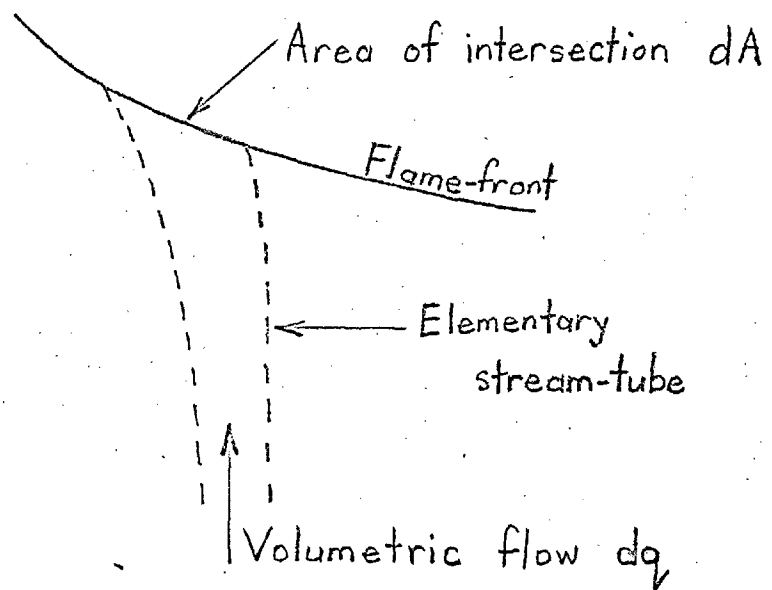


Fig. 34 Definition of S_u

Table III
Flows in Stream-tubes for P 39.

	Diameter of Stream-tube at section y_1 (cm.)	Calculated Flow in Stream-tube:-	
		at section y_1 (cm ³ /sec)	at section y_2 (cm ³ /sec)
1.	0.2	1.16	1.13
2.	0.3	2.60	2.77
3.	0.4	4.64	4.50

The diameters given in the table refer to the actual size, not the dimensions on the print. It is seen that the largest discrepancy between the two flow values obtained for a stream-tube was about 7%. The main sources of this inaccuracy were probably (a) the difficulty of sketching in the stream-tubes precisely, and (b) the difficulty of constructing the velocity profiles owing to the scatter of the individual particle velocities.

The variation in local burning velocity over the flame-front was calculated as follows. With the convention adopted, the burning velocity, S_u , is defined as the component of the cold air velocity perpendicular to the flame-front. (This definition is based on that for a pre-mixed gas flame.) Considering a small area of the flame-front dA cut by an elementary stream-tube, as in fig. 34, if the volumetric air flow along the tube based on ambient

conditions is dq , then the burning velocity over area dA is given by dq/dA . The volumetric air flows calculated for the stream-tubes were based on ambient conditions, since the velocity profiles used were sufficiently far from the flame to be at atmospheric temperature, according to the temperature profile given below. From the stream-tube flows, the air flows into the central area of the flame-front a_1 , and the annular areas a_2 , a_3 , a_4 (shown in section in fig. 35) were obtained. The areas themselves were obtained from measurements made on the print; where necessary allowance was made for the curvature of the flame-front by approximating its shape to that of a portion of a sphere. Division of the flows by the corresponding areas gave the mean burning velocities over the zones a_1 , a_2 , a_3 , a_4 of the flame-front. The results for each flame are given in graphical form in fig. 36, where the burning velocities for each zone are plotted against the mean radius of the zone; e.g. for P.39, the central zone of the flame-front, corresponding to a_1 , has a radius of 0.165 cm, and the mean radius was therefore taken as 0.083 cm; the annular area corresponding to a_2 has an inner radius of 0.165 cm and an outer radius of 0.331 cm, the mean of which is 0.248 cm. The outer edge of the flame is shown in each case.

The overall burning velocity for each flame, \bar{S}_u , was obtained by dividing the total air flow into the flame-front.

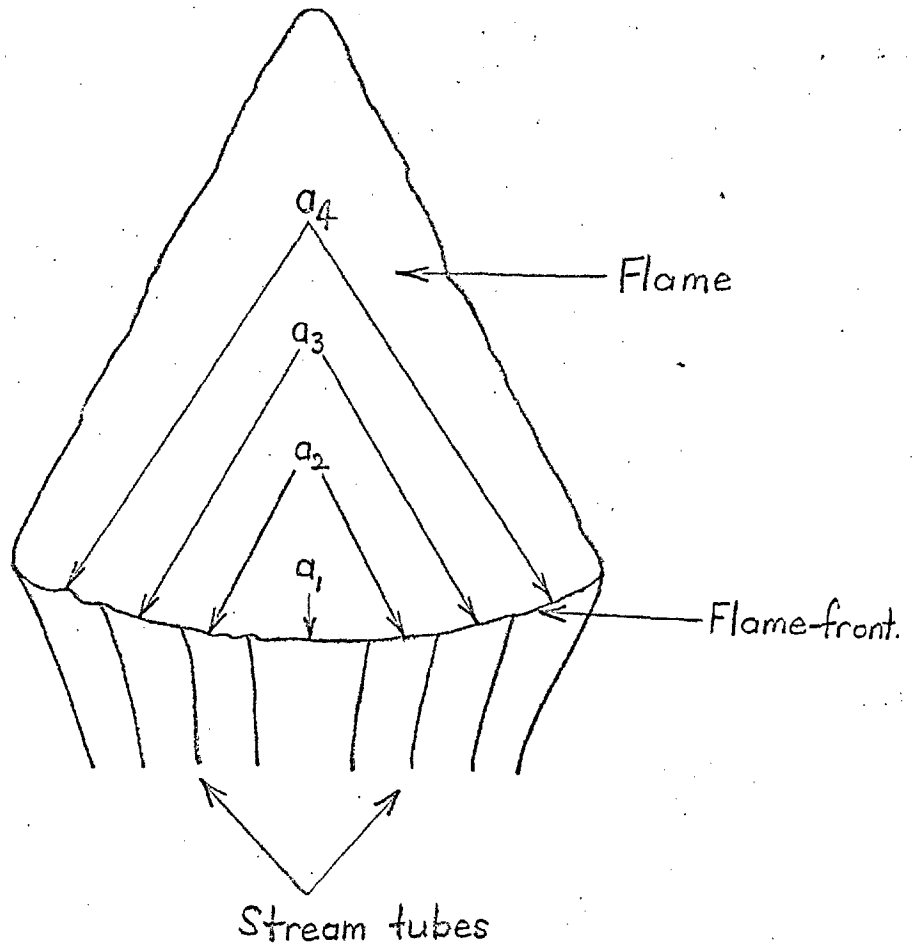


Fig.35 Areas of flame-front cut off by Stream-tubes

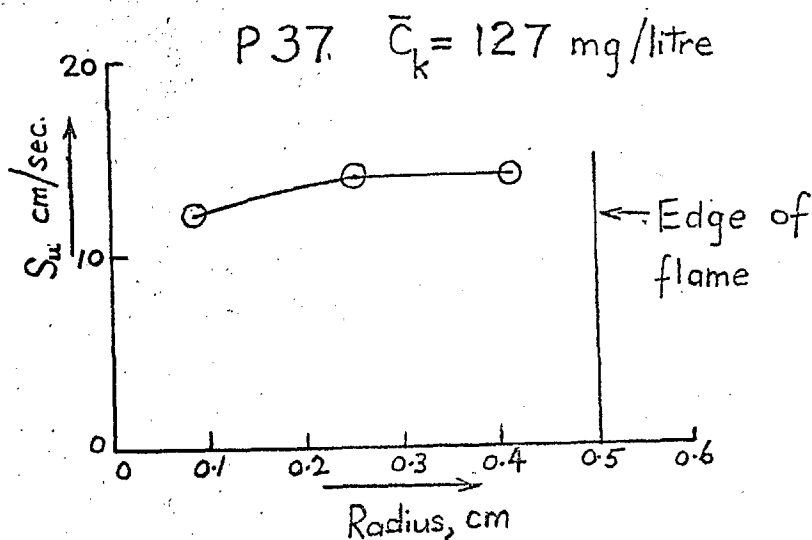
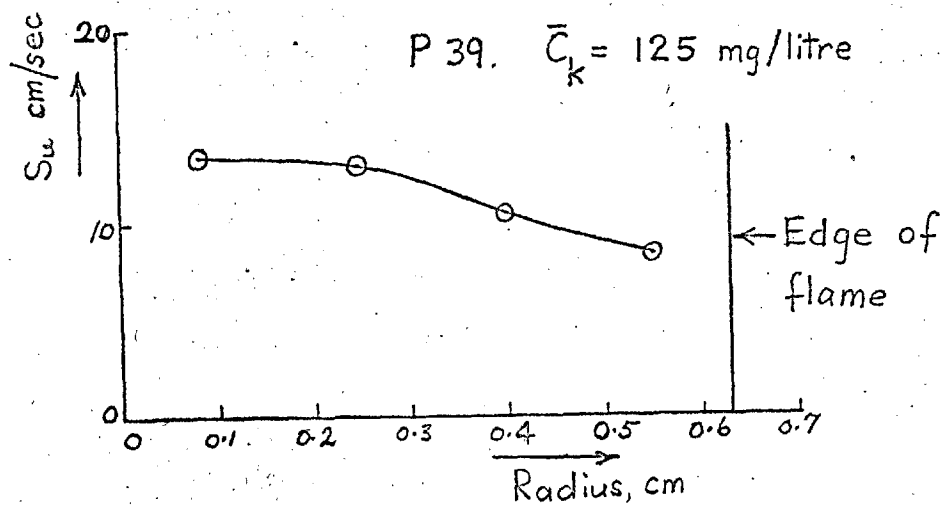


Fig 36. Variation of S_u over flamefronts (i)

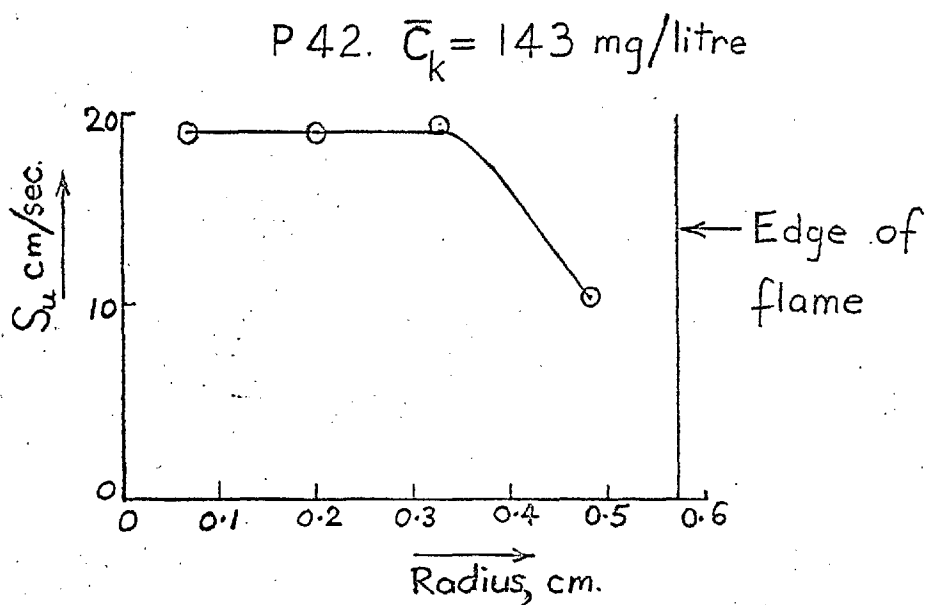
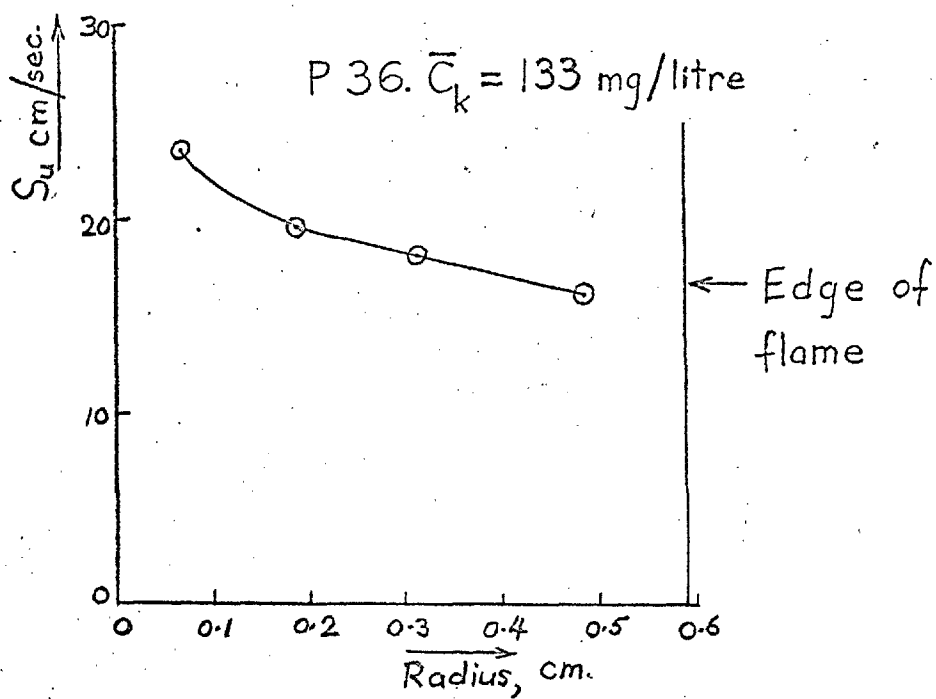


Fig. 36. Variation of S_u over flamefronts. (ii)

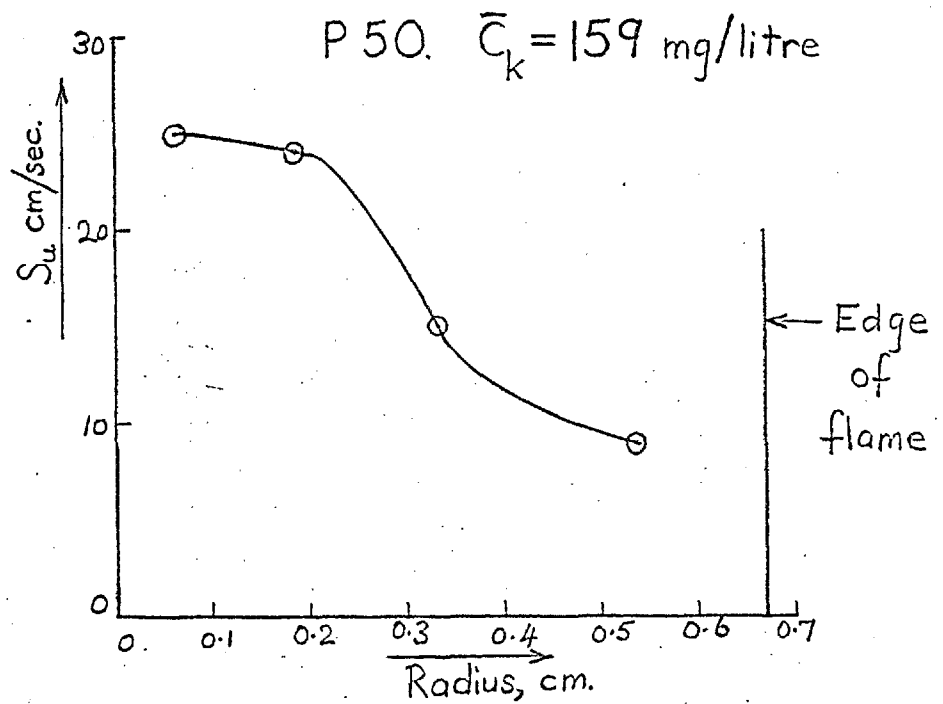
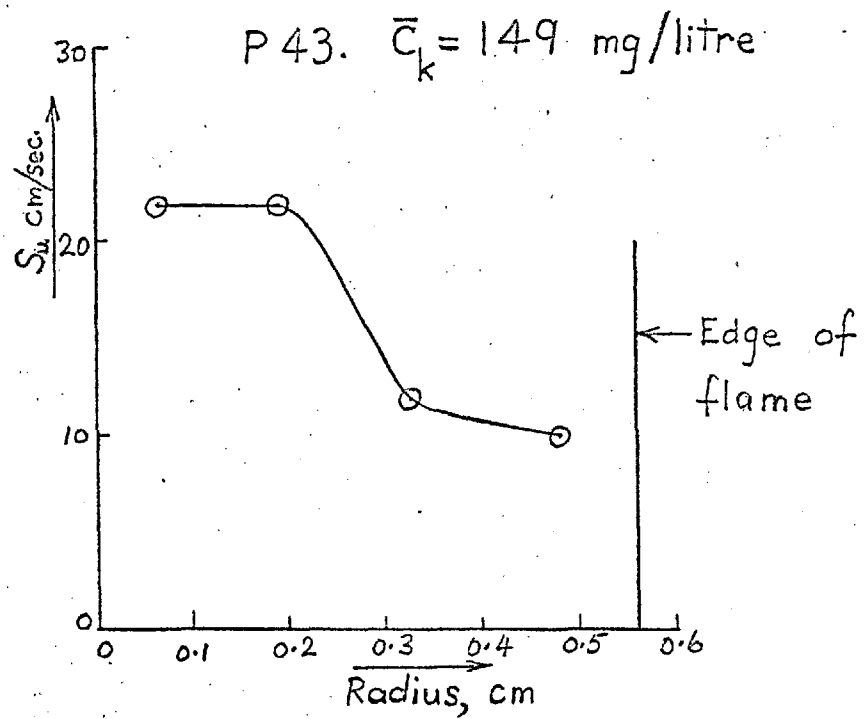


Fig. 36. Variation of S_u over flamefronts (iii)

by the total area of the flame-front.

The information obtained from measurement and analysis of the particle-track photograph^s, apart from the local burning velocities plotted in fig. 36, is summarised in Table IV (p.128). This gives the mean kinetic concentration (\bar{C}_k), the burner flowrate (q), the overall burning velocity (\bar{S}_u), the flamefront area (A) and the vertical height (h_1) of the lowest point of the flame-front above the burner rim. In fig. 37 the maximum local burning velocity for each flame (S_{max}) is plotted against \bar{C}_k . From the figures given in Table III for P39, it appears that the values of local and overall burning velocities obtained may be accurate to the order of $\pm 10\%$.

3. Temperature Measurements.

In Table V which gives the results of the thermocouple measurements, the following symbols are used, in addition to those already defined:-

T . is the temperature given by the thermocouple.

h_2 is the vertical co-ordinate of the thermocouple junction relative to the flamefront, + signifying above the flamefront and - below, e.g. + 2mm. indicates that the junction was 2mm. vertically above the flamefront, and - 2 mm. that it was 2 mm. below the flamefront.

No correction for heat losses by radiation has been made to the thermocouple temperature, as it is difficult to allow for the effect of the particles present.

TABLE IV.

Data from Analyses of Particle-Track Photographs.

Photograph.	\bar{C}_k (mg/litre)	q (litres/min)	\bar{S}_u (cm/sec)	A_2 (cm)	h_1 (cm)
P.27	156	1.37	- *	1.31	0.15
P.36	133	1.43	13.0	1.09	0.28
P.37	127	1.51	- *	0.81	0.41
P.39	125	1.50	11.0	1.22	0.58
P.41	127	1.39	- *	1.74	0.69
P.42	143	1.53	14.5	1.01	0.32
P.43	149	1.54	14.0	1.01	0.34
P.50	159	1.40	12.5	1.39	0.22
P.59	125	1.58	- No flame -		

* In these cases the particle tracks near the edge of the flame were too indistinct to permit the evaluation of \bar{S}_u

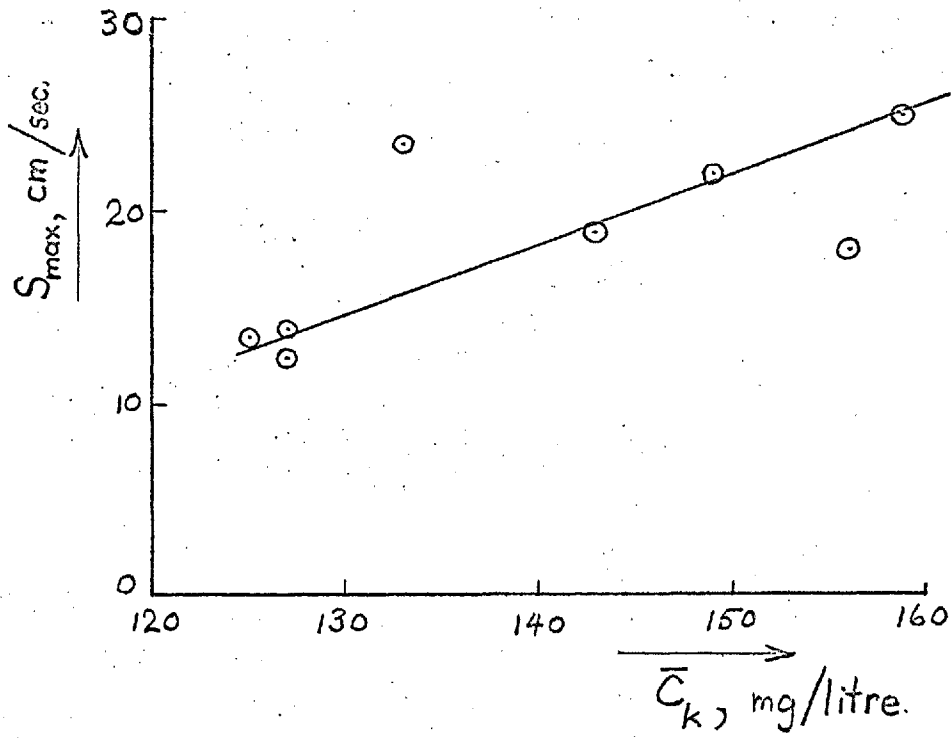


Fig. 37. Variation of S_{\max} with \bar{C}_k

Table V Flame Temperatures.

\bar{C}_k (mg/litre.)	q (litres/min.)	h_2 (mm.)	T (°C)
143	1.53	+1.9	1550
150	1.23	+1.5	1550
163	1.19	+1.5	1510

Table VI . Temperature Profiles.

	\bar{C}_k (mg/litre.)	q (litres/min.)	h_2 (mm.)	T (°C)
Flame A	143	1.53	-0.6 to -0.9	52
			-0.3 to 0	1180
			+1.9	1550
Flame B	137	1.56	-1.9 to -2.6	20
			-1.3 to -0.9	68
			-0.3 to -0.6	750

Adiabatic Flame Temperature.

In order to obtain an adiabatic flame temperature for comparison with the values given above, the calorific value of the lycopodium was measured in a bomb calorimeter. This measurement yielded a gross calorific value of 7500 cal/g. and a net value of 7000 cal/g for lycopodium containing 3% moisture.

Analysis of the lycopodium gave the following ultimate composition:-

Carbon	65.3% by weight
Hydrogen	9.6% " "
Nitrogen	1.1% " "
Moisture	3.0% " "
Oxygen	21.0% " " (by difference)

This analysis agrees closely with that given by Line, Rhodes and Gilmer⁴⁷, who also determined the ash content as 1% by weight. The moisture content of the lycopodium as burnt was about 5%; making the necessary corrections, it appears that the stoichiometric concentration of the suspension under ambient conditions of 20°C and 760 mm. is 124 mg/litre. The adiabatic flame temperature of this mixture was calculated using the graphical method of Underwood⁶⁰, which gave a value of 1970°C. As no value could be found for the heat required to volatilise lycopodium, a value of 100 cal/g. was assumed for this calculation.

4. Quenching Measurements.

The suspensions emerging from the burner tubes were ignited by passing a 1 in. long gas diffusion flame over the top of the tubes. The distances the resulting flames travelled down the tubes are given in Table VIII.

Table VIII Flame Propagation in Tubes.

Burner Tube.	\bar{c}_k (mg/litre)	q (litres/min)	Results of 10 trials
11 mm. bore	140	0.63	All propagated between 2 cm. & 4 cm. down tube
11 mm. bore	123	0.545	7 propagated less than 0.5 cm., 3 propagated 1 to 2 cm.
13.5 mm. bore	128	1.11	5 propagated 2.5 cm., 3 propagated 4 cm., 2 propagated whole length of tube, and continued to burn on gauze at bottom.

5. Refraction by the tube wall.

In order to find if refraction by the burner wall caused the particle tracks to appear at a position significantly different from their actual position, the following experiment was carried out. The actual burner tube was not available, but a tube of similar dimensions was used. Equally spaced lines were scribed lengthwise on a strip of brass having a width equal to the tube bore, and the strip was inserted into one end of the tube, so that a portion of it remained sticking out (fig.38). The scribed lines were thus in the same position as the zone of illuminated particles. A travelling microscope was set up and used to observe the position of the lines and the edges of the strip as they appeared out side and inside the tube. The greatest apparent displacement of the lines by refraction occurred at the edges of the strip; however, the particle tracks used in analysing the photographs all lay within 0.45 cm of the tube axis, and it was found that in this region the maximum error of position due to refraction was 0.011 cm. This error can be neglected in comparison with the other errors involved in the measurements.

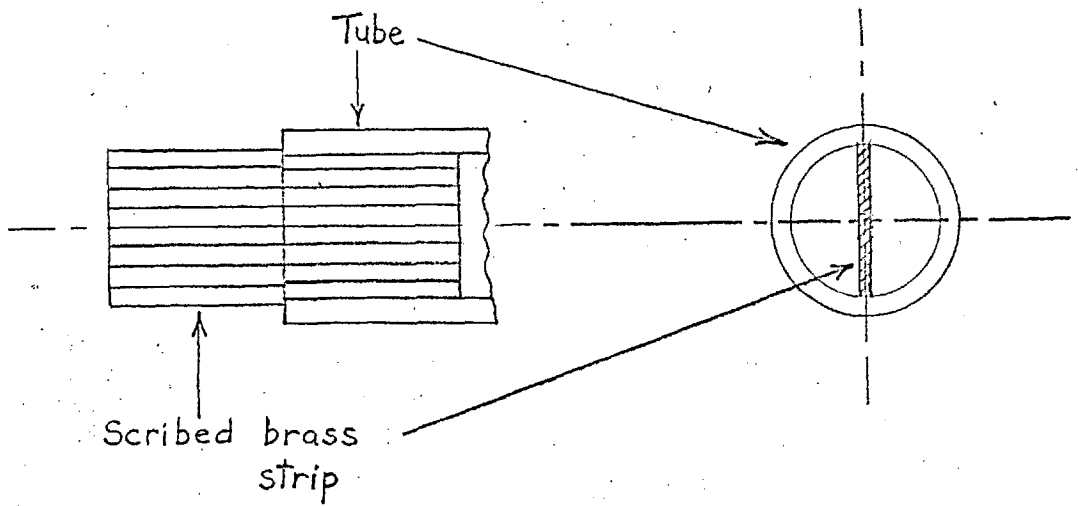


Fig. 38. Measurement of refraction at tube wall.

CHAPTER 6.

Discussion and Conclusions.

The significance of the experimental results obtained will be discussed under three main headings:-

- 1). Performance of the dust dispersing system.
- 2). The flow of dust suspensions in tubes,
- 3). Dust flames.

1. Performance of the dust dispersing system.

The dust dispersing system developed for carrying out flame studies proved to be simple and flexible in operation. Mean kinetic concentrations up to about 190 mg. of lycopodium per litre could be obtained with burner flows in the neighbourhood of 1.5 litres/min. (The kinetic concentration of the burning suspension considerably exceeded the mean kinetic concentration of the whole flow, for reasons which will be discussed later.) The dispersion apparatus was very compact in comparison with systems using hoppers and mechanical conveyors, and the quantity of dust required to produce a flame was as little as 15g. The concentrations of the suspensions produced, measured over 1-minute sampling periods, remained constant to within 3 to 4% for up to 30 mins. Flames could only be burnt for periods of about $\frac{1}{2}$ minute, since over longer periods the accumulation of dust on the burner rim was sufficient to cause disturbances of the flow pattern, leading to asymmetry of the flame. However, this difficulty is common to all forms of apparatus

for burning laminar dust flames.

The elutriation of particles from a fluidised bed is essentially an unsteady process, since it takes place by the bursting of 'bubbles' at the surface of the bed. In the transition zone above the bed, the local concentration and velocity of the suspension fluctuate rapidly. Above the transition zone these fluctuations die out, and the flow of suspension appears homogeneous to the eye. However, it is possible that small fluctuations persist in the apparently uniform flow, and affect the stability of the flames. Since the concentrations were measured by sampling over a period of 1 minute, such fluctuations would not affect the measured concentration values significantly if their durations were only of the order of 1 second or so. It was observed that flames burning at concentrations near the lower limit of stability tended to go out abruptly, (p.109), and it seems likely that small fluctuations in suspension concentration were responsible for this. The flames burning at higher concentrations, which were more stable in position and shape (p.110), were evidently less sensitive to any fluctuations.

Mean kinetic concentrations greater than about 190 mg/litre could not be obtained without increasing either the fluidising air flow or the bed depth to values which caused instability of the suspension in the cone. This limitation was produced by the dimensions of the apparatus rather than the dispersion method itself. Higher concentrations could

have been obtained by increasing the overall height of the cylindrical column and the cone. These modifications would permit the use of higher fluidising velocities or deeper beds.

The kinetic concentrations of the suspensions produced were found to be dependent on the burner flow-rate. At burner flows in the region of 1.2 to 1.5 litres/min., as required for stable flames, the mean kinetic concentration increased slightly with increase of burner flow. It will be demonstrated later that this effect is due to the settling of the particles relative to the air, and is therefore unavoidable.

Since the elutriation rate from a fluidised bed increases as a high power of the gas velocity through the bed (see p. 21), the concentration of the suspension produced was very sensitive to changes in the fluidising air flow. A fine-control needle valve was therefore desirable for controlling the latter; however, no valve of this type having the required pressure drop/flow characteristics was available, and the control valve actually used did not permit fine adjustment of the fluidising flow. It was therefore impracticable to maintain a constant kinetic concentration at the burner while varying the burner flow. Because of this limitation, it was not possible to study the effect of variation in the burner flow on flames burning at constant concentration.

At burner flows less than about 0.8 litres/min., the mean kinetic concentration at the burner fell off sharply with decreasing flow, in a manner similar to that shown by the sampling measurements given in fig. 15. (It should be noted that the latter were made with the earlier form of the apparatus, in which the sampling tube was of smaller diameter than the burner tube used later.) To obtain flash-back conditions for the quenching experiments it was necessary to use burner flows in the range 0.5 to 0.6 litres/min., and at these low flows only a narrow range of inflammable concentrations could be obtained, so that only a few measurements of quenching diameter could be made. For systematic measurements of quenching diameter, the apparatus would need to be modified to enable higher concentrations to be achieved, on the lines already suggested.

It has been pointed out (p.11) that local variations in the concentrations of flowing suspensions can easily arise. In the case of flames stabilised on burner tubes or nozzles, concentration differences may be set up during the flow of the suspension through the tube or nozzle. Most of the workers studying combustion in dust systems have made no attempt to check the uniformity of concentration of their suspensions, on account of the experimental difficulties involved. Since any variations in the suspension concentration arising during flow will have an important effect on the flame, the flow of dust suspensions in tubes will now be discussed in detail.

2. The flow of dust suspensions in tubes.

Information about the behaviour of suspensions in laminar

flow through tubes is given by (a) the experiments on sampling, reported on p.63 (figs. 14 and 15), (b) the experiments on tube flow described in chapter 3, and (c) the particle track photographs obtained as described in chapter 4. Since the presence of a flame stabilised on the burner tube affects the flow inside the tube to some extent, only the photograph P.59, (fig. 39), will be considered at present. This was the only photograph taken in the absence of a flame which was analysed in detail.

In interpreting any of the particle-track photographs, the following points must be borne in mind:-

- (i) The illuminated tracks lie in a narrow zone of the flow, whilst the entire flame appears in the photograph, since the burning particles are photographed by their own light.
- (ii) The intensity of the tracks depends to some extent on the orientation of the respective particles, which are irregular in shape.
- (iii) Refraction at the tube wall causes the initially parallel light beam to diverge slightly, so that it becomes wider and less intense as it crosses the tube, (from right to left in the photographs).
- (iv) The tube wall appears thicker on the photographs than is actually the case, owing to refraction effects (see p. 133).
- (v) The number of tracks intersecting a line of unit length drawn horizontally across the tube in any

part of the photograph is a function of both the local air velocity and the local particle concentration.

- (vi) The view of the illuminated zone of the suspension is partly obstructed by the suspension flowing in the portion of the tube between this zone and the camera. The thickness of this obstructing layer of suspension is greatest for tracks lying close to the tube axis, and least for those lying near the tube wall. It would therefore be expected that tracks lying near to the tube wall would appear the most clearly defined in the photographs.

A satisfactory account of the flow of suspension in the burner tube must take account of the following experimental data:-

- (a) The velocity profile of the flow measured from photograph P.59.
- (b) The existence of a region practically free of tracks near to the tube walls, as seen in photographs P.4 and P.59, (fig. 39.) This region was less prominent at the lower flowrates used for the sampling measurements described on p.63.
- (c) The behaviour of this apparently particle-free region as observed in the experiments on tube flow described in Chapter 3.
- (e) The variation of \bar{C}_k with tube flow observed in the sampling experiments, (fig. 15, p.64.)

Consider first the particle-free space adjacent to the tube walls, as seen in photographs P.4 and P.59. In the former, the light beam illuminating the tracks was about 1mm. wide, much wider than that used for the other photographs. The absence of tracks in this region may be due to (i) low air velocity near the walls, (ii) low particle concentration near the walls, or (iii) a combination of both these effects (see point (v) above.) Since the velocity profile is known for P.59, the effect of the local velocity on the number of tracks crossing different parts of the line $y = -0.27\text{cm}$ (i.e. the section for which the profile was measured) may be calculated. The calculation, details of which are given in Appendix A, was made on the assumption of uniform static concentration over the tube cross-section; the reason for this assumption will become apparent later. The line $y = -0.27\text{ cm}$, was divided up into 0.04cm lengths, and the number of particles crossing each of these lengths during the period of illumination (1/200 sec) was obtained. The results of this calculation are shown in Table VIII; column I gives the position of each 0.04cm length in terms of the distance of its ends from the tube axis, and column II gives the average number of particles crossing each length during the period of illumination.

Table VIII

Calculated Distribution of Particle Tracks for
Photograph P.59.

I	II
Distance from Tube Axis (cm.)	Average number of Tracks crossing length
0 - 0.04	1.9
0.04 - 0.08	1.9
0.08 - 0.12	1.9
0.12 - 0.16	1.8
0.16 - 0.20	1.7
0.20 - 0.24	1.7
0.24 - 0.28	1.6
0.28 - 0.32	1.5
0.32 - 0.36	1.4
0.36 - 0.40	1.2
0.40 - 0.44	1.1
0.44 - 0.48	0.9
0.48 - 0.52	0.6
0.52 - 0.55 (tube wall)	0.2

The results in Table VIII refer to one-half of the tube cross-section. The calculation therefore indicates that a total of about 39 particles should cross the line $y = -0.27$ cm. in the illuminated zone during the period of illumination ($1/200$ sec); this compares with about 26 tracks actually visible crossing this line on the photograph. The discrepancy is probably caused by the presence of agglomerates containing two or more

particles, (see p.68), and also by overlapping of tracks. This comparison indicates that the number of tracks actually visible on the photograph is about two-thirds of the calculated number. Now no track is visible crossing the line considered on either side of the photograph beyond a point 0.36 cm. from the tube axis, while from the calculation about 4 particles would be expected to cross in the illuminated zone beyond this point on either side of the photograph. This suggests that the assumption of uniform static concentration over the whole tube cross-section is invalid, and that the static concentration in the apparently particle-free region at the walls is much lower than elsewhere.

Particle-track photographs of flames burning several mm. above the burner rim show a particle-free space up to the top of the tube similar to that in P.59, e.g. P.56 and P.43, (fig. 28) but in the case of flames closer to the burner, e.g. P.50 (fig. 29) the particle flow-lines diverge to some extent within the topmost portion of the tube itself.

In accounting for this region of low particle concentration near the tube walls, the following factors may be important:-

- (a) Effects at the tube entrance, e.g. inertial effects causing the particles to follow paths different from the air flow-lines,
- (b) The convergence of the flow-lines towards the tube axis as the velocity profile becomes fully developed,
- (c) The Magnus effect, which would cause rotating



Plate P.4.



Plate P.59.

← Level of top of
burner tube

Fig 39. Flow of Suspension from the Burner Tube

particles to experience a force impelling them towards the tube axis,

- (d) At points very close to the tube wall, the upward air velocity is less than the settling velocity of lycopodium particles.

The contributions of these factors will be discussed in order.

(a) Effects at the tube entrance.

In the experiments with flames, direct observation of the flow at the burner tube entrance was not possible, as a result of the position of the cone. However, information about these flow conditions may be deduced from the observations on tube flow described in chapter 3. The sketch of the particle flow-lines at the entry to the plain tube given there, (fig. 24a), shows the particle-free space of the order of several mm. wide observed immediately below the tube rim. The result of an increase in the air flow was to reduce the width of this space (fig. 24b). This effect may be explained as follows. The situation is illustrated by the sketch in fig. 40, which shows the observed particle paths, (dotted), and the air flow lines (solid) inferred from the observed particle motion. Consider the air flow-line from point A onwards; the vertical velocity component of particles in the neighbourhood of point A is less than that of the air surrounding them, since they are settling with respect to it, whilst their horizontal velocity component is approximately equal to that of the

surrounding air, provided inertial effects are small. (It will be shown later that particle inertia effects are negligible in the present situation.) The particles therefore follow paths less steeply inclined to the horizontal than the air flow-lines from point A onwards. At point C, adjacent to the tube wall, the particles originally in the neighbourhood of the air flow-line at A are all some way below it, and as a result a particle-free space is present below the tube rim, and in the tube itself. An increase in the air flow through the system results in an increase of the vertical and horizontal velocity components of the air along the flow-line, so that the angle between the air and particle flow-lines is reduced. This reduces the thickness of the particle-free region below the tube rim. This corresponds to the effect observed experimentally (fig. 24b.)

A simple experiment was used to test the picture just suggested. If this explanation is valid, the width of the particle free space will increase with increase of the lateral distance the streamline moves from A to C in fig. 40. If the small-diameter tube is displaced to one side of the main tube as in fig. 41, the particle-free region should be reduced in width on the side where the lateral movement of the flow-lines is least, i.e. the right-hand side in the figure, and increased on the opposite side. This experiment was carried out using the same system as for the tube flow experiments described in chapter 3. It was found that using a flowrate of 2.0 litres/min, with the 13.5 mm. bore tube mounted as shown in fig. 41, the column of suspension

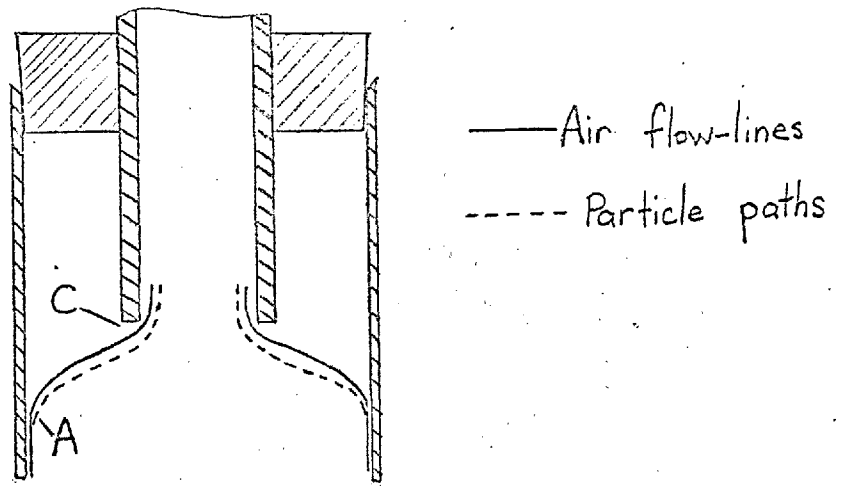


Fig. 40. Flow pattern at entry to plain tube

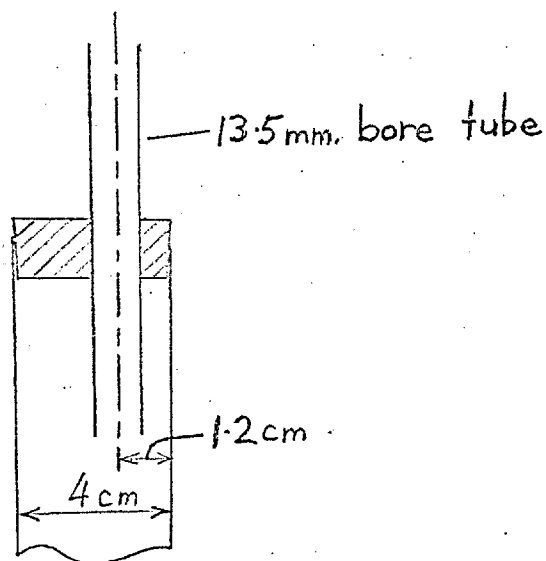


Fig. 41 Position of displaced outlet tube

emerging from the top of the latter was displaced towards the right-hand side as predicted. The widths of the particle-free spaces, measured at the top of the tube, were approximately 2mm. and 4.5mm. on the right-hand and left-hand sides respectively.

The observations made using the tube with the bell-mouthed entrance may be explained on a similar basis. The situation is sketched in fig. 42, which shows why the particle-free space was observed to be present from the widest part of the bell onwards. The shape of the air and particle flow-lines is basically similar to that for the plain tube, which explains why the diameters of the columns of suspension emerging from the two tubes were practically the same. (p. 88). Similar considerations apply in the case of the disc with an orifice.

The situation in the apparatus used for flame studies differed from that in the experiments just discussed, since in the former case only a portion (about a quarter) of the suspension flow from the bed passed into the burner tube. A tentative sketch of the flow pattern in the combustion apparatus is given in fig. 43. The upward velocity of the air at points DD just above the bottom of the burner tube is likely to be quite low, with the result that particles do not penetrate into this region. The settling of the particles relative to the air in the flow approaching the tube entrance will give rise to a particle-free space in the manner already described. With low flow-rates

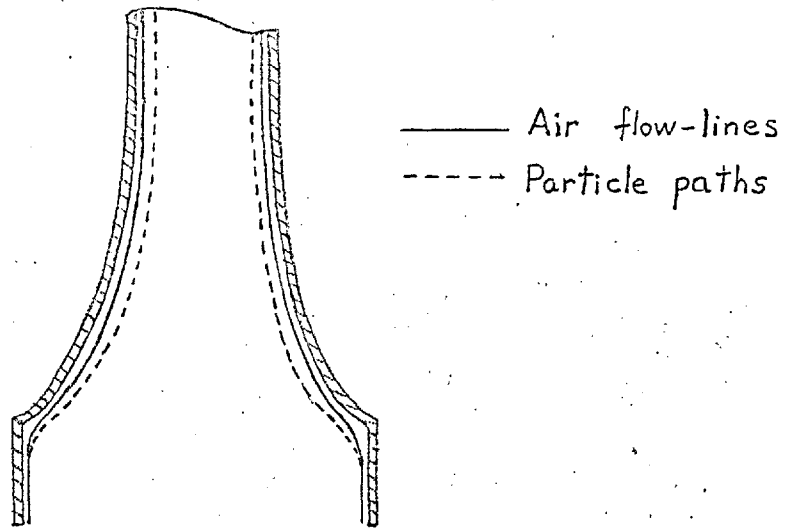


Fig. 42. Flow pattern at entry to bell-mouthed tube.

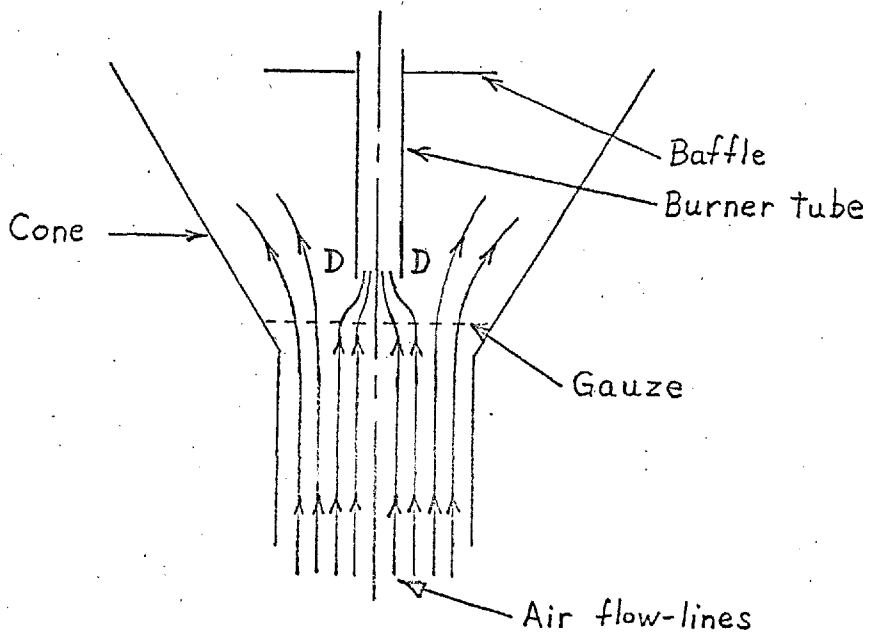


Fig 43. Flow pattern at entry to burner tube.

in the burner tube or sampling tube, the lateral displacement of the air flow-lines approaching the tube entry is small, and as a result the particle-free region is narrower. Thus it was observed that at low sampling flows the particle-free space was hardly noticeable. (p.66).

The entry effects just discussed are solely due to the settling of the particles relative to the air, and it has been assumed that particle inertia effects are negligible in this situation. This assumption will now be examined. The significance of particle inertia effects may be estimated by reference to the value of the particle parameter, P. The value of this dimensionless parameter gives an indication of the extent to which the path of a particle suspended in an air flow deviates from the air flow-line as a result of particle inertia when the air flow-line curves round an obstacle or into a sampling nozzle. (see e.g. RICHARDSON⁶¹.) The value of P may be expressed as:-

$$P = \frac{\rho d^2 U}{9D\eta}$$

where in the case of flow into a sampling tube, the symbols have the meanings:-

- ρ is the particle density,
- d is the particle diameter,
- U is the mean velocity in the sampling tube
- D is the sampling tube diameter,
- η is the air viscosity.

For values of P less than about $1/3$, in the viscous flow regime, inertial effects in sampling may be neglected, i.e. the particles will not deviate significantly from the air flow-lines as a result of their inertia.^{62, 63} It was found that the maximum value of P for any of the tube flow experiments carried out, including the flame studies, was 0.17. It appears, therefore, that effects due to particle inertia at the entrance to the sampling tube or burner tube were negligible in the present work.

b). Convergence of flow-lines in the tube.

The velocity at entry to the burner tube may be taken as substantially uniform over the tube cross-section, and a measured profile is available for a cross-section near the top of the tube. From these two profiles the radial displacement of an infinitesimal volume of air moving from one of these cross-sections to the other may readily be calculated, using continuity equations. Considering the outermost particle track visible in the tube on photograph P.59, which is at a radial distance of 0.43cm. from the tube axis, the radial displacement suffered by this particle in travelling from the tube entrance as a result of the convergence of the air flow-lines was calculated. (Appendix B.) It is shown that the air flow-tube having a radius of 0.43cm. at the top of the tube has a radius of 0.49cm. at the tube entrance. Hence in travelling up the tube, the outermost particles experience a radial displacement of 0.06cm. towards the tube axis as a result of convergence of the air flow lines.

C). The Magnus effect.

When spherical particles are suspended in a laminar flow of fluid having a velocity gradient, they experience a couple tending to make them rotate. It has been shown theoretically by JEFFREY⁶⁴ that the equilibrium angular velocity of a sphere rotating freely under the influence of this couple is given by $G/2$, where G is the velocity gradient. This has been experimentally verified by MASON and BARTOK⁶⁵, who used glass spheres from 50μ to 300μ in diameter suspended in corn-oil with velocity gradients in the range 0 to 40 sec^{-1} . As mentioned in the introduction, p. 17, if the spheres settle relative to the fluid flowing up a vertical tube, the orthodox Magnus force resulting from the rotational and translational velocities of the spheres relative to the fluid should impel the spheres towards the tube axis. Experimental evidence quoted in the introduction (p. 18) indicates that this simple picture is inadequate, but a rough calculation of the order of magnitude of the radial movement of the particles predicted by the conventional analysis was made for the present situation. This calculation again applies to the outermost particle visible in P59. (Particles closer to the tube axis experience a smaller velocity gradient, and hence a smaller value of the Magnus force.)

RUBINOW and KELLER⁶⁶ have calculated the Magnus force experienced by a rotating sphere moving in a viscous fluid at small values of Reynolds number (i.e. at values of particle Reynolds number much less than 1.) Their analysis

applies strictly to a uniform flow field, but they indicate that it will probably give a value of the right order of magnitude when applied to particles in a suspension flowing through a tube. The value of Reynolds number for the particles in the present case, based on a particle diameter of 30μ and a settling velocity relative to the air of 2 cm/sec, is 0.04, so the application of Rubinow & Keller's result is justified. From the measured velocity profile for the upper part of the tube (fig.31), the velocity gradient experienced by the outermost particle visible was estimated as 100 sec.^{-1} . According to Rubinow & Keller the Magnus force F experienced by a sphere of radius a rotating with angular velocity ω and moving with velocity V relative to a fluid of density ρ is given by
$$F = \pi \omega a^3 \rho V$$

(the axis of rotation being perpendicular to the direction of the relative velocity V .)

In the present case, $\omega = G/2 = 50 \text{ radians/sec.}$

Making the various substitutions, F is 5.5 dynes.

At equilibrium, this force is equal to the Stokes' law drag on the particle, thus:-
$$F = 3\pi u_r d \eta$$

where u_r is the radial velocity component of the particle due to the Magnus force, d the particle diameter, and the air viscosity is η . Substituting, the value of u_r at equilibrium is 0.011 cm/sec. The vertical velocity of the particle up the burner tube is 18 cm/sec. (from the velocity profile) and if these velocities remain constant over

the length of the burner tube, (14 cm.) the particle would move 0.009 cm. radially towards the tube axis as a result of the Magnus force in travelling up the tube. This value is probably an overestimate, since the time required for the particle to accelerate to the equilibrium values of angular velocity and radial migration velocity have been neglected. Also, the value taken for the velocity gradient only applies to that portion of the tube in which the flow is fully developed; in the lower part of the tube the velocity gradient at the radius considered is smaller. Moreover, it is possible that the particles do not rotate, since they are not spherical, and may be sufficiently asymmetrical to resist the turning moment of the couple produced by the velocity gradient. It is clear from this discussion that even if the Magnus effect is operative in the present case, its contribution to the particle-free space is negligible.

d). Low air velocity close to the walls.

It may be seen from the velocity profile for P59 that the zone adjacent to the wall in which the air velocity is below the lycopodium settling velocity is quite narrow, only of the order of 0.1mm thick.

It appears, therefore, that the effects discussed under (c) and (d) make only a very small contribution to the observed particle-free space, and that the effect of particle inertia at the tube entrance may be neglected. Thus it is concluded that this space arises largely from the

effects of the particles settling relative to the air in the approach to the tube entrance. The convergence of the flow-lines in the tube makes only a small contribution to the space. This accounts for the observation that the column of suspension was approximately constant in width over most of the tube length. (p. 89). In order to obtain more information about the behaviour of the particle-free space, further measurements were made on some of the particle track photographs available. The photographs used were taken in the absence of flames, similar to No. P.59, which has already been discussed. The poor definition of the tracks in most of these photographs made them unsuitable for detailed analysis, but it was possible to measure the diameter of the column of suspension in the tube. Isolated particle tracks away from the main column were ignored in making this measurement. The same measurement was made on three photographs with flames in which the flames were some distance above the burner; in these cases the diameter of the column was taken at a point before any divergence of the tracks took place. These measurements are given in Table IX below.

Table IX.

Diameters of Suspension Columns in the Burner Tube.

Plate Number	Burner flowrate (litres/min)	\bar{c}_k (mg/litre)	Diameter of suspension column. (cm.)
P.59	1.58	125	0.74
P.70	1.43	181	0.77
P.60	1.27	115	0.74
P.64	1.40	165	0.76
P.63	1.56	138	0.75
P.77	1.26	150	0.77
P.73	1.58	158	0.75
P.62	1.25	133	0.76
P.41*	1.39	127	0.73
P.43*	1.54	149	0.74
P.39*	1.50	125	0.76

The photographs marked * were taken with flames present. These measurements show that in the absence of a flame the diameter of the column of suspension approaching the top of the tube is practically independent of the suspension concentration or flowrate, over the range of these variables used. They also show that flames burning at heights of several mm. above the tube rim have little effect on the width of the particle-free space in the tube.

Since effects due to particle inertia and the Magnus force may be neglected, it is possible to apply a modified form of Walton's first theorem on the sampling of suspen-

sions, and so to obtain important information on the concentration distribution over the tube cross-section. The original form of this theorem has been given on p. 16; the modified form may be stated:-

Consider a suspension of uniform particles in air in steady flow. Then if air density changes and particle inertia effects are negligible, the static concentration of the suspension will remain constant along any particle flow-tube.

This theorem may be proved as follows, adapting Walton's treatment.

Initially, assume the particles to be of the same density as the air, so that their settling velocity is zero. There is then no relative motion between the particles and air at any point. Since any small group of particles remains associated with the same volume of air throughout the motion, the static concentration remains constant along any particle flow-tube. (A particle flow-tube is a volume bounded by particle flow-lines). If the particles are now given a settling velocity v , their resultant velocity at any point will be the vector sum of v and the air velocity at that point. Since v is constant over the whole system, the resulting particle flow-field will be the same as that of particles having zero settling velocity in an air flow formed by superimposing a uniform velocity v on the original air flow-field. In the latter case, as already shown, the static concentration remains

constant along any particle flow-tube; therefore the static concentration must also remain constant along any particle flow-tube in the more general case when the particles settle with respect to the air.

When this theorem is applied to the present case, it indicates that any variation in static concentration over the cross-section of the column of suspension flowing up the tube (excluding the particle-free space) originates in the body of suspension flowing up from the fluidised bed. In the transition region above the bed, conditions are highly turbulent as a result of the violent 'boiling' of the bed, and it would be expected that eddy diffusion would produce a fairly uniform concentration of suspension over the column cross-section. The suspension flowing up from the transition zone appeared quite uniform to the eye. Previous ^wworkers studying laminar dust flames, e.g. Hattori³⁰, Kaesche-Krischer and Zehr²⁸, and Long³¹, have assumed that the concentrations of their dust suspensions were uniform over the cross-sections of the burner tubes they employed, but were unable to verify this experimentally. In the present case, however, it was possible to make a check on the concentration distribution over the burner cross-section by applying the theorem derived above to the sampling results presented in fig.15. The significance of these results may be seen by reference to fig. 44, which shows the flow of suspension entering the bottom of the sampling or burner

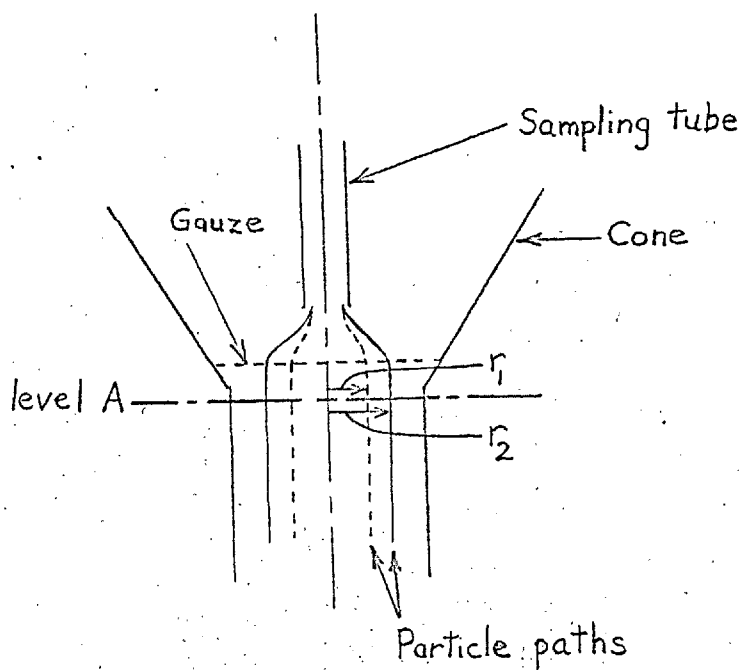


Fig. 44. Flow entering tube.

tube. Level A is a cross section just before the streamlines begin to converge at the approach to the tube entry. On account of the presence of the gauze near the bottom of the cone, the upward air velocity may be taken as uniform over this cross-section, except in the immediate neighbourhood of the cone walls. At a certain sampling flowrate q_1 the air and the particles flow into the sampling tube from a circular area of radius r_1 , and at a higher rate q_2 from a circular area of radius r_2 . If the static concentration of the suspension is uniform over both these areas, it follows from continuity that the values of \bar{C}_k for the samples taken at the two flowrates will be equal, since the air velocity is also uniform over these areas. This does not apply for sampling flows below about 0.3 litres/min, for which the velocities in the sampling tube were less than those outside it; also, at sampling flows below 0.4 litres/min., aggregates of particles had been observed falling down the sampling tube, as described in Chap. 2. Since these aggregates were not collected in the sampling filter, concentration values obtained under these conditions were lower than the true values. Inspection of the sampling measurements (fig.15), leaving out of account the values obtained at flowrates less than 0.4 litres/min., shows that \bar{C}_k remains substantially constant over a wide range of flowrate; at flows between 0.6 litres/min and 1.07 litres/min. \bar{C}_k did not deviate by more than $\pm 4\%$ from its mean value over this range. This result shows that the static concentration of the suspension was practically uniform over the area of the flow in the

cone from which the sample was withdrawn, and the application of the theorem derived above shows that this uniformity would persist in the column of suspension flowing up the sampling tube. In the flame studies, the burner tube flows used were up to 50% higher than the sampling flows just mentioned, but as the fluidised bed flows for the flame studies were also up to 25% higher than the maximum values used in the sampling experiments, the flow conditions in the two sets of experiments are comparable. It is therefore concluded that for the flame experiments also the static concentration of the suspension flowing up the burner tube was practically uniform over the cross-section, except for the particle-free space adjacent to the tube wall.

The picture so far built up of the flow approaching the stationary flamefront is that it consists of a central column of suspension having a substantially uniform static concentration over its cross-section, surrounded by a layer of particle-free air. The thickness of this particle-free space was almost constant for all the burner flows employed, except over a few mm. at the top of the tube, where it was in some cases reduced in width by the presence of a flame. The concentration actually experienced by the stationary flamefront is the ratio of the particle and air flows into it, i.e. the kinetic concentration for a stationary reference plane. The velocity profiles of the flows approaching the flame, e.g. P.27 and P.50, show considerable variations in velocity across the flamefront, so

that different parts of the flames will experience different kinetic concentrations although the static concentrations are uniform. (The relation between the local static and kinetic concentrations, C_s and C_k respectively, for a vertically upward air flow of velocity u , and particles of settling velocity v is given by:-

$$C_s = C_k \left(\frac{u}{u-v} \right)$$

The concentrations measured were mean kinetic values, based on the total flow of air and particles through the burner tube. However, owing to the presence of the particle-free region, the kinetic concentration in the column of suspension was much higher than this measured value. A detailed analysis of the flow was carried out for photograph P.59, in order to find the concentration in the column of suspension, and to account for the measured velocity profile. The diameter of the column of suspension in the tube was found to be approximately 0.74cm., by measurement from the photograph; the rest of the tube diameter was occupied by the particle-free space. The air flow within the column diameter was obtained from the measured velocity profile, and by assuming that all the particles collected in the sampling filter were carried in this column, the mean kinetic concentration of the column C'_k was obtained. This was 210 mg/litre, compared with the \bar{C}_k value of 125 mg/litre. The mean air velocity within the suspension column was obtained from the measured profile as 36.5 cm/sec, and since the settling velocity of

lycopodium is 2 cm/sec, the static concentration in the column is given by:-

$$C_s = 210. \left(\frac{36.5}{36.5-2} \right) = 222 \text{ mg/litre}$$

A theoretical analysis of the flow was attempted, using the following model. The problem was treated as being analogous to that of the pipe flow of two immiscible fluids, one of which flows in a layer at the pipe walls. The suspension was assumed to behave as a Newtonian fluid of greater density than the particle-free air flowing adjacent to the walls. The density of the suspension is the sum of its static concentration and the air density. The viscosity of suspensions of spherical particles may be obtained from the equation due to EINSTEIN⁶⁷:-

$$\eta_s/\eta = 1 + 2.5c$$

where η_s and η are the viscosities of the suspension and pure air respectively, and c is the concentration of the particles expressed as a fraction of the total volume. The equation was derived for low concentrations, and experimental evidence suggests that it applies for values of c up to about 0.01.^{68, 69.} Taking the density of lycopodium particles as 1.2 g/cc.⁵⁹, it is found that the highest value of c in the present work is of the order of 0.19×10^{-3} , for which η_s does not differ significantly from η , so the viscosities of air and suspension were taken as equal. On this basis, the equations for fully-developed laminar viscous flow were set up, and solved to obtain the equations of the velocity profile. The complete derivation is lengthy, and so is

given separately in Appendix C.

The particle tracks visible in photograph P.59 are parallel, which indicates that the flow is fully developed in the upper portion of the burner tube, and the theoretically derived profile may therefore be compared with that measured from the photograph. For comparison, the entry length was calculated for air flow through the tube from the formula due to BOUSSINESQ⁷⁰. Since the developing velocity profile approaches full development asymptotically, the entry length is defined as the distance downstream of the tube entry at which the velocity on the tube axis reaches 99% of its fully developed value. Boussinesq's formula gives X, the entry length, in terms of the tube radius, r, and the Reynolds' number, Re:-

$$X = 0.13r.Re$$

where Re is based on the tube diameter. Substituting a value of air flow equal to the flow of suspension for P.59 (1.58 litres/min.), and the appropriate air density and viscosity, gives an entry length of 14.3 cm., which is slightly greater than the burner tube length (14 cm).

The equations derived for the velocity profile were:-

$$u = \frac{(P - \rho g h)}{4\eta h} \cdot (a^2 - r^2) - \frac{b^2 g}{2\eta} \cdot (\rho_s - \rho) \cdot \ln\left(\frac{a}{r}\right)$$

and

$$u_s = \frac{(\rho - \rho_s g h)}{4\eta h} \cdot (a^2 - r^2) + \frac{(\rho_s - \rho) g}{4\eta} \cdot [a^2 - b^2 - 2b^2 \ln\left(\frac{a}{b}\right)]$$

where

u is the air velocity in the particle-free space,

u_s is the air velocity in the column of suspension,

r is the radial distance from the tube axis,

a is the inside radius of the tube,

b is the radius of the column of suspension,

P is the pressure drop over length h of the tube,

η is the air viscosity,

ρ is the air density,

ρ_s is the density of the suspension,

g is the acceleration due to gravity,

and the symbol \ln indicates natural logarithm.

In both these equations, P is unknown, since the pressure drop was not measured. It was therefore necessary to fix a value of the velocity at one point in order to plot the profile, and this was done by making the value of u_s on the axis equal to the measured axial velocity, 44cm/sec.

Substitution of this value in the equation for u_s gave a value for P/h and permitted the plotting of the complete profile, which is given in fig. 45, together with the measured profile for comparison. Although the latter shows slight asymmetry, the general shapes of the profiles agree closely.

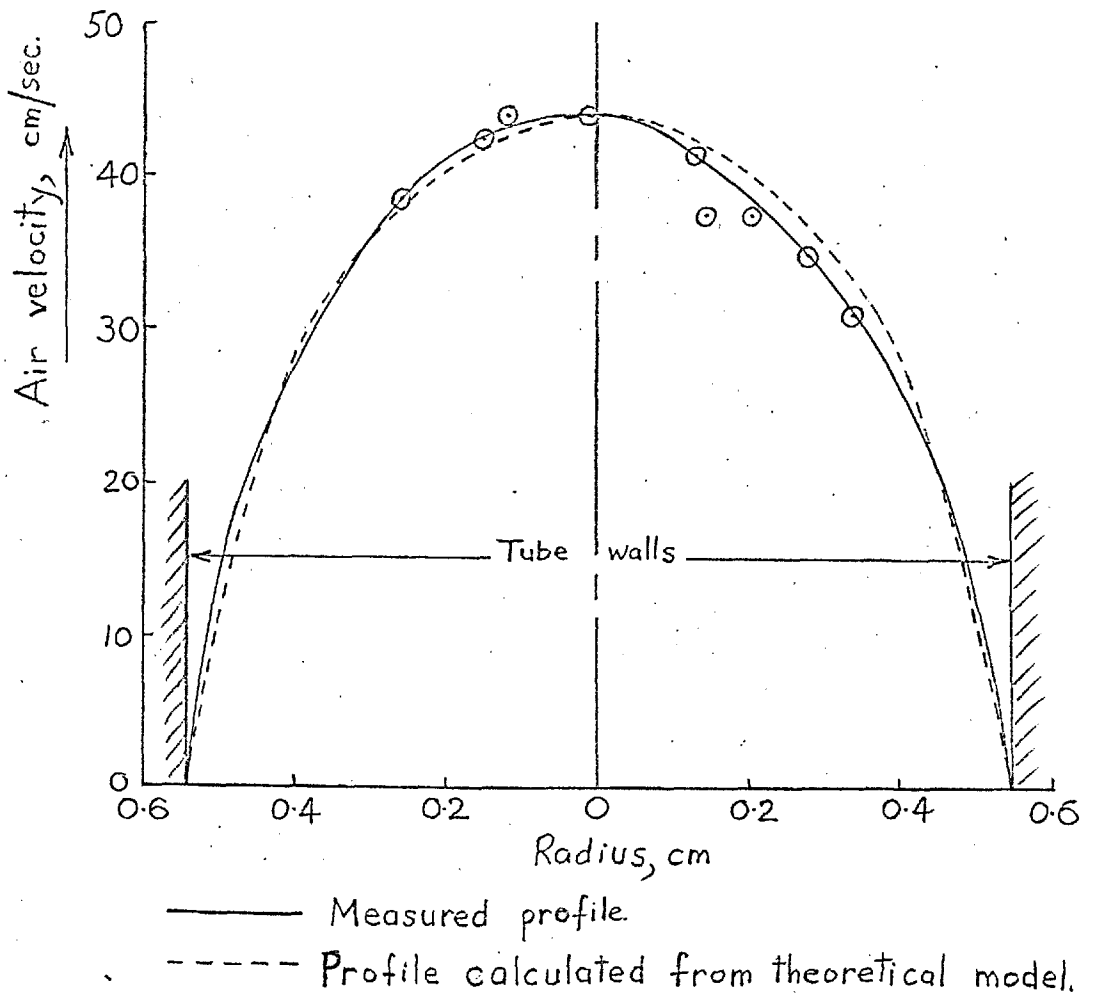


Fig. 45. Comparison of measured and calculated velocity profiles for plate P59, (i).

The total flowrate corresponding to the theoretical profile was calculated (see Appendix C), and was found to be 1.50 litres/min., compared with the value of 1.58 litres/min. measured by soap-film meter during the experiment. (The value of the total flowrate obtained from the measured profile by graphical integration was 1.48 litres/min. Since errors of the order of $\pm 5\%$ can easily arise in the construction and integration of the velocity profile - see p.121- this value agrees well with the soap-film meter measurement.) In fig.46 the measured profile is compared with a simple Poiseuille velocity distribution having the same axial velocity; the total flowrate corresponding to the simple Poiseuille profile is 1.23 litres/min., much less than the measured value. It is seen that over most of the tube cross-section, the measured velocity is higher than that corresponding to the simple Poiseuille profile.

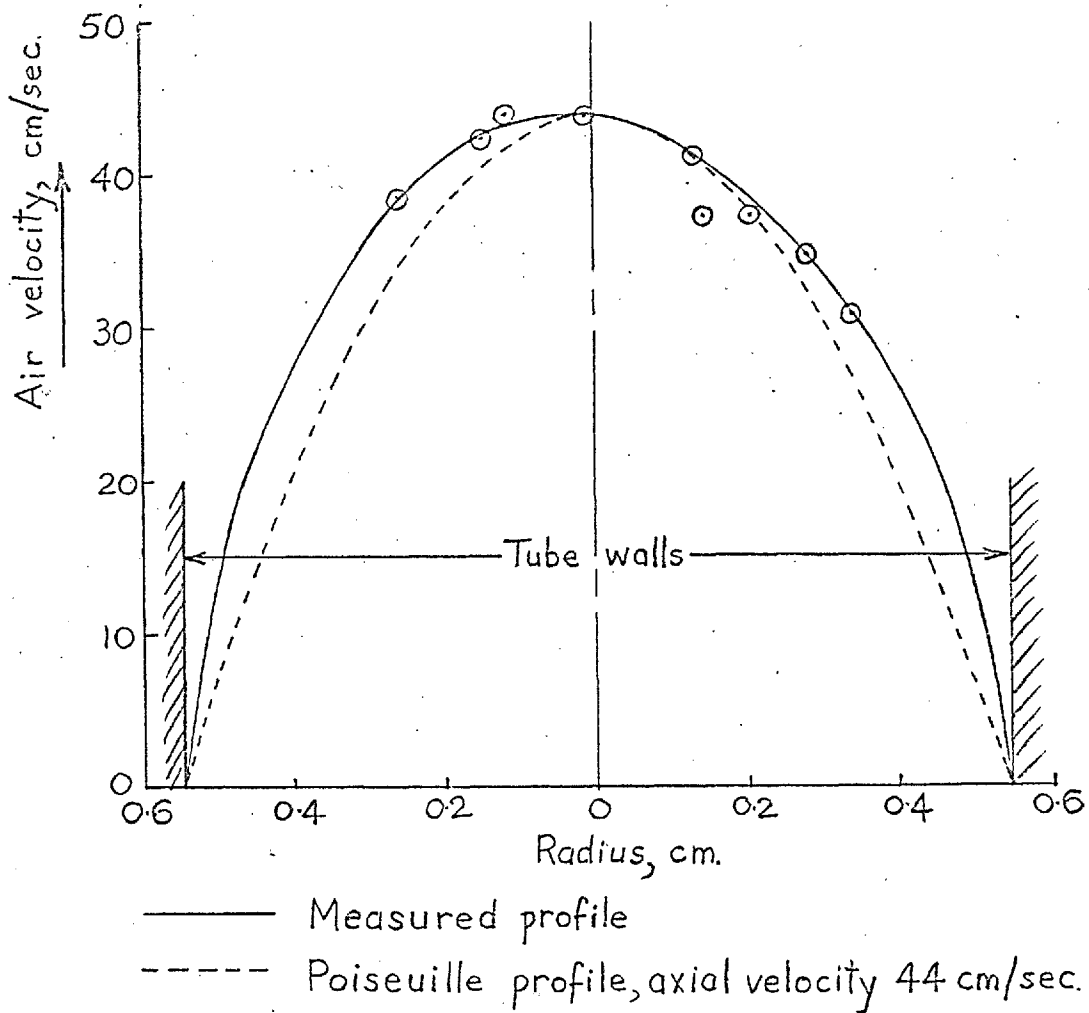


Fig. 46. Comparison of measured and calculated velocity profiles for plate P59, (ii).

From these comparisons, it is seen that the theoretical two-fluid model suggested gives a velocity profile and total flowrate which agree reasonably well with the experimental observations, whilst the profile and flowrate obtained from the simple Poiseuille analysis differ considerably from those observed. The theoretical model suggested therefore appears to be a plausible one.

The theoretical two-fluid model is further compared with the simple Poiseuille model in fig. 47, which shows the velocity profile as already calculated for the conditions of photograph P.59. using the two-fluid model, and a simple Poiseuille profile calculated for the same total flowrate, i.e. 1.50 litres/min. It is seen that the two-fluid model profile has the flatter shape, and a lower axial velocity, as a result of the presence of the particles. According to the two-fluid model, this flattening of the profile arises from the density of the column of suspension being greater than that of the air in the particle-free space. It follows that if a similar particle-free space were present in a vertically downward flow of suspension, the axial velocity would exceed that of a homogeneous fluid with the same total flow-rate, and the velocity profile would be more peaked than that of the

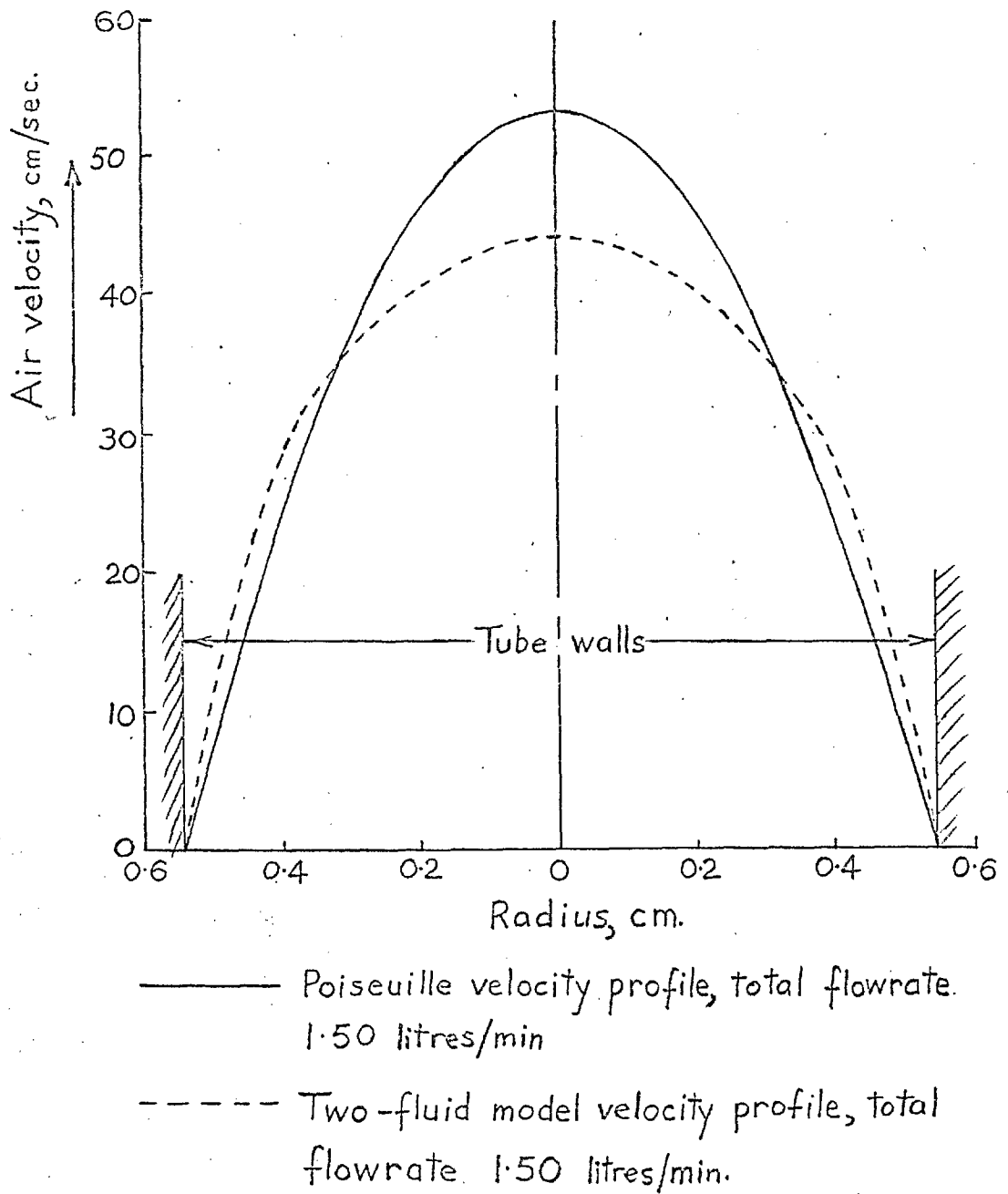


Fig. 47. Comparison of two theoretical profiles.

homogeneous fluid. Also, if the particle-free space were absent, and the static concentration of the suspension were uniform over the whole tube cross-section, the velocity profile would be identical with that of a homogeneous fluid flowing at the same rate,

3. Dust Flames.

It is clear from the preceding discussion of the flow of dust suspensions that the actual kinetic concentrations in the dust flames are much higher than the measured \bar{C}_k values, as a result of the presence of the particle-free space at the burner wall. The mean kinetic concentration, C'_k , in the column of suspension flowing into the flame was therefore calculated for each flame photograph. The calculation was carried out by the same method as that described for photograph P59 on p. 162 ; the diameter of the column of suspension was measured from the photograph, and the air flowrate q_s in the column of suspension was calculated from the measured velocity profile. C'_k was then obtained from the relation:-

$$C'_k = \bar{C}_k \cdot \frac{q}{q_s}$$

where q is the total air flowrate up the burner tube. The values of \bar{C}_k , q/q_s and C'_k are given in table X.

Table \bar{X} .
 Values of \bar{C}_k , q/q_s and C'_k

Photograph	\bar{C}_k (mg/litre)	q/q_s	C'_k (mg/litre)
P.27	156	1.37	214
P.36	133	1.57	209
P.37	127	1.28	162
P.39	125	1.54	193
P.41	127	1.83	243
P.42 [⊗]	143	-	-
P.43	149	1.48	220
P.50	159	1.47	234

⊗ For this photograph, the particle tracks at the outer edge of the flame were not sufficiently clear to permit the evaluation of q/q_s .

The model of the suspension flow discussed above suggests that the value of the ratio q/q_s is a function of both C'_k and q . It is seen from table \bar{X} that if the flames are arranged in order of increasing C'_k , the arrangement is similar to that in order of increasing \bar{C}_k , the main exception being no. P 41. The latter has a value of q/q_s considerably higher than the other flames; the reason for this is not clear, but might be due to some asymmetry of the flow not obvious in the photograph. The values of C'_k obtained are subject to considerable error, as the diameter of the suspension column is not sharply

defined, and the velocity profile cannot be measured with high accuracy. This emphasises a basic difficulty in the study of small dust flames, i.e. while particle concentrations may vary widely over the flame as a result of the properties of dust suspensions already discussed, it is impracticable to measure local concentrations at different parts of the flamefront.

A graph of S_{\max} against C'_k , the kinetic concentration of the suspension approaching the flamefront, is given in fig. 48. Although the individual values show a wide scatter, there appears to be a tendency for S_{\max} to increase with increase of concentration over the range studied.

The main features of the lycopodium flames studied may be summarised as follows:-

- a). The luminosity of the flames was not uniform like that of a gaseous diffusion flame, but arose from discrete sources within the flame. This gave rise to the streaky appearance of the flames in the photographs.
- b). The dead space at the burner rim was very large in comparison with that usually observed in pre-mixed gas flames at atmospheric pressure; e.g. for the flames analysed in detail, the flame-fronts were between 1.5 mm. and 6.9 mm. above the burner rim.
- c). The flamefronts were flat or saucer-shaped in profile.
- d). Flames could only be stabilised at values of C'_k well

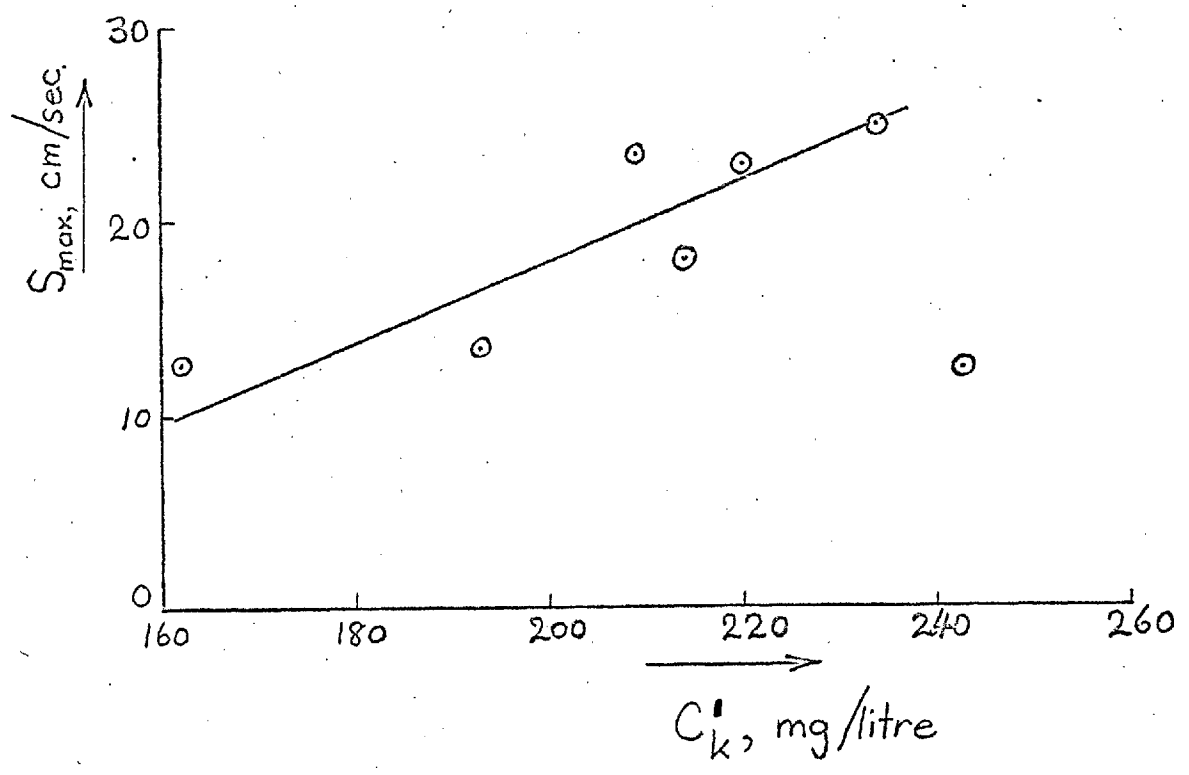


Fig. 48 Variation of S_{max} with C'_k

- above the stoichiometric value.
- e). The local burning velocity was only constant over a small portion of the flame area in most cases.
 - f). The maximum burning velocity of the flames S_{\max} , tended to increase with concentration over the range investigated.
 - g). Interpolation of the quenching measurements (Table VII) indicates that a suspension in upward flow, with a \bar{C}_k value of 126 mg/litre has a quenching distance of about 13 mm. for downward propagation of the flame.
 - h). The temperature profile (Table VI) of a flame with a \bar{C}_k value of 137 mg/litre shows that the temperature of the air in the suspension begins to rise significantly at a point about 2 mm. ahead of the visible flamefront.

These features will now be compared with those shown by pre-mixed gas flames, and by the flames of liquid-in-air and solid-in-air suspensions described in the literature, and the significance of these features in relation to flame structure will be discussed.

The large dead space at the burner rim and the flat or saucer-shaped flame-front of the flames studied (figs 28,29) are in marked contrast to the typical appearance of pre-mixed laminar gas flames burning on tubes, which normally have conical flamefronts, and dead spaces much less than 1 mm. An exceptional type of pre-mixed gas flame with a

flat flamefront has however been described by WOHL, GAZLEY and KAPP,⁷¹ who stabilised very lean butane-air flames on a 1.03 in. diameter burner tube; these flames had flat or saucer-shaped flamefronts similar to the lycopodium flames under discussion, and also resembled the latter in having a large dead space at the burner tube rim.

The particle track photographs show that the dead space at the burner rim has an important influence on the flow pattern of the suspension approaching the lycopodium flames. Comparing photograph P59, taken without a flame, with any of the flame photographs, it is seen that the flame causes a marked divergence of the flow emerging from the tube, while in the absence of a flame the particle tracks continue practically undeviated up to 1 cm. or more beyond the tube mouth. (The divergence of the flow emerging from the tube mouth seen in photograph P4 was exceptional, and arose through inadequate protection from draughts; this was remedied for subsequent photographs.) It appears that the pressure drop across the flame causes the flow emerging from the tube to diverge radially outwards through the large dead space between the tube and the flamefront into the surrounding atmosphere. The pressure drop across a pre-mixed gas flame has a similar effect on the flow of gas mixture at the burner mouth, but the area of the dead space for typical pre-mixed gas flames is so small in comparison with the

area of the flame-front that the quantity of mixture flowing through it has no significant effect on the pattern of flow into the flame-front. The flow-lines in these flames therefore remain parallel up to a point very close to the flame-front, as shown by the particle-track photographs of LEWIS and VON ELBE⁷². The lycopodium flames, however, are stabilised in a diverging flow field; if any portion of the flame-front moves down towards the burner rim, it enters a region of higher velocity, which causes it to move back to its original position. This mechanism of stabilisation may be contrasted with that usually operative in pre-mixed laminar gas flames, where the stability is determined by the velocity gradient at the tube wall. It is interesting that Wohl, Gazley and Kapp account for the flat flame-fronts of their lean butane-air flames by suggesting that the velocity profile of the flow approaching these flames is flattened by the pressure drop across the flames themselves. This shows some similarities with the mechanism of stabilisation just suggested for lycopodium flames.

Most of the lycopodium flames in the present work show a marked difference in shape from the lycopodium flames obtained by Käsche-Krischer and Zehr²⁸; the latter had conical flame-fronts similar to those of pre-mixed gas flames, whereas the former mostly had flamefronts which were flat or convex towards the burner. It has been pointed

out in the literature survey that flat-fronted flames have been observed in other dust suspensions; e.g. Ghosh, Basu and Ray stabilised coal dust/oxygen-enriched air flames in the open air which had flat flamefronts and a streaky appearance similar to the lycopodium flames shown in figs. 28 and 29. The coal dust flames obtained by Long, on the other hand, had conical flamefronts. One possible reason for the existence of the two types of flame-front in the case of lycopodium is suggested by the observation in the present work that flames burning at the higher values of \bar{C}_k gradually moved down onto the burner, and developed conical flamefronts (p. 110.) It is considered that this was caused by gradual heating of the burner tube, which in turn preheated the suspension flowing through it, and liberated some volatiles from the lycopodium, thus causing a change to a type of flame approaching the pre-mixed gas flame. It is possible that similar preheating of the suspension took place in Kaesche-Krischer and Zehr's work; they do not mention any precautions taken to avoid this. If such preheating took place, it could account for their obtaining the inner-cone type of flame-front. In the present work, heating of the burner tube was minimised by photographing the flames as soon as possible after ignition (p. 101). The temperature profile obtained for a typical flame shows that preheating of the suspension by the tube was negligible. (Table VI).

It is interesting to compare the lycopodium flames

obtained in the present work with the flames in suspensions of tetralin droplets in air studied by COHEN.⁷³ Cohen used suspensions which were practically mono-disperse and varied the droplet size from 7μ to 55μ . He concluded that with droplet sizes below 10μ , the droplets evaporated completely in the pre-heating zone of the flame, and the flame-front was essentially that of a homogeneous air-vapour mixture. With droplet sizes above 40μ , the flames were completely 'particularised', i.e. only a small proportion of the fuel evaporated in the pre-heating zone, and the flame itself was made up of diffusion flames round individual droplets. For droplet sizes between 10μ and 40μ , the flame structure was of an intermediate type. Tetralin suspension flames stabilised on an 11 mm. diameter burner tube showed two types of structure; with droplet sizes below 10μ , the flames had a blue inner cone, while for droplets above 10μ the flames were flat-fronted and made up of discrete burning droplets. The latter type of flame was similar in appearance to the lycopodium flame in figs. 28 and 29, which suggests a similarity of structure. The following structure is therefore put forward for the lycopodium flames studied in the present work. In the preheating zone of the flame, some volatiles are liberated from the lycopodium particles; these volatiles mix with the surrounding air and ignite in the flamefront, the combustion of this mixture giving rise to the blue colour of the latter, (p.109). The particles continue to

volatilise as they pass through the flame-front, and diffusion flames form round each particle; the tracks of these diffusion flames form the streaks visible with ⁱⁿ the flame envelope on the photographs. Only that portion of the fuel which is volatilised in the preheating zone is available for combustion in the flamefront, so that the effective concentration of fuel at the flamefront is much less than the actual concentration of the suspension. This may partly explain why flames could only be stabilised at concentrations well above the stoichiometric value. Since the burning suspensions are fuel-rich, oxygen from the atmosphere must diffuse into the upper part of the flames to complete the combustion of the particles. Particles in the axial region of the flame, which are furthest from the secondary oxygen supply, therefore have the longest burning times, and since the velocities are highest in the axial region, the flames would be expected to have a roughly conical outline, as was actually the case.

The flame temperatures given in Tables V and VI are not corrected for radiation losses from the thermocouple, as the effect of the burning particles is not known. The flames are not homogeneous in structure, and the temperature of the particles both in the preheat zone and in the flame itself will differ from that of the surrounding gases. The thermocouple will indicate the temperature of the gas rather than that of the particles, e.g. the temperature profiles obtained (Table VI) indicate the air temperature ahead of

the flame-front, rather than that of the particles. The value of 2 mm. for the thickness of the pre-luminous zone (i.e. the zone of pre-heating ahead of the visible flame-front,) is of the same order as that for pre-mixed gas flames of low burning velocity; e.g. the corresponding value for a hydrogen/oxygen/nitrogen flame with a burning velocity of 8 cm/sec. studied by DIXON-LEWIS and ISLES⁷⁴ is about 3 mm.

In most of the pre-mixed gas flames which have been studied in detail, the burning velocity was constant over most of the flame-front, except at the extreme edges, and at the tips of conical flamefronts. LEWIS and VON ELBE⁷⁵ give values for a natural gas/air flame on a rectangular burner which show that the burning velocity was constant over about 70% of a section through the conical flamefront, which was 1 cm. wide at its base. For most of the lycopodium flames analysed, however, the burning velocity was only constant over less than half of the flame-front area, (fig.36) and consequently the overall burning velocities, \bar{S}_u , are much less than the values for the central regions of the flames, S_{max} . The decrease in local burning velocity towards the edge of the flame is probably partly caused by quenching effects, and will be discussed in more detail later. In comparing the burning velocities of lycopodium flames with those of pre-mixed gas flames, it therefore seems appropriate to use the values of S_{max} rather than those of \bar{S}_u , since the burning velocities of

pre-mixed gas systems are usually obtained under conditions where quenching effects have negligible influence on the result. Considering first the relationship of S_{\max} to C'_k , (fig. 48), the lycopodium flames show an important difference from the behaviour of pre-mixed gas flames. The latter normally show a well-defined burning velocity maximum at or near the stoichiometric concentration, above which the burning velocity falls; e.g. according to data given by VON ELBE and LEWIS⁷⁶, methane/air mixtures have a maximum burning velocity of 36.6 cm/sec. at 1.02 times the stoichiometric methane concentration, which falls steadily to 16.0 cm/sec at 1.5 times stoichiometric. The values of C'_k for the lycopodium flames are all well above the stoichiometric concentration (124 mg./litre) yet the burning velocities show a general tendency to increase with concentration. Other workers have also found that the relationship of burning velocity to concentration for dust suspensions differs from that of pre-mixed gas flames, e.g. Kaesche-²⁸ Krischer and Zehr reported that the overall burning velocity of their lycopodium flames remained constant at 26 cm/sec over the concentration range 180 mg./litre to 300 mg./litre, while Long³¹ found that the overall burning velocities of coal-dust suspensions increased with concentration until the latter reached almost twice the stoichiometric value. The overall burning velocities obtained by Kaesche - Krischer and Zehr for lycopodium flames are approximately double the \bar{S}_u values obtained in the present work

for flames in the same range of concentrations. This difference may be due to (a) the larger diameter burner used by Kaesche-Krischer and Zehr, (2 cm in diameter) for which quenching effects would be smaller, (b) possible preheating of their suspension, as already mentioned.

It is interesting to compare the quenching diameter obtained with those for ~~gas~~^{gas} flames. Since the burner tube flows used in the quenching experiments were considerably lower than those required to stabilise flames, the particle-free spaces would be smaller than in the latter case, and so the kinetic concentration of the suspension ahead of the flame would not be much greater than the value of \bar{C}_k measured, i.e. 126 mg/litre, approximately the stoichiometric concentration. According to the data of HARRIS, GRUMER et al,⁷⁷ the quenching diameter of a stoichiometric methane/air mixture is 3.2 mm, for downward flame propagation through a quiescent mixture, and the value for a stoichiometric propane/air mixture is 2.8 mm. These hydrocarbon/air mixtures show minimum quenching diameters at the stoichiometric concentration; the methane/air mixture has a quenching diameter of 13 mm at a methane concentration of 1.4 times stoichiometric, and the propane/air mixture has a 13 mm quenching ~~distance~~^{diameter} at a propane concentration of 1.7 times stoichiometric. No data on quenching diameters appears to be available for other dust systems, but Cassel, Das Gupta and Guruswamy³² mention that they found it impossible to stabilise flames less than

$\frac{1}{2}$ in. diameter in aluminium dust clouds. Long³¹ suggested that quenching distances for dust suspensions should be larger than those for gas mixtures, basing his predictions on calculations of the radiant heat transfer in dust flames.

It has been mentioned that at the lowest values of \bar{C}_k with which flames could be stabilised, the flames sometimes went out abruptly, without either blowing off or flashing back; also that when the burner flowrate was reduced, these flames went out without flashing back into the tube. From these observations, it appears that the flames were burning under conditions close to quenching. In these circumstances their behaviour will be considerably influenced by heat losses to the surroundings; the magnitude of these losses is a function of the dimensions of the flames, and of their position relative to the burner. Since these variables could not be controlled independently, and varied widely from one flame to another, it is likely that the heat losses also varied widely. This may account for the erratic variation of S_{\max} with C_k^1 . Long, who made a large number of measurements of overall burning velocities of laminar coal-dust flames on a $\frac{5}{8}$ in. burner, also found a very wide scatter in the values for a particular concentration and particle size; in some cases values obtained under similar conditions differed by 40%.

An increase in the diameter of the flames, other conditions remaining constant, would lead to a reduction in the proportion of generated heat lost to the surroundings.

Hence it seems likely that flames could be stabilised at lower concentrations on a burner of larger diameter. Line, Clark & Rahman³⁴ obtained a value of 40 mg/litre for the lower inflammable concentration of lycopodium suspended in an oxygen/nitrogen mixture containing only 18.7% by volume of oxygen, in a 2 in. diameter tube. This is very much below the lowest concentration at which flames could be stabilised in the present work.

The reasons for the existence of the large dead space at the burner rim, which was a prominent feature of the lycopodium flames stabilised, will next be discussed. The flame quenching experiments indicate that quenching distances for the lycopodium flames are much larger than for comparable pre-mixed gas flames, and this may partly account for the large dead spaces observed. Apart from wall quenching, two other factors may contribute to these large dead spaces. These are:- (i) the existence of the particle-free space at the walls, and (ii) the variation of kinetic concentration with suspension velocity. As a result of the second effect the flame experiences a maximum concentration on the tube axis where the air velocity is greatest, and a lower concentration towards the edges. The magnitude of this effect can be estimated from the results showing the variation of burning velocity over the flame cross-section, since the local burning velocity is defined as the air velocity normal to the flame-front. In the case of plate P42, for example, the burning velocity was 18 cm/sec on the tube axis, and 11 cm/sec near the edge of the flame (fig.36). Since the flamefront ^{is} flat,

these burning velocities represent the vertical components of the local air velocities. Assuming uniform static concentration over the cross-section of the column of suspension, the ratio of the kinetic concentration at the edge of the flame to that at the centre is seen to be roughly 0.92:1, using the relation given on p. 162. It is possible that in flames near the lower concentration limit of stability the kinetic concentration at the edge of the column of suspension is too low to support combustion, with the result that the dead space is increased. Particle inertia effects in the region of diverging flow upstream of the flame-front may also contribute to the concentration differences over the flame cross-section. Although it has been concluded that these effects may be neglected at the entry to the burner tube, the velocities of particles emerging from the tube exceed those of particles approaching the tube entry by a factor of 3 or 4, so inertia effects could be significant near the flame. These would result in the particle flow-lines diverging less sharply than the air flow-lines, causing increased concentrations near the centre of the flame, and corresponding decreases near the edge.

With the exception of flame P 37, the flames analysed in detail show a marked decrease in local burning velocity with increasing distance from the flame axis. This has already been contrasted with the behaviour of pre-mixed gas flames of similar size, for which the burning velocity

is constant over most of the flame-front, and only shows a decrease, due to quenching, at the edge of the flamefront. This difference may be partly accounted for as follows. From the quenching experiments in the present work, it appears that the quenching diameter of a lycopodium flame is much greater than that of a comparable pre-mixed gas flame, and therefore quenching effects penetrate more deeply into the former; as a result the area of constant burning velocity in the lycopodium flame is smaller than in a pre-mixed gas flame of similar size. Apart from this quenching effect, the variation of kinetic concentration over the flamefront, just discussed, will also contribute to the decrease of burning velocity towards the edge of the flame. In the case of plate P.42, it has just been shown that the kinetic concentration at the edge of the flamefront is about 92% of the value at the centre. From the relationship of burning velocity with C'_k , (fig.48) it is seen that this decrease in concentration towards the edge of the flame corresponds to a decrease of about 3 cm/sec. in burning velocity. The observed decrease in burning velocity is 7 cm/sec, the remainder of which is probably accounted for by the quenching effect.

The relatively large quenching distances observed may be the result of radiation contributing to heat transfer in these flames. Long³¹ gives some calculations which suggest that in dust flames radiant heat transfer is effective over much longer distances than conductive transfer, and on this

basis he predicted that dust flames would have quenching distances much larger than gas flames. Apart from mathematical complexities, the major obstacle to reliable calculation of radiant heat transfer in dust flames is the lack of information on the size and emissivity of the flamelets surrounding the individual dust particles.

In conclusion, a few remarks may be made about the experimental limitations of the present work, and the possibilities for its extension. The most serious limitations of the apparatus used were:-

- 1). The presence of the particle-free space at the tube walls causes difficulty in the accurate measurement of concentration, and modifies the characteristics of the flames.
- 2). As the flames are stabilised under conditions approaching quenching, they are very sensitive to heat losses, which depend upon factors that cannot be independently controlled, such as the position of the flame relative to the burner.
- 3). At the higher concentrations, particle-track photography was unsuccessful, as a result of the large number of particles passing between the illuminated zone of the suspension and the camera.

The first limitation might be overcome by modifying the design of the apparatus, but the other two pose a dilemma, since the use of larger flames less sensitive to heat losses would make particle-track photography still more

difficult. The discussion has shown that dust flames of the type studied modify the suspension flow to a marked extent, and therefore some means of observing the flow of suspension is essential.

It is also clear that for a detailed understanding of the structure of dust flames, more information is required about the factors controlling the burning rate of single particles, and the relative magnitudes of radiant and conductive heat transfer in such flames.

Appendices.

	Page
Appendix A	191
Appendix B	194
Appendix C	195
List of References	199

Appendix A.

Calculation of the number of particle tracks crossing the line $y = -0.27$ cm in photograph P.59.

First, the relationship between \bar{C}_k and C_s will be derived. Assume that C_s is uniform over the tube cross-section (see p.141 and p.161). Using the same notation as in the text, let u be the local air velocity up the tube at any point on the tube cross-section with a radial distance x from the tube axis. Consider a velocity profile in the tube, symmetrical about the axis, given by $u=f(x)$, where $f(x)$ is some function of x . If the particles settle with a velocity v relative to the air, then u_p , the local velocity of the particles up the tube at any point on the cross-section, is given by $u_p = u - v$.

Then \bar{C}_k , the mean kinetic concentration over the tube cross-section, is given by:-

$$\bar{C}_k = \frac{\int_0^a 2\pi x \cdot u_p \cdot C_s \cdot dx}{\int_0^a 2\pi x \cdot u \cdot dx}$$

where a is the tube radius. This follows from the definition of \bar{C}_k , p.109. (The small region at the tube wall where u is less than v is neglected.)

Then

$$\bar{C}_k = \frac{C_s \int_0^a [f(x) - v] x \cdot dx}{\int_0^a f(x) \cdot dx} = \frac{C_s \left[\int_0^a f(x) \cdot dx - \frac{va^2}{2} \right]}{\int_0^a f(x) \cdot dx}$$

since C_s is independent of x .

$$\text{Now } 2\pi \int_0^a f(x) dx = \pi a^2 u_m$$

where u_m is the mean air velocity up the tube, and hence

$$\bar{C}_k = C_s \left(\frac{u_m - v}{u_m} \right)$$

This is identical in form with the relation between C_k and C_s given on p.19.

In the present case, for P59, $\bar{C}_k = 125$ mg/litre, and the burner flow is 1.58 litres/min, i.e. $u_m = 28.2$ cm/sec., also $v = 2$ cm/sec, so

$$C_s = 125 \times \frac{28.2}{26.2} \text{ mg/litre}$$

The line $y = -0.27$ cm is divided up into 0.04 cm. lengths for the purpose of the calculation, and since the light beam was 0.007 in. wide, each of these lengths represents an illuminated area of the tube cross-section equal to $(0.04 \times 0.007 \times 2.54) \text{ cm}^2 = 7.1 \times 10^{-4} \text{ cm}^2$.

Taking the number of lycopodium particles per g of powder as 9.4×10^7 (Gregory⁵⁹), and denoting the mean particle velocity through an illuminated area by u_p , the number of particles crossing an an area per second is given by:-

$$u_p (7.1 \times 10^{-4} \times 125 \times \frac{28.2}{26.2} \times 10^{-6} \times 9.4 \times 10^7)$$

or approximately $9u_p$.

The total time of illumination for the photograph was $1/200$ sec., and therefore if the assumption of uniform C_s is valid, the number of particle tracks crossing the corresponding 0.04 cm. length of the line $y = -0.27$ cm

should be $\frac{9}{200} \cdot u_p$, although the number actually visible on the photograph may be less than this, due to the presence of agglomerates, and overlapping.

An example will serve to illustrate the method of calculation used to obtain the figures in Table VIII, p.143. Consider the first length given in the table, commencing on the tube axis, and ending 0.04 cm. from it. From the velocity profile, fig. 32a, it is seen that the mean value of u for this length is 44 cm/sec., and hence the mean value of u_p is 42 cm/sec. Evaluating $\frac{9}{200} \cdot u_p$, the number of tracks crossing this length should be 1.9.

Appendix B.

Convergence of the air flow-lines in the burner tube. (p.151)

Consider the flow-tube having a radius of 0.43 cm. on the photograph P 59. By graphical integration of the velocity profile (fig. 32a) it is found that the total air flow in this tube is $19.7 \text{ cm}^3/\text{sec.}$, compared with a flow of $24.7 \text{ cm}^3/\text{sec.}$ over the whole cross-section of the burner tube. Now at the entrance to the burner tube, the air velocity is uniform over the cross-section. Hence if the flow-tube considered has a radius r_1 at the burner tube entrance,

$$\frac{4r_1^2}{(1.09)^2} = \frac{19.7}{24.7}$$

$$\text{and } r_1 = 0.49 \text{ cm.}$$

Therefore the flow-tube having a radius of 0.43 cm. at the cross-section $y = -0.27 \text{ cm.}$ has a radius of 0.49 cm. at the tube entrance.

Appendix C.

Derivation of the equations for the velocity profile in a suspension flow. (see p.164.)

Consider the flow of suspension in a tube of radius a , between sections (1) and (2), fig. A1. The particles are assumed to be concentrated in the central column, radius b , in which the static concentration C_s is uniform, and the concentration of particles in the annular space between this column and the tube walls is ~~is~~ taken to be negligible. The flow is assumed to be fully developed, i.e. the velocity profile does not change along the tube. Consider the equilibrium of a cylinder of fluid, co-axial with the tube, of radius r and height h .

For $r < b$, a force balance for steady flow gives:-

$$(p_1 - p_2) \pi r^2 - \pi r^2 h \rho_s g + 2 \pi r h \eta \left(\frac{du_s}{dr} \right)_r = 0 \quad (1)$$

where p_1 , p_2 are the pressures at sections (1) and (2) respectively, ρ_s is the density of the suspension column, u_s is the local air velocity up the tube in the suspension column, $\left(\frac{du_s}{dr} \right)_r$ is the gradient of u_s at radius r , η is the viscosity of the suspension, - taken as equal to the viscosity of dust-free air, see p.165 - and g is the gravitational acceleration.

For $b < r < a$, the steady flow force balance is:-

$$(p_1 - p_2) \pi r^2 - \pi b^2 h \rho_s g - \pi (r^2 - b^2) h \rho g + 2 \pi r h \eta \left(\frac{du}{dr} \right)_r = 0 \quad (2)$$

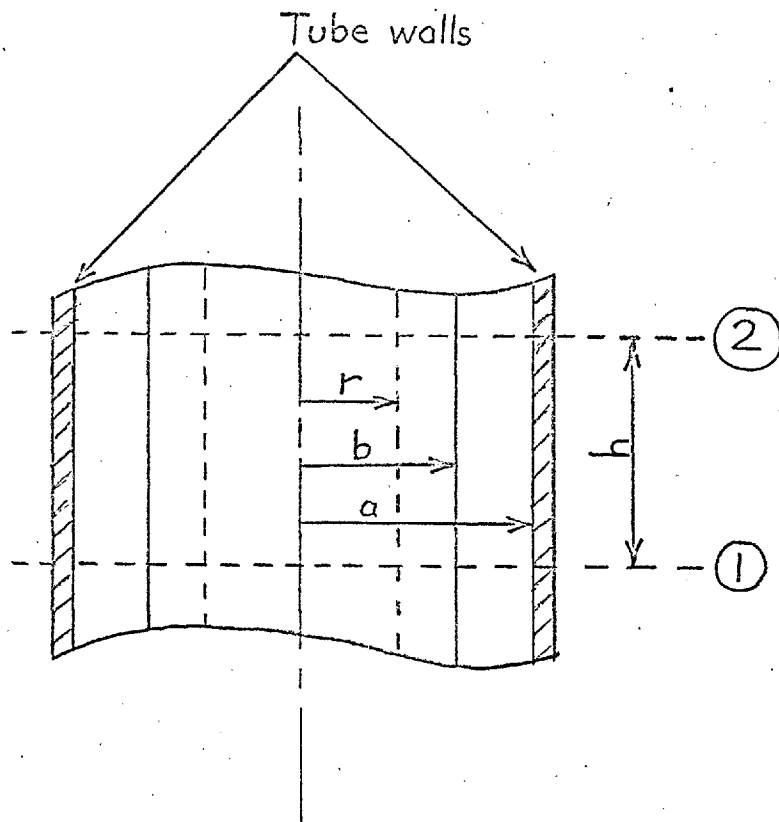


Fig A1. Suspension flow in tube.

where ρ is the density of dust-free air, u is the local air velocity up the tube in the particle-free space, and $\left(\frac{du}{dr}\right)_r$ is the gradient of u at radius r .

$$\text{Rearranging (1), } \left(\frac{du_s}{dr}\right)_r = \frac{(\rho_s g h - P)r}{2\eta h} \quad (3) \quad \text{where } P = p_1 - p_2$$

$$\text{Integrating, } u_s = \frac{(\rho_s g h - P)r^2}{4\eta h} + A \quad (4)$$

where A is a constant of integration.

$$\text{Similarly from (2), } u = \frac{(\rho g h - P)r^2}{4\eta h} + \frac{b^2 g}{2\eta} (\rho_s - \rho) \ln r + B \quad (6)$$

where B is a constant of integration.

At the tube wall, $r=a$ and $u=0$. Using these boundary conditions to evaluate B in (6), it is found that

$$u = \frac{(P - \rho g h)}{4\eta h} (a^2 - r^2) - \frac{b^2 g}{2\eta} (\rho_s - \rho) \ln\left(\frac{a}{r}\right) \quad (\text{for } b < r < a) \quad (7)$$

At $r=b$, $u=u_s$, since there can be no slip at the interface, and substituting (7) in (4) at $r=b$ to evaluate A ,

$$u_s = \frac{(P - \rho_s g h)}{4\eta h} (a^2 - r^2) + \frac{(\rho_s - \rho)g}{4\eta} [a^2 - b^2 - 2b^2 \ln\left(\frac{a}{b}\right)] \quad (\text{for } r < b) \quad (8)$$

Equation (7) represents the velocity profile for the air in the particle-free space, and equation (8) the profile for the air in the suspension column.

P/h is unknown, and was evaluated by putting the value of u_s on the axis equal to the value obtained from the measured velocity profile (fig. 32a), i.e. 44 cm/sec.

Substituting the values:-

$$a=0.545 \text{ cm,}$$

$$b=0.37 \text{ cm, (measured from the photograph)}$$

$$\eta = 180 \times 10^{-6} \text{ poise for air at } 20^{\circ}\text{C.}$$

$$\rho = 1.21 \times 10^{-3} \text{ g/cm}^3 \text{ for air at } 20^{\circ}\text{C.}$$

$$C_s = 222 \text{ mg/litre, therefore } \rho_s = (1.21 + 0.222) \times 10^{-3} \text{ g/cm}^3$$

$$\text{and at } r=0, u_s = 44 \text{ cm/sec.}$$

in (8),

$$u_s = 93(a^2 - r^2) + 16.4 \text{ cm/sec} \quad (9) \quad (r < b)$$

and similarly,

$$u = 396(a^2 - r^2) - 83 \ln(a/r) \text{ cm/sec} \quad (10) \quad (b < r < a)$$

From (9) and (10) the calculated profile in fig. 45 was plotted.

Calculation of the total air flow.

Let the total air flow in the tube be F , and let the air flows in the suspension column and the particle-free space be f_s and f respectively.

$$\text{Then } F = f + f_s$$

$$\text{Also, } f = 2\pi \int_b^a u r \cdot dr, \quad f_s = 2\pi \int_0^b u_s r \cdot dr$$

The total air flow was then obtained by substituting for u and u_s from (10) and (9) respectively, and evaluating the integrals. The value of F was found to be 1.50 litres/min.

References.

1. Torobin, L.B. and Gauvin, W.H., Can. J. Chem. Eng., 37, 129, 167, 224, (1959), and 38, 142, (1960).
2. Hawksley, P.G.W., B.C.U.R.A. Bulletin, 15, 105, (1951), and 16, 117, 181, (1952).
3. Hawksley, P.G.W., 'The Physics of Particle Size Analysis' p.S1, (Supplement no. 3 to Brit. J. Appl. Phys., 5, (1954).
4. Davies, C.N., Symposium on Particle Size Analysis, p.25, (Supplement to Trans. Inst. Chem. Eng. 25, (1947).
5. Banister, J.R., Proc. 6th Mid-Western Conf. on Fluid Mechanics, Austin, Texas, (1959).
6. Kynch, G.J., J. Fluid Mech., 5, 193, (1959).
7. Smoluchowski, M.A., Bull. Acad. Sci. Cracow, 1a, 28, (1911).
8. Burgers, J.M., Proc. K. Ned. Akad. Wetensch., 44, 1045, 1177, (1941), and 45, 9, 126, (1942).
9. Kynch, G.J. 'The Physics of Particle Size Analysis' p.S5. (See no. 3 above).
10. Hawksley, P.G.W., in 'Some Aspects of Fluid Flow' p.114. (Inst. of Physics, London, Edward Arnold & Co., 1951).
11. Maude, A.D. and Whitmore, R.L. Brit. J. Appl. Phys., 9, 477, (1958).
12. Rowe, P.N. and Henwood, G.A., Trans. Inst. Chem. Eng., 39, 43, (1961).
13. Kaye, B.H. and Boardman, R.P. 3rd Congress Europ. Fed. Chem. Eng., Proc. Symp. on Interaction between Fluids and Particles, p.17, (London, 1962).

14. Happel, J., Amer. Inst. Chem. Eng. Journal, 4, 197, (1958).
15. McNoon, J., and Lin, P.-N., Reprint in Engineering no. 109
State University of Iowa, U.S.A.
16. Picknett, R. G., 'Aerodynamic Capture of Particles', ed.
E. G. Richardson, (Pergamon, London, 1960.)
17. Palmer, K. N., Private communication.
18. Khudyakov, G. N., Izvest. Akad. Nauk SSSR, Otdel. Tekh.
Nauk, (1953), p.1022.
19. Walton, W. H., Symposium on Particle Size Analysis, p.136
(see ref. no. 4, above.)
20. Tollert, H., Chem.-Ing.-Tech., 26, 141, (1954).
21. Starkey, T.V., Brit. J. Appl. Phys., 6, 34, (1955) and
7, 52, (1956).
22. Segre, G. and Silberberg, A., Nature, 189, 209, (1961).
23. Oliver, D. R., Nature, 194, 1269, (1962).
24. Taylor, H. D., Ph. D. Thesis, 'Flame Propagation through
Liquid-in-Air Suspensions', University of London, 1957.
25. e.g. Goldstein, S., (ed.), 'Modern Developments in Fluid
Mechanics', vol.I, p.299. (Oxford, 1938)
26. Happel, J. and Brenner, H., Amer. Inst. Chem. Eng.
Journal, 3, 506, (1957).
27. Brown, K. C. and James, G. J., Min. of Power, Safety in
Mines Research Estab., Research Rept. 201, (1962).
28. Kaesche-Krischer, B. and Zehr, J., Zeit. Phys. Chem.
N.F. 14, 384, (1958).
29. Ray, N. K., Basu, D. and Ghosh, B., J. Sci. and Ind.
Research, 16B, 470, (1957).

30. Hattori, H., 6th Symposium (International) on Combustion, (1956), p.590.
31. Long, V. D., Ph.D. Thesis, 'Flame Propagation in Suspensions of Coal Dust in Air', University of London, /1956.
32. Cassel, H. M., Das Gupta, A. K. and Guruswamy, S., 3rd Symposium (International) on Combustion, (1948), p.185.
33. Yagi, S. and Kunii, D., 5th Symposium (International) on Combustion, (1954), p.231.
34. Line, L.E., Clark, W.J. and Rahman, J.C., 6th Symposium (International) on Combustion, (1956), p.779.
35. Kane, L.J., Wright, H.C. and Shale, C.C., U.S. Bureau of Mines, Rept. Investign. 5637, (1960).
36. Hyman, D., Ph.D. Thesis, M.I.T., Cambridge, Mass., 1952.
37. Lang, P.M., Ph.D. Thesis, M.I.T., Cambridge, Mass., 1955.
38. Richards, R.L., jun., Ph.D. Thesis, M.I.T., Cambridge, Mass., 1955.
39. Thomas, W.J., Grey, P.J. and Watkins, S.B., Brit. Chem. Eng., 6, 80, 176, (1961).
40. Hartmann, I., Cooper, A.R., and Jacobson, M., U.S. Bureau of Mines, Rept. Investign. 4725, (1950).
41. Orning, A.A., Trans. ASME, 64, 497, (1942).
42. Audibert, E., Rev. Ind. Minerale Mémoires, 4, 1, (1924).
43. Taffanel, J. and Durr, A., Colliery Guardian, 103, 227, /((1912)).
44. De Grey, A., Rev. Métall., 19, 645, (1922).
45. Kislig, F., Thesis, 'Contributions to the Knowledge of Dust Flames', E.T.H., Zurich, 1950.
46. Essenhigh, R.H., and Woodhead, D.W., Combustion and Flame, 2, 365, (1958).

47. Line, L.E., Rhodes, H.A. and Gilmer, T.E., *J. Phys. Chem.*,
63, 290, (1959).
48. Fuhrmann, E.A. and Köttgen, H., *Zeit. Phys. Chem.* 169,
388, (1934).
49. Wolfhard, H.G. and Parker, W.G., *Proc. Phys. Soc. B*,
62, 523, (1949).
50. Cueilleron, J. and Scartazzini, H., *C.R. Acad. Sci.*
Paris, 228, 489, (1949).
51. Scartazzini, H., *C.R. Acad. Sci. Paris*, 231, 1144, (1950).
52. De Salins, R., *C.R. Acad. Sci. Paris*, 234, 2437, (1952).
53. Stubbs, J.J., Thesis, Leeds University, 1954.
54. Cassel, H.M., Liebman, I. and Mock, W.K., 6th Symposium
(International) on Combustion, (1956), p.602.
55. Orning, A.A., as ref. no. 54, p.562-4.
56. Ghosh, B., Basu, D. and Ray, N.K., as ref. no. 54, p.595.
57. Orning, A.A., as ref. no. 55.
58. Beer, J.M., and Essenhigh, R.H., *Nature*, 187, 1106, (1960)
59. Gregory, P.H., *Annals of Applied Biol.*, Cambridge,
38, 357, (1951).
60. Underwood, A.J.V., in 'Technical Data on Fuel', ed.
H.M. Spiers, 6th edn., London, 1962, p.89.
61. Richardson, E.G., in 'Aerodynamic Capture of Particles,'
p.199.(see ref. no. 16, above.)
62. Davies, C.N., 'The Physics of Particle Size Analysis',
p.S17, (see ref. no. 3 above.)
63. Richardson, E.G., as ref. no. 16, p.5.

64. Jeffery, G.B., Proc. Roy. Soc., 102A, 161, (1922).
65. Mason, S.G. and Bartok, W., in 'Rheology of Disperse Systems', ed. C.C. Mill, p.19. (Pergamon, 1959).
66. Rubinow, S.I. and Keller, J.B., J. Fluid Mech., 11, 447, (1961).
67. Einstein, A., Ann. Phys., (Leipzig), 19, 289, (1906);
54, 591, (1911).
68. Roscoe, R., in 'Flow Properties of Disperse Systems', ed. J.J. Hermans, p.3. (North-Holland Pub. Co., Amsterdam, 1953)
69. ~~Hawksley, P.G.W.~~, ^{Kynch, G.J.,} as ref. no. ~~9~~, above.
70. see e.g. Prandtl, L. and Tietjens, O.G., 'Applied Hydro- and Aeromechanics', p.26. (Dover Publications, New York, ¹⁹⁵⁷).
71. Wohl, K., Kapp, N.M. and Gazley, C., 3rd Symposium (International) on Combustion, (1948), p.3.
72. Lewis, B. and Von Elbe, G., 'Combustion, Flames and Explosion of Gases', p.266. (2nd. edn., New York, 1961.)
73. Cohen, L., Ph.D. Thesis, 'Flame Propagation in Liquid Aerosols', University of London, 1953.
74. Dixon-Lewis, G., and Isles, G.L., 8th Symposium (International) on Combustion, (1960), p.448.
75. Lewis, B. and Von Elbe, G., as ref. no. 72, p.269.
76. Von Elbe, G. and Lewis, B., 3rd Symposium (International) on Combustion, (1948), p.68.
77. Harris, M.E., Grumer, J. et.al., 3rd Symposium (International) on Combustion, (1948), p.80.